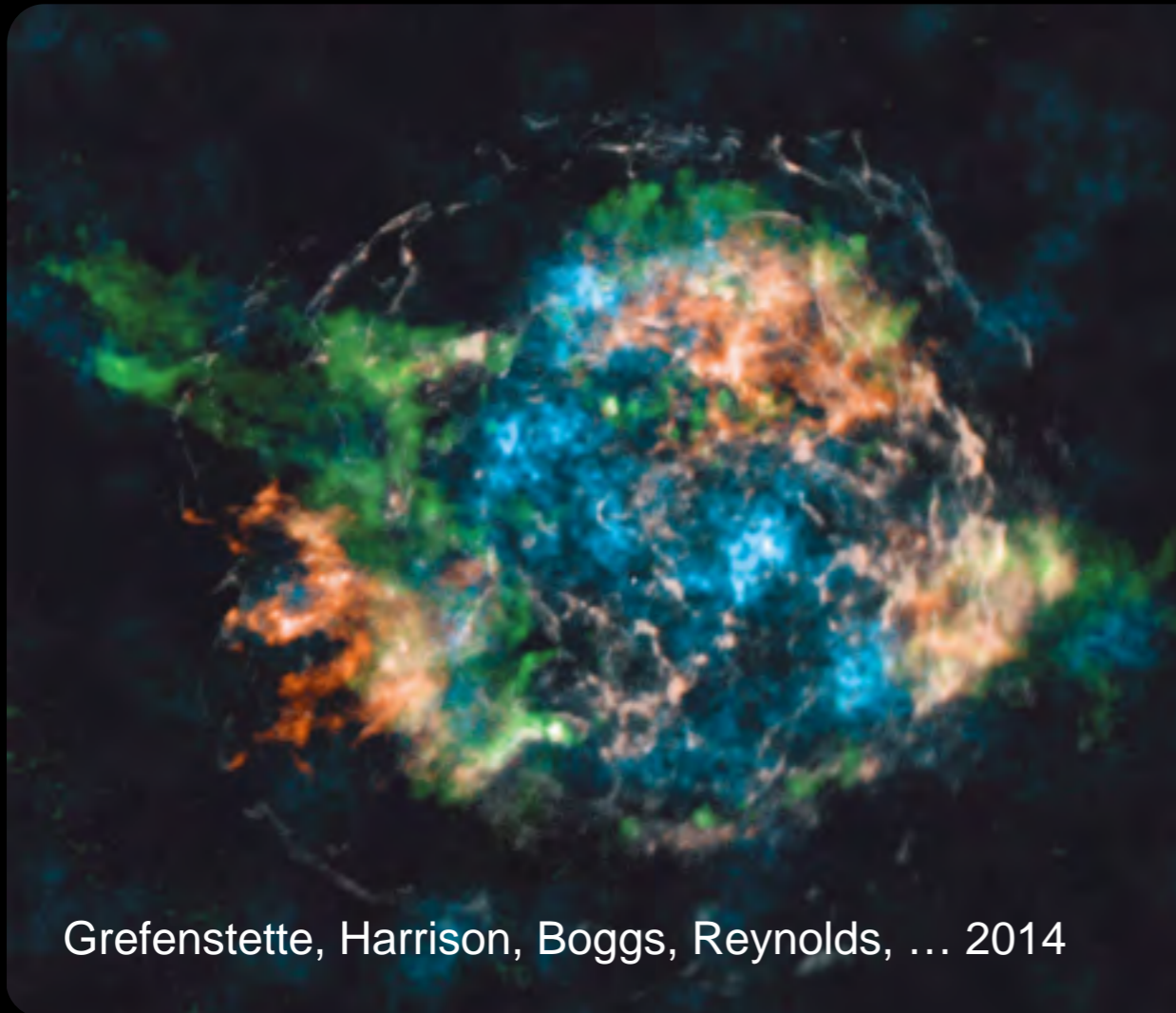
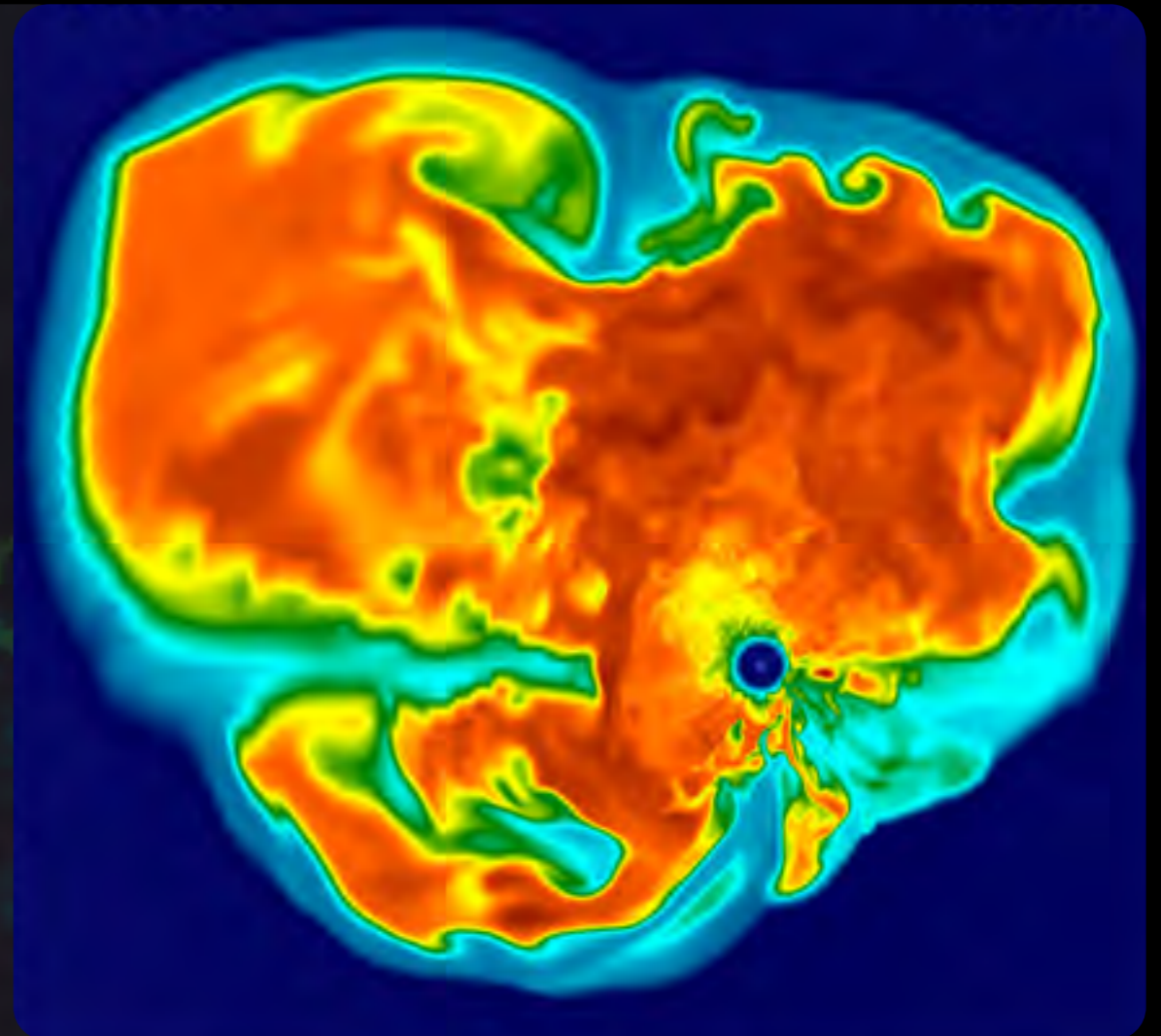


# MULTIDIMENSIONAL SIMULATIONS OF CORE-COLLAPSE SUPERNOVAE



Grefenstette, Harrison, Boggs, Reynolds, ... 2014

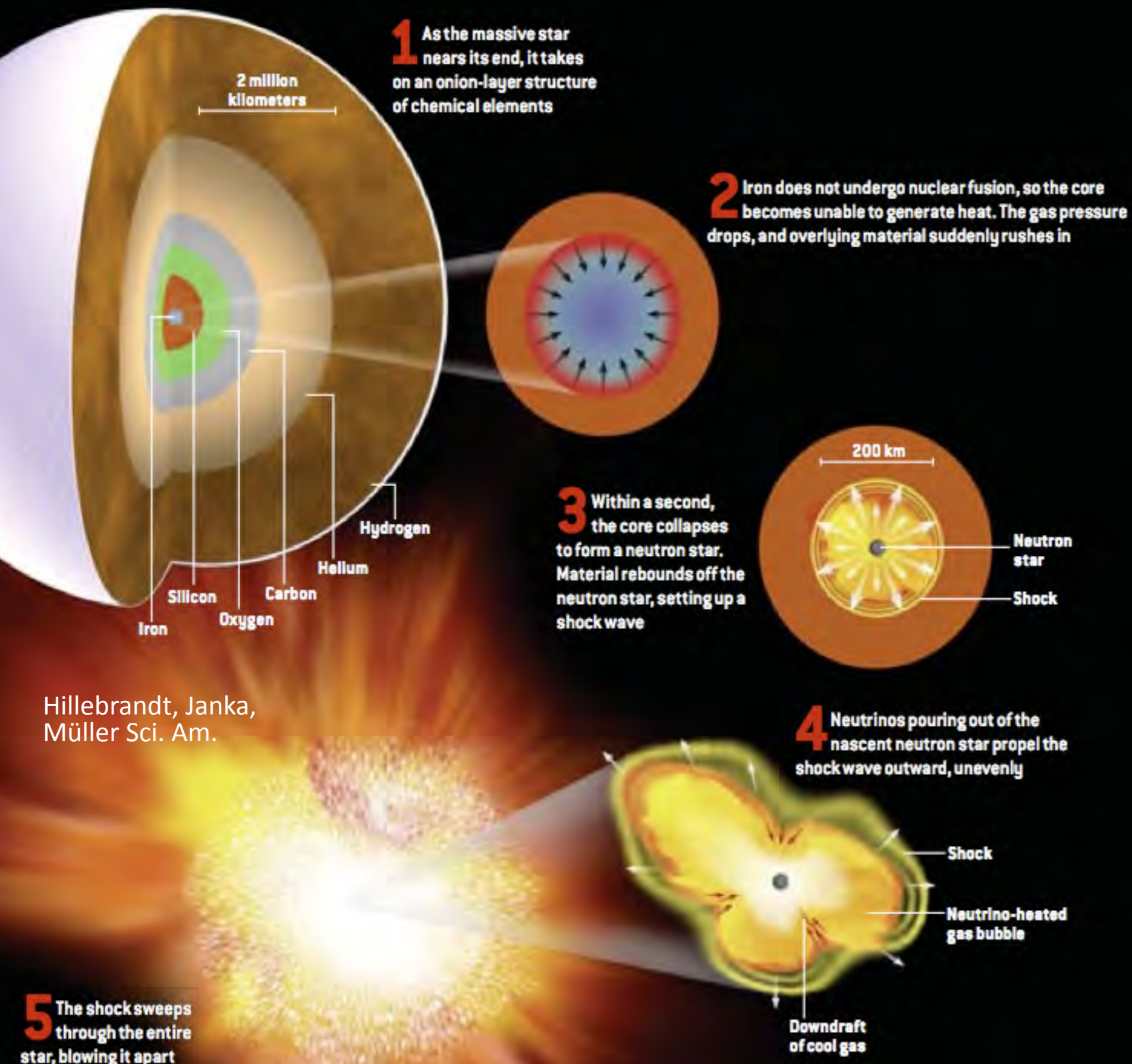


## & THEIR IMPACT ON SN NUCLEOSYNTHESIS

William Raphael Hix (ORNL/U. Tennessee)

Blondin, Bruenn, Endeve, Fröhlich, Harris, Lentz, Marronetti, Messer, Mezzacappa &  
Yakunin (Florida Atlantic U., NC State U., ORNL, UT, LBL)

# TEXTBOOK SUPERNOVA



Hillebrandt, Janka,  
Müller Sci. Am.

A Core-Collapse Supernova is the **inevitable death** knell of a massive star ( $\sim 10+ M_{\odot}$ ).

The explosion enriches the **interstellar** medium with elements from **Oxygen to Nickel** and potentially the **r-process** elements as well.

# CHIMERA



CHIMERA has 3 “heads”

Spectral Neutrino Transport (MGFLD-TRANS, Bruenn)  
in Ray-by-Ray Approximation

Shock-capturing Hydrodynamics (VH1, Blondin)

Nuclear Kinetics (XNet, Hix & Thielemann)

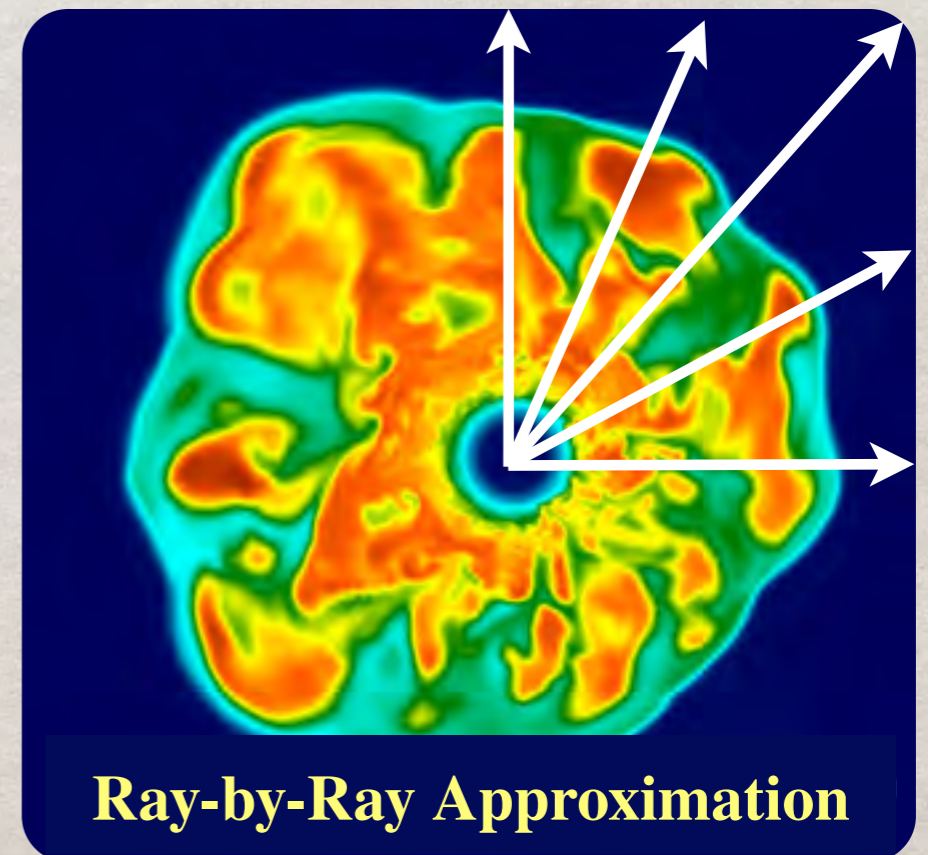
Plus Realistic Equations of State, Newtonian Gravity  
with Spherical GR Corrections.

Models use a variety of approximations

**Self-consistent** (*ab initio*) models use  
full physics to the center.

**Leakage** & **IDSa** models simplify the  
transport.

**Parameterized** models replace the core  
with a specified neutrino luminosity.

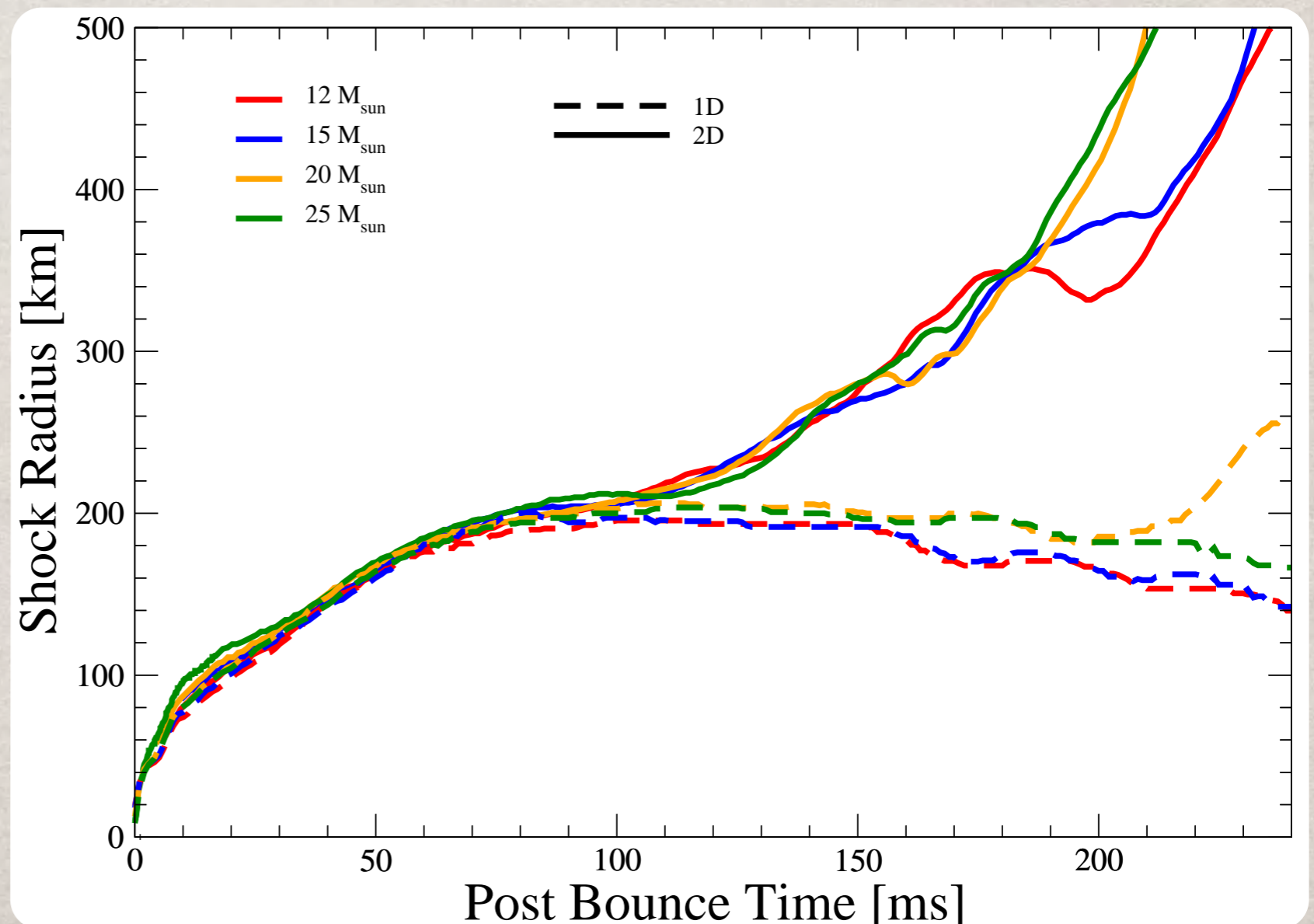


**Ray-by-Ray Approximation**

# THE EARLY PHASE

For the first  $\sim 0.1$  s after bounce, the supernova shock is **essentially spherical**, with 1D models identical to 2D models.

In multi-dimensions, fluid instabilities begin to **deform the shock** and gradually **push it outwards**.

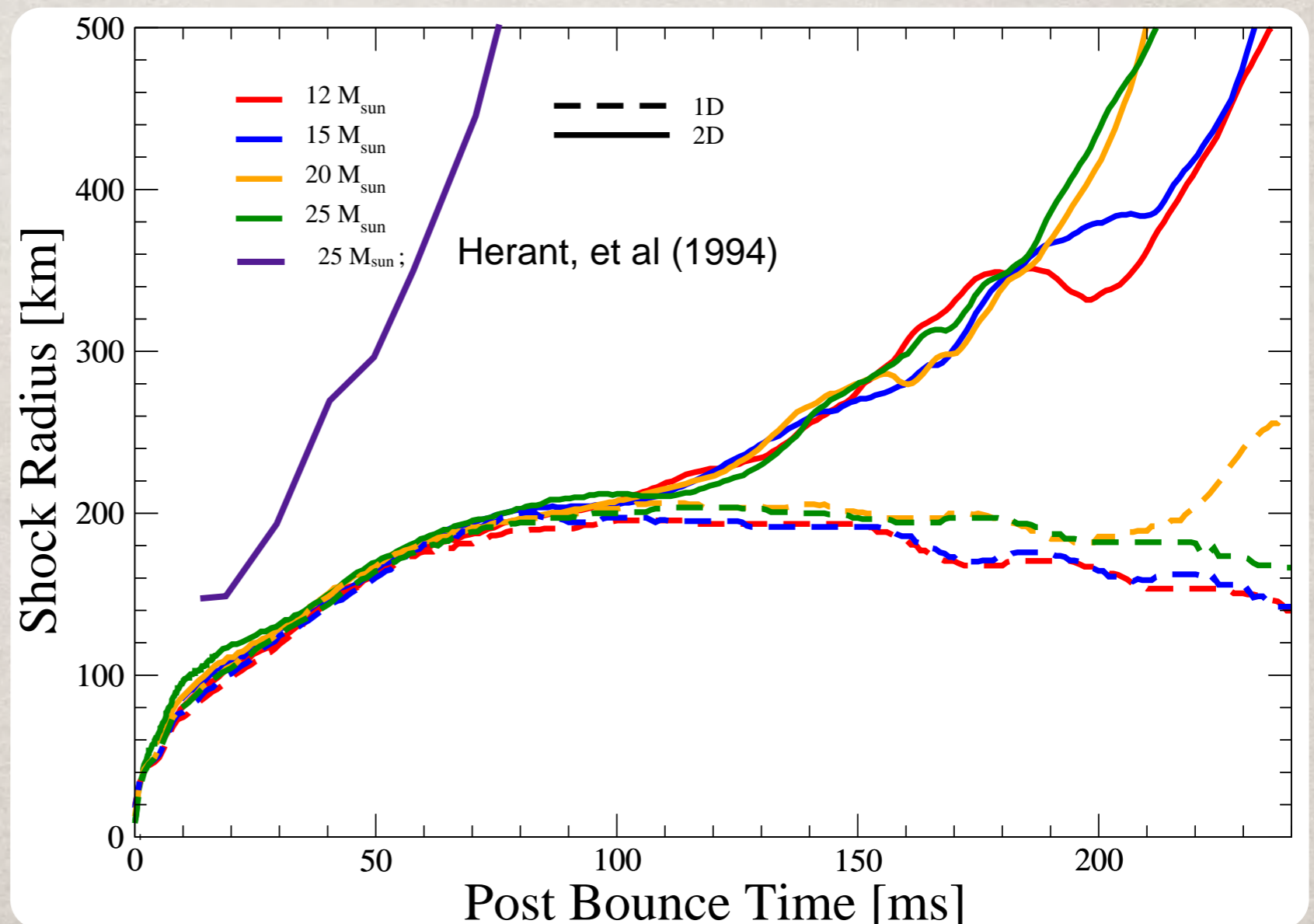


# THE EARLY PHASE

For the first  $\sim 0.1$  s after bounce, the supernova shock is **essentially spherical**, with 1D models identical to 2D models.

In multi-dimensions, fluid instabilities begin to **deform the shock** and gradually **push it outwards**.

Compared to **older models**, there is a considerable delay ( $\sim 0.2$  s) in launching an explosion.



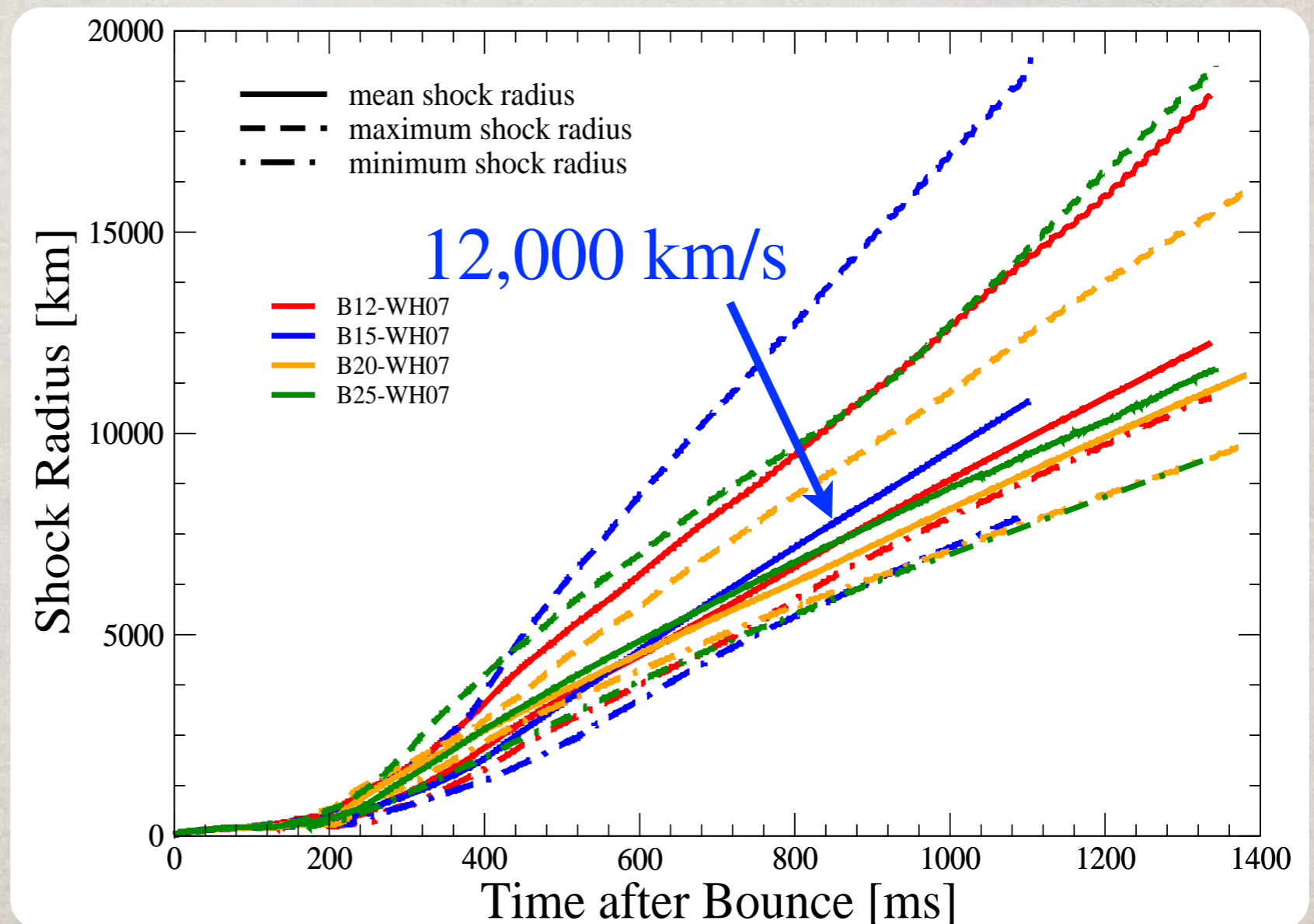
# THE EARLY PHASE

For the first  $\sim 0.1$  s after bounce, the supernova shock is **essentially spherical**, with 1D models identical to 2D models.

In multi-dimensions, fluid instabilities begin to **deform the shock** and gradually **push it outwards**.

Compared to **older models**, there is a considerable delay ( $\sim 0.2$  s) in launching an explosion.

Shock accelerates to free expansion.



# THE EARLY PHASE

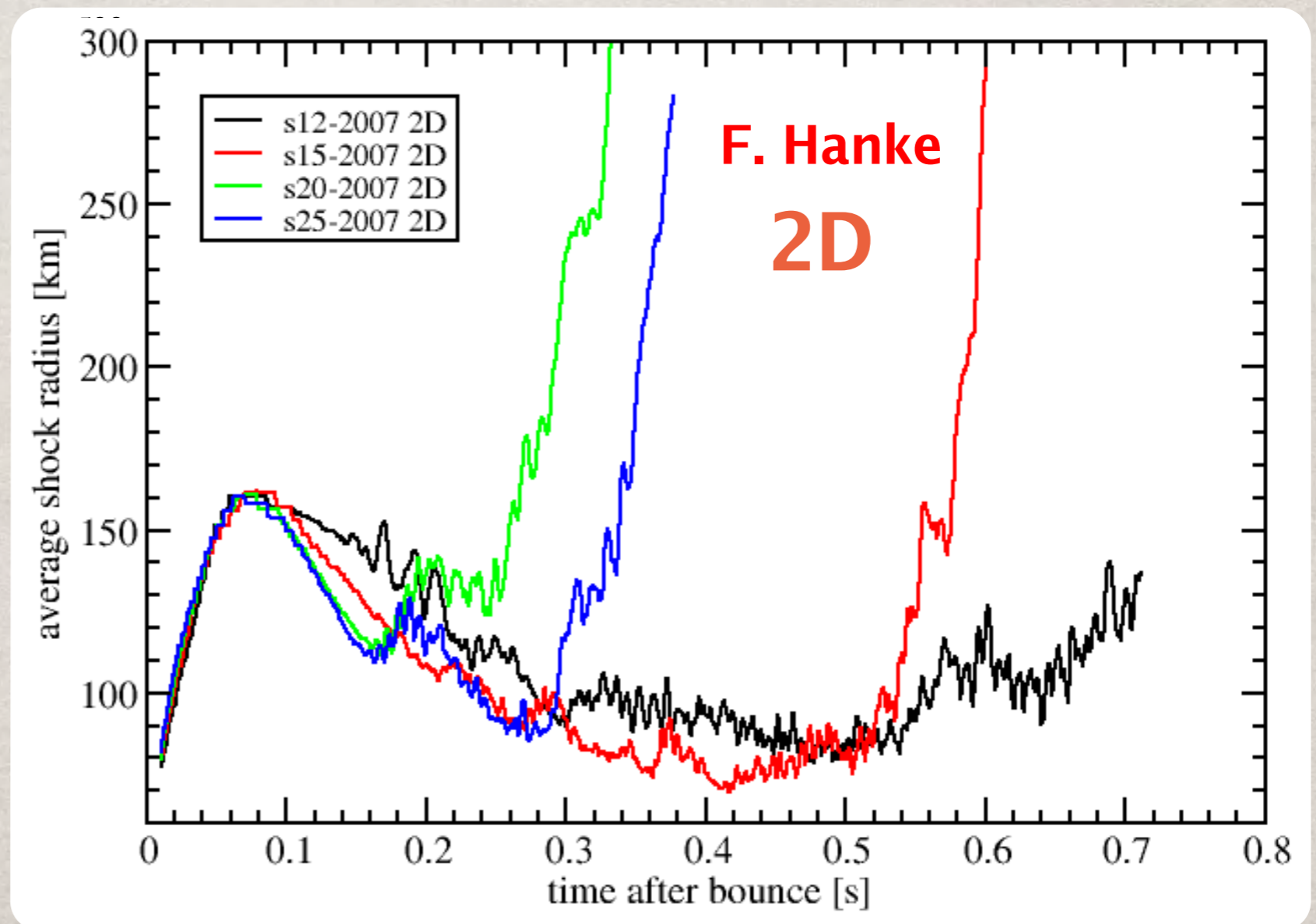
For the first  $\sim 0.1$  s after bounce, the supernova shock is **essentially spherical**, with 1D models identical to 2D models.

In multi-dimensions, fluid instabilities begin to **deform the shock** and gradually **push it outwards**.

Compared to **older models**, there is a considerable delay ( $\sim 0.2$  s) in launching an explosion.

Shock accelerates to free expansion.

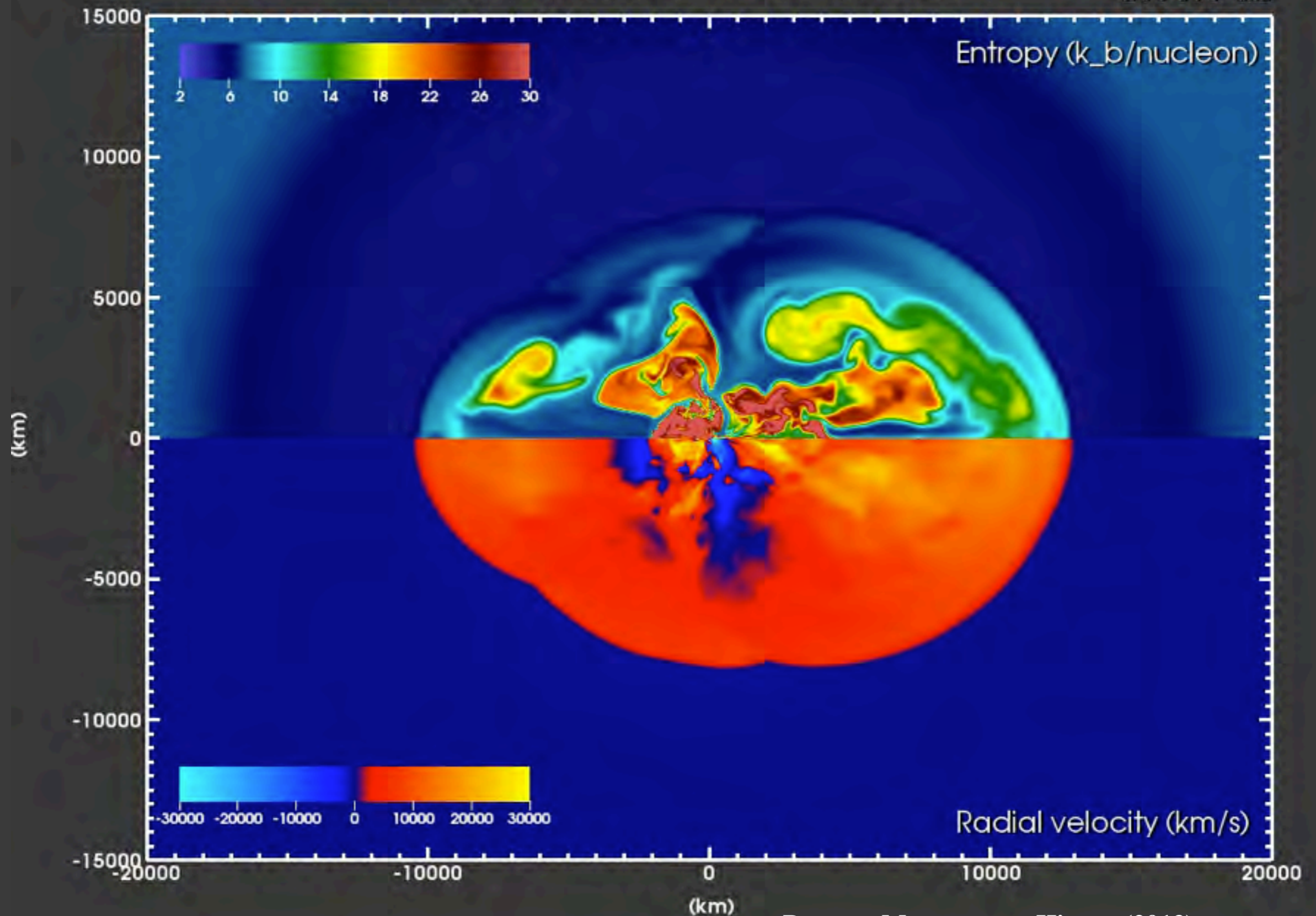
Competitive models exhibit **even longer delays**.



# SUPERNOVA: THE MOVIE

Chimera model: B12-WH07

1004.0 ms



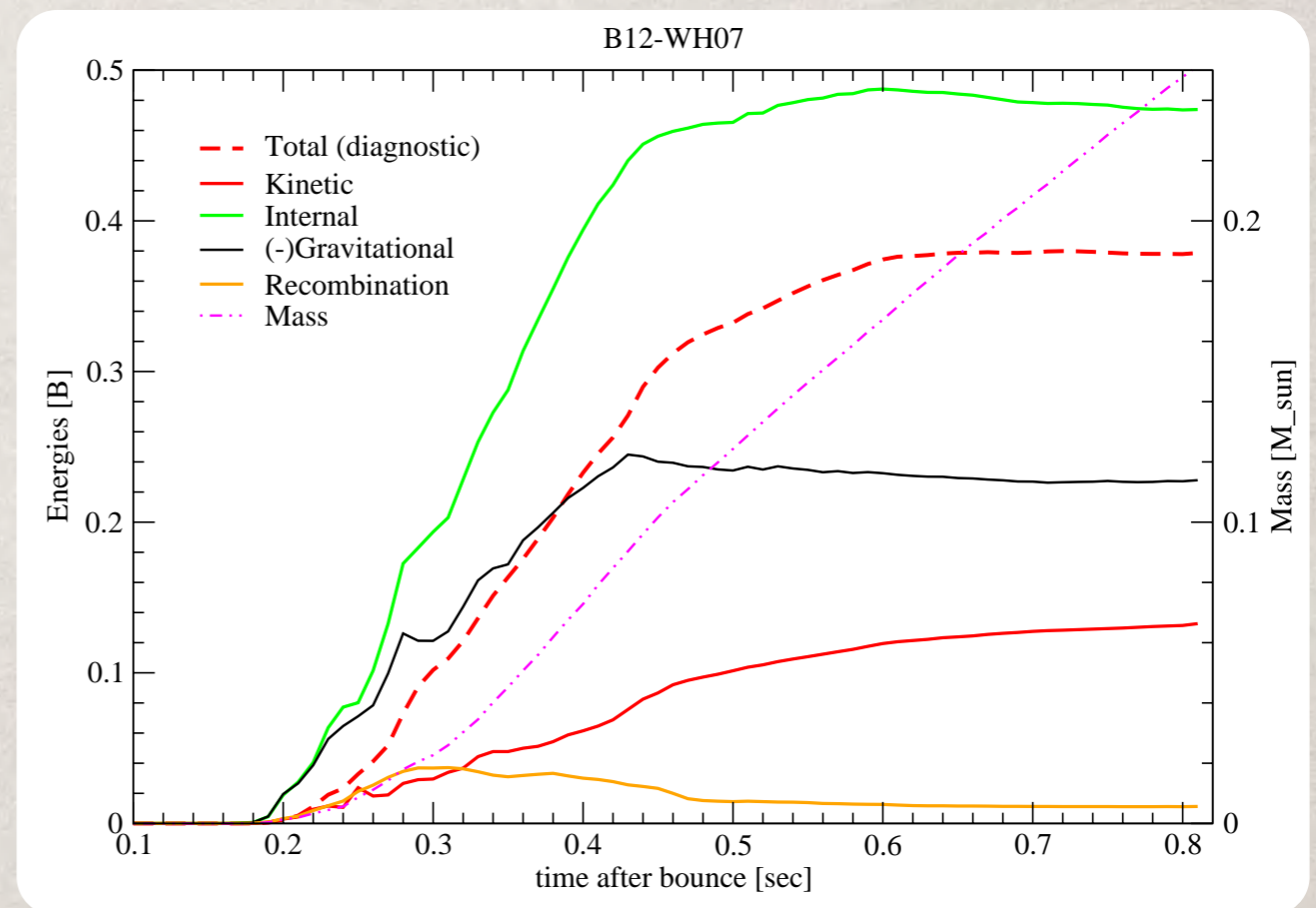
Bruenn, Mezzacappa, Hix, ... (2013)

# EXPLOSION ENERGIES

Once we achieve the most basic observable, an explosion, we can begin to compare to the myriad of other potential observations.

Foremost is the kinetic **energy** of the explosion.

Unfortunately, models are still in the stage where **internal energy dominates**, so we must estimate the explosion energy by assuming efficient conversion of  $E_i \Rightarrow E_k$ .

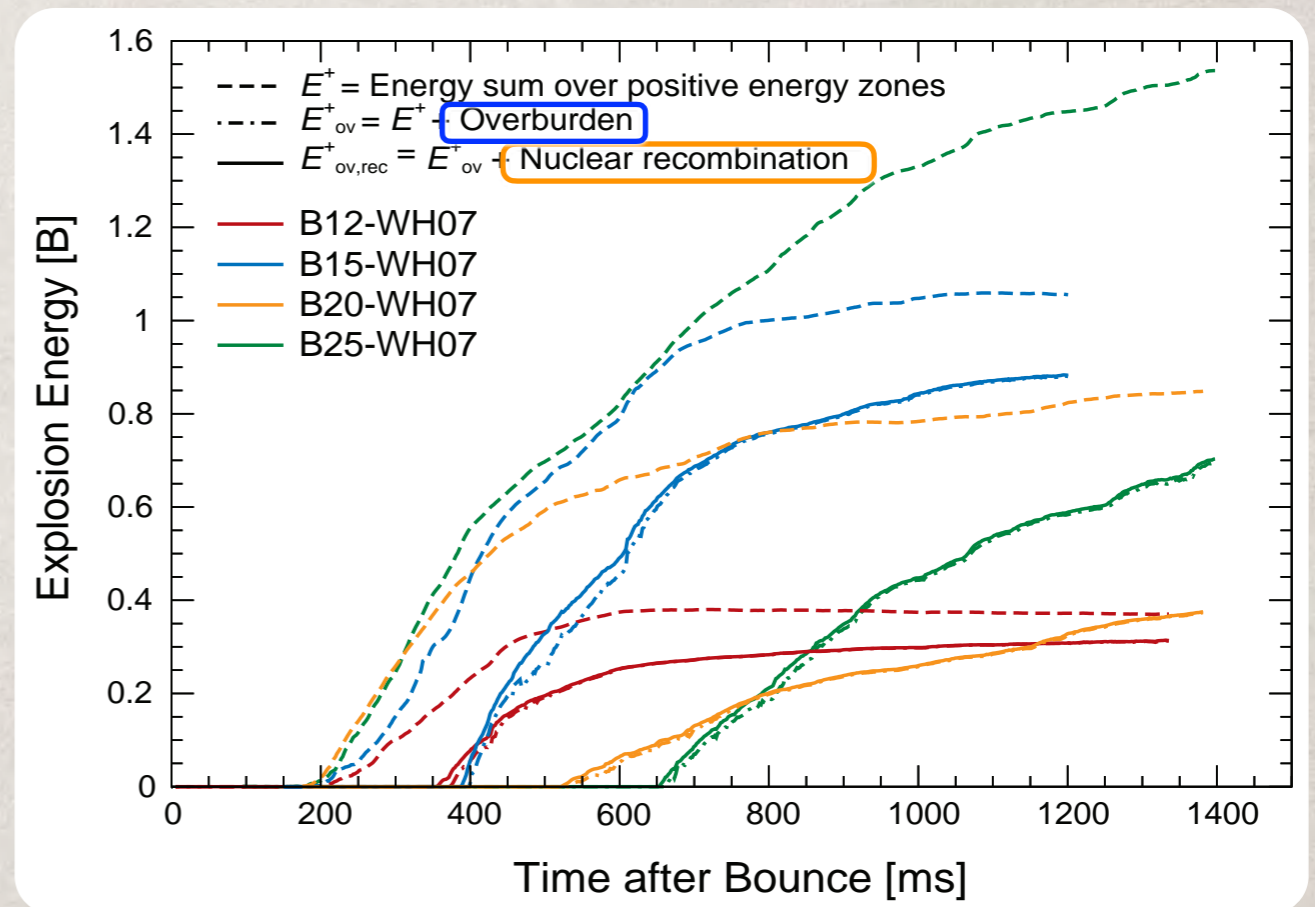


# EXPLOSION ENERGIES

Once we achieve the most basic observable, an explosion, we can begin to compare to the myriad of other potential observations.

Foremost is the kinetic **energy of the explosion**.

Unfortunately, models are still in the stage where **internal energy dominates**, so we must estimate the explosion energy by assuming efficient conversion of  $E_i \Rightarrow E_k$ .



One can construct a “**diagnostic**” **energy**,  $E^+ = E_i + E_g + E_k$ , summed over zones where  $E^+ > 0$ .

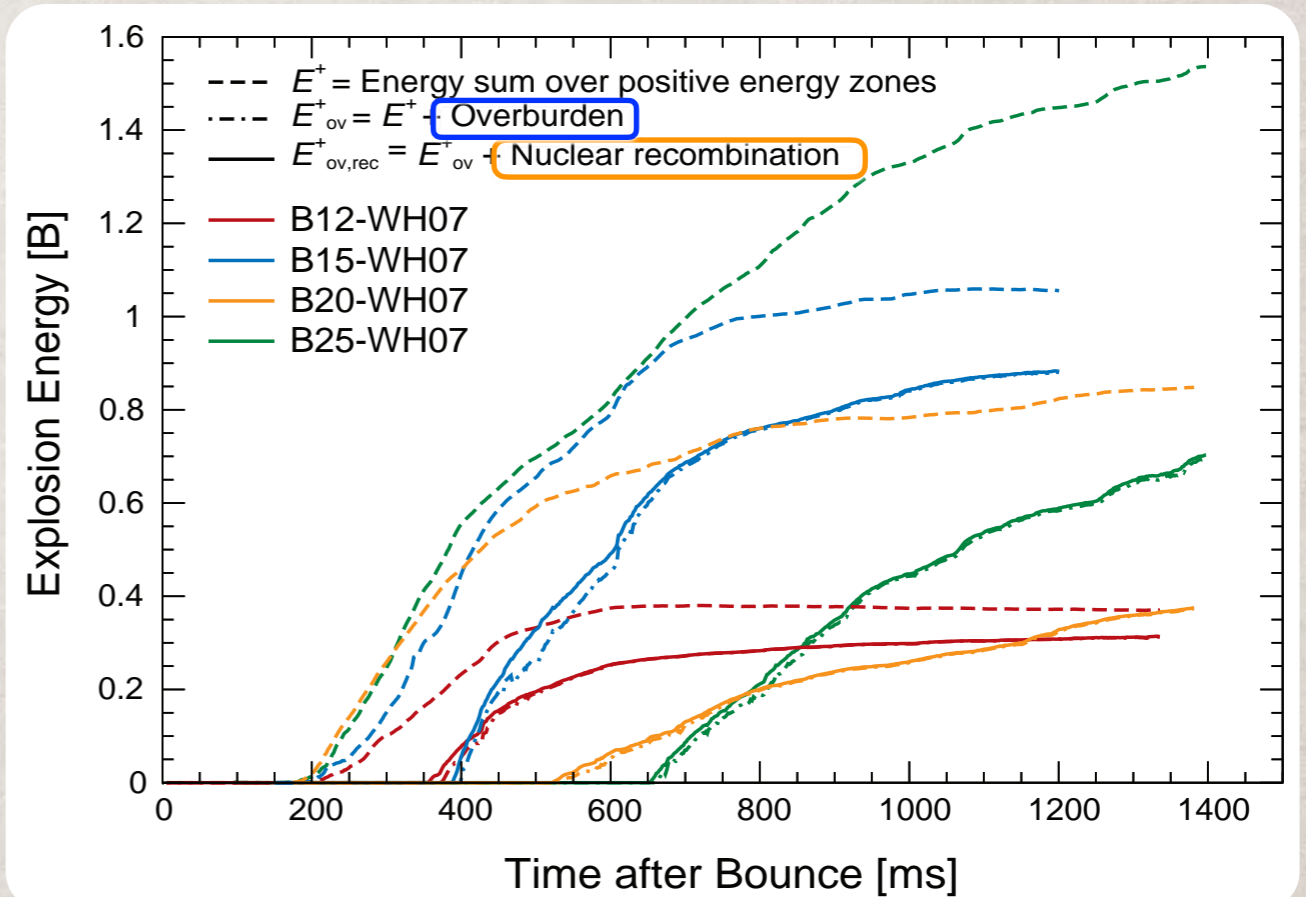
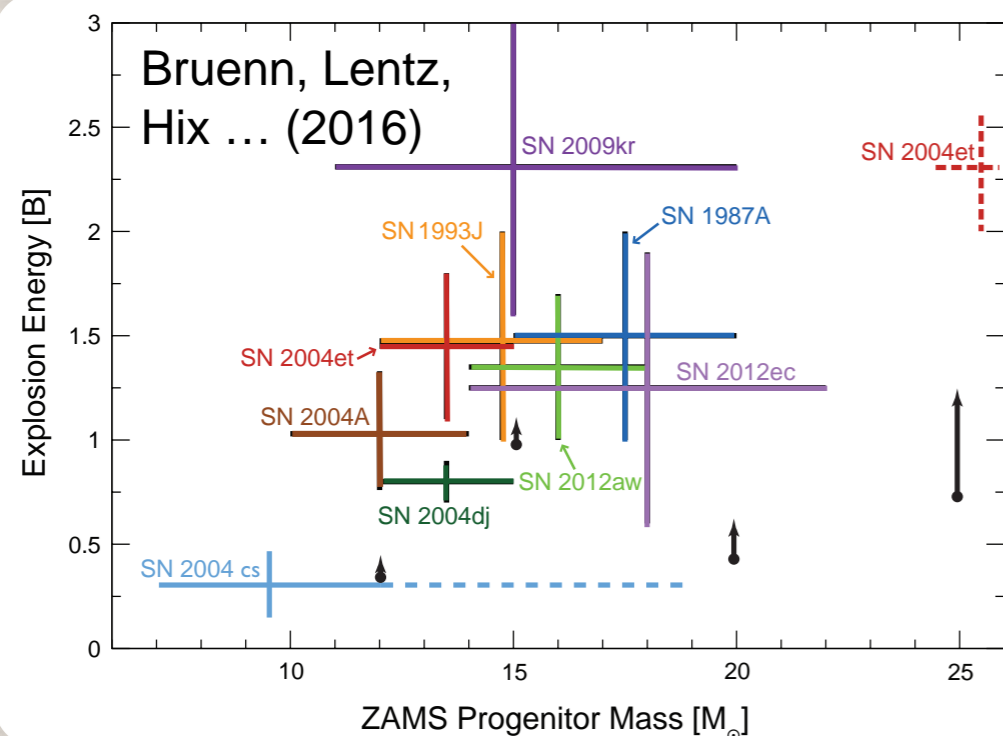
To this we add contributions from **nuclear recombination** and **removing the envelope**.

# EXPLOSION ENERGIES

Once we achieve the most basic observable, an explosion, we can begin to compare to the myriad of other potential observations.

Foremost is the kinetic **energy** of the explosion.

Unfortunately, models are still in the stage where **internal energy dominates**, so we must estimate the explosion energy by assuming efficient conversion of  $E_i \Rightarrow E_k$ .



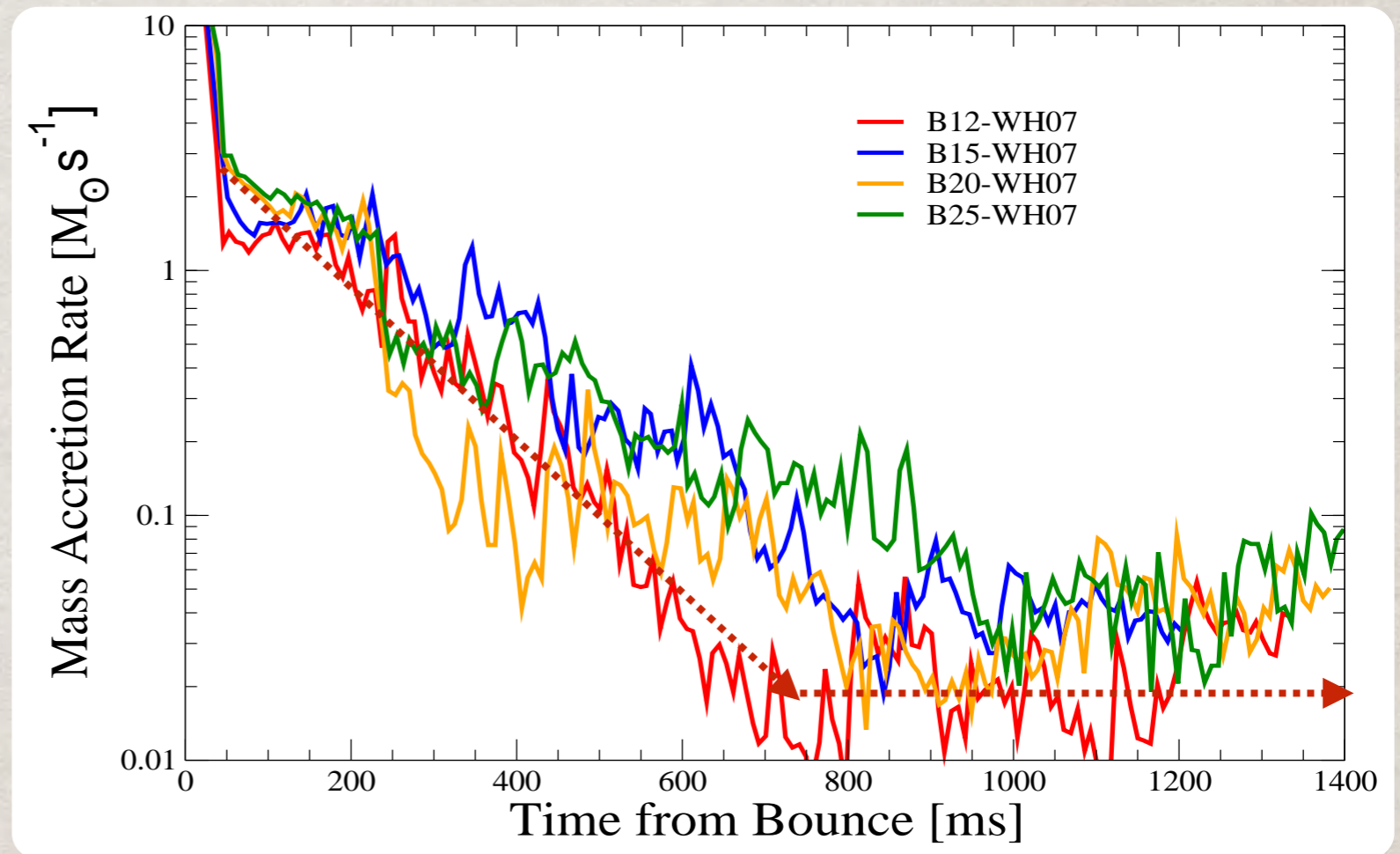
One can construct a “**diagnostic**” **energy**,  $E^+ = E_i + E_g + E_k$ , summed over zones where  $E^+ > 0$ .

To this we add contributions from **nuclear recombination** and **removing the envelope**.

# END OF THE EXPLOSION?

Even in our most fully developed model, the explosion energy **has not leveled off** 1.3 seconds after bounce.

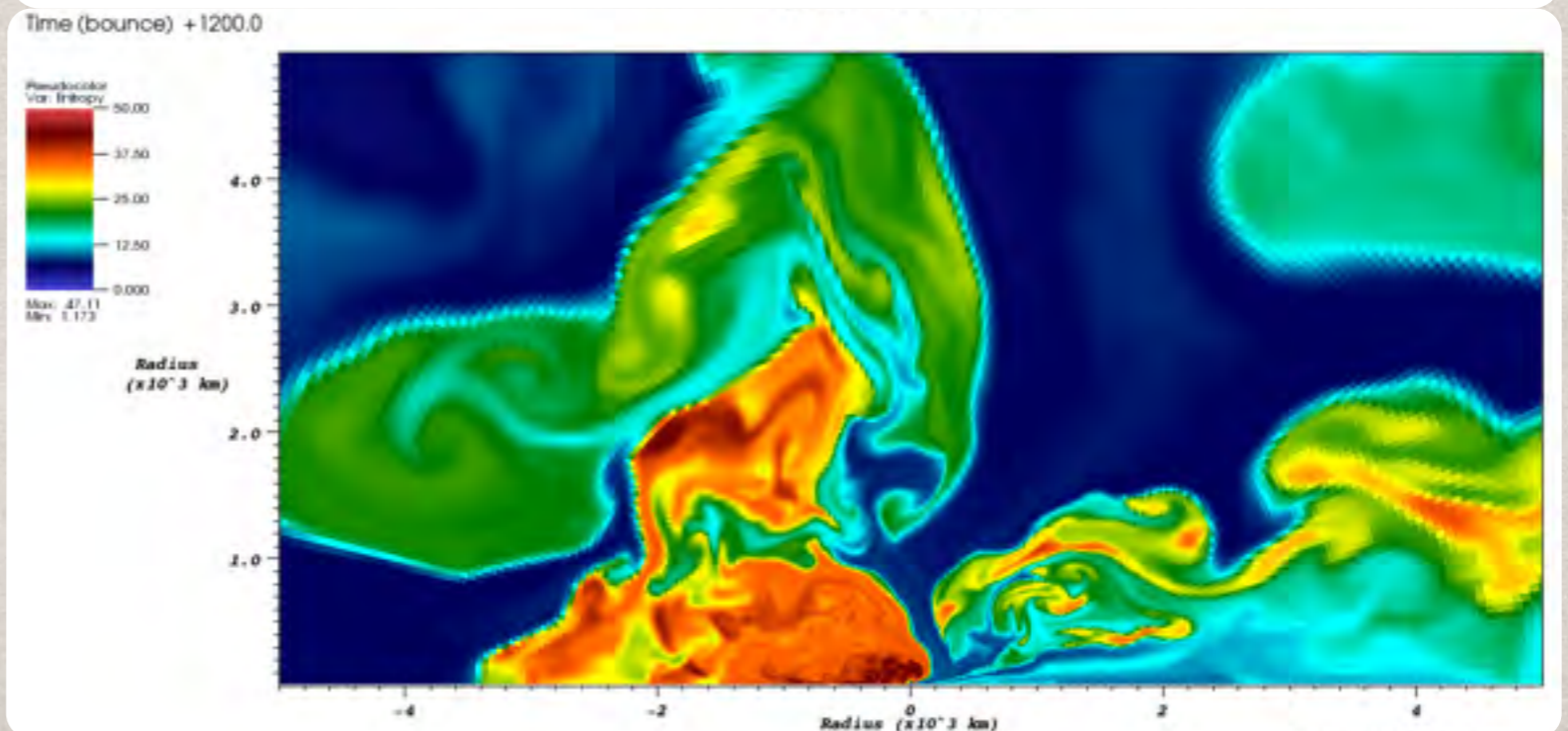
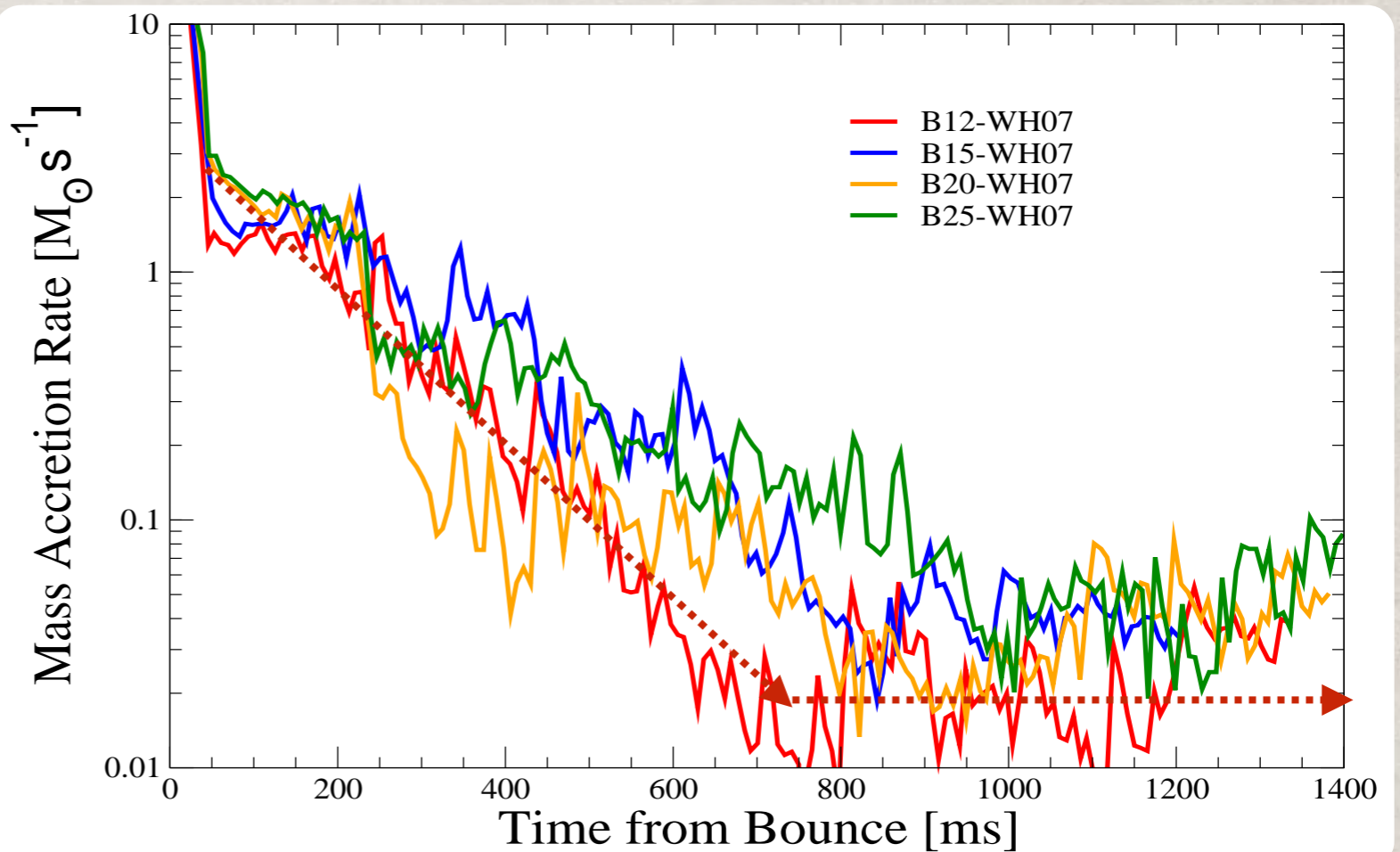
The reason is that **accretion continues** at an appreciable rate, showing no sign of abating.



# END OF THE EXPLOSION?

Even in our most fully developed model, the explosion energy **has not leveled off** 1.3 seconds after bounce.

The reason is that **accretion continues** at an appreciable rate, showing no sign of abating.

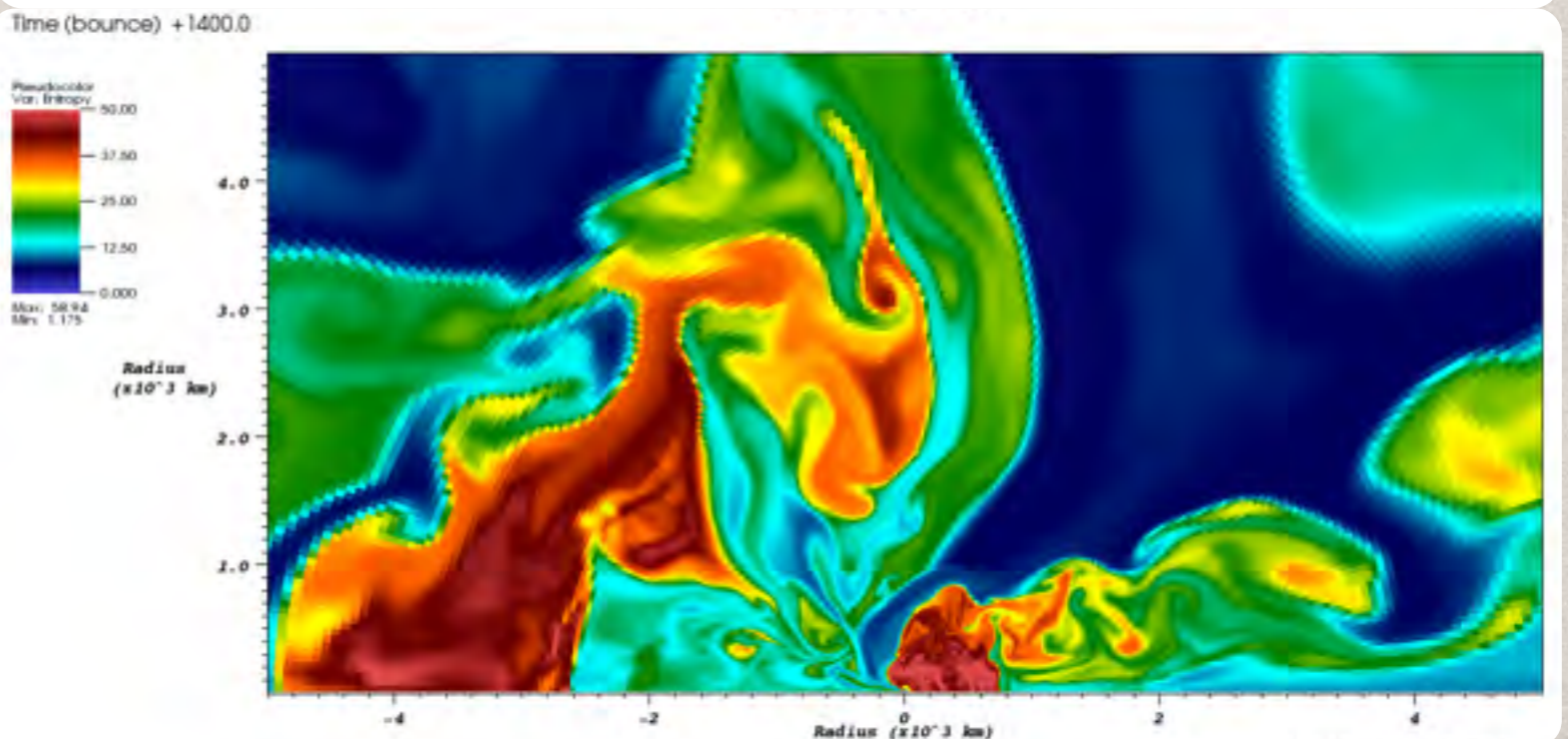
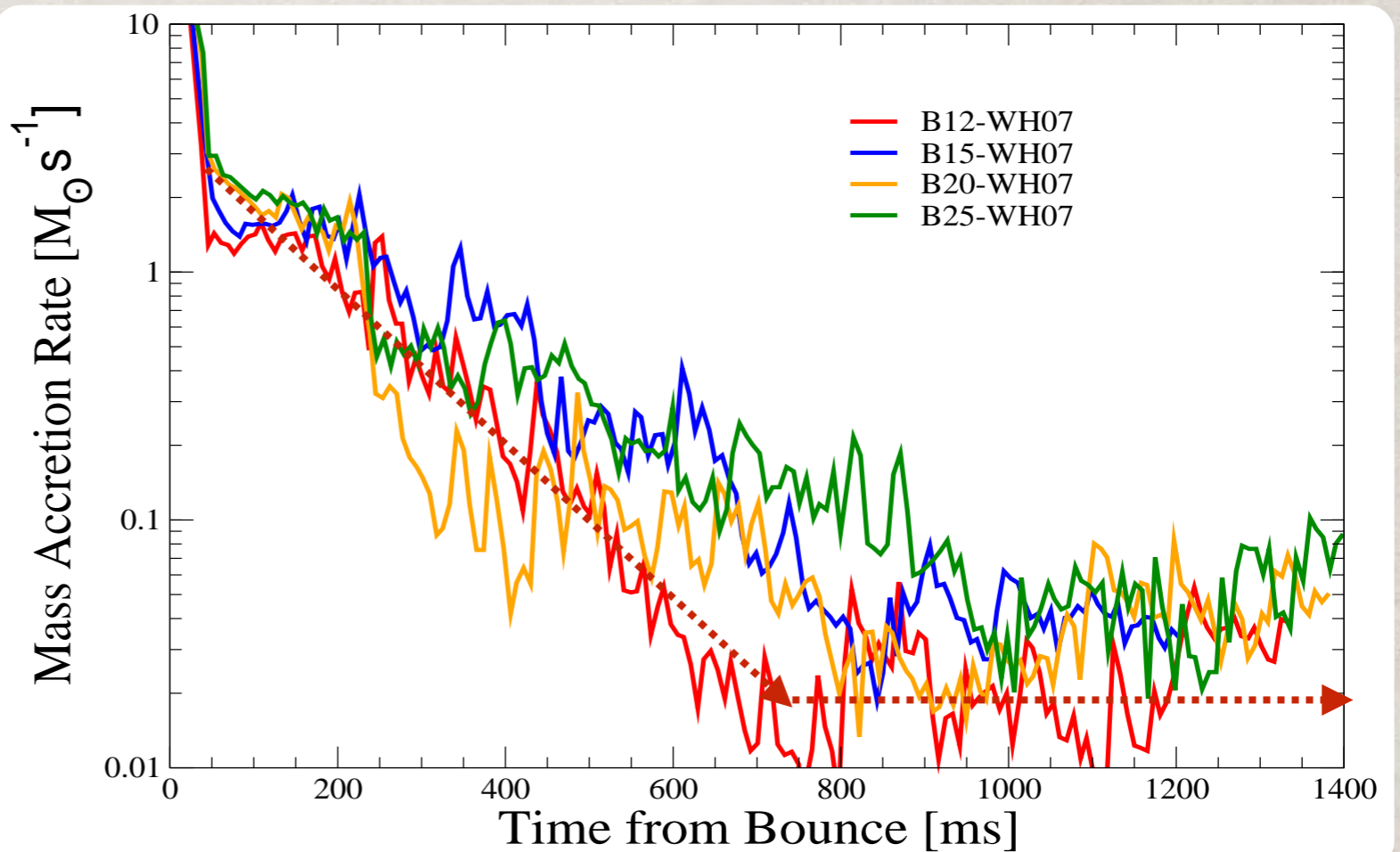


# END OF THE EXPLOSION?

Even in our most fully developed model, the explosion energy **has not leveled off** 1.3 seconds after bounce.

The reason is that **accretion continues** at an appreciable rate, showing no sign of abating.

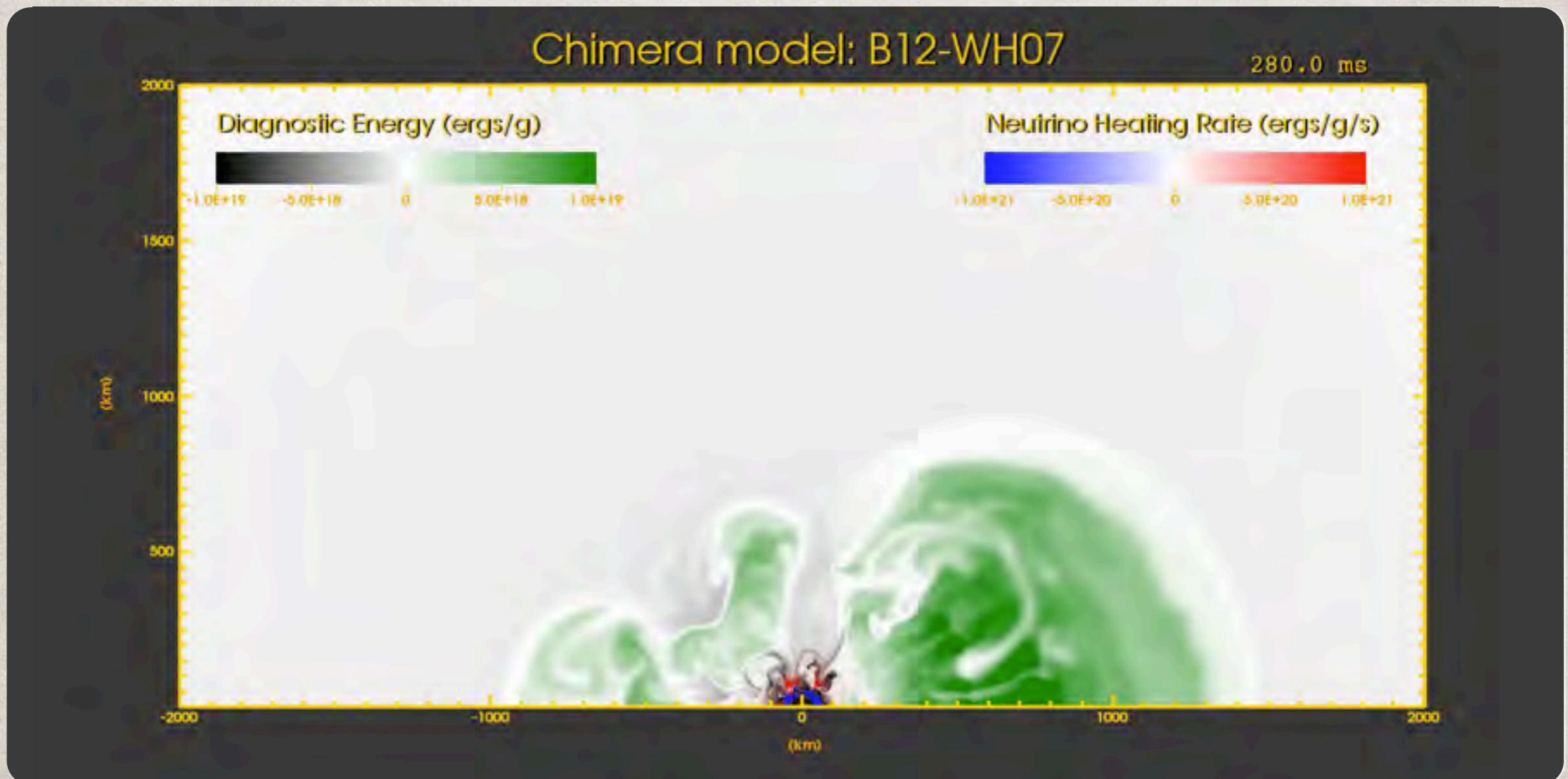
This extends the “hot bubble” phase and **suppresses** the development of **the PNS wind**.



# THE PROBLEM OF FALLBACK

Some of the infalling matter at late times is making its **first approach** to the PNS, but much of the matter has been here before, having **expended energy** lifting the remainder of the star.

This continued accretion & heating impacts the **nucleosynthesis**.



# ANATOMY OF A GW SIGNAL

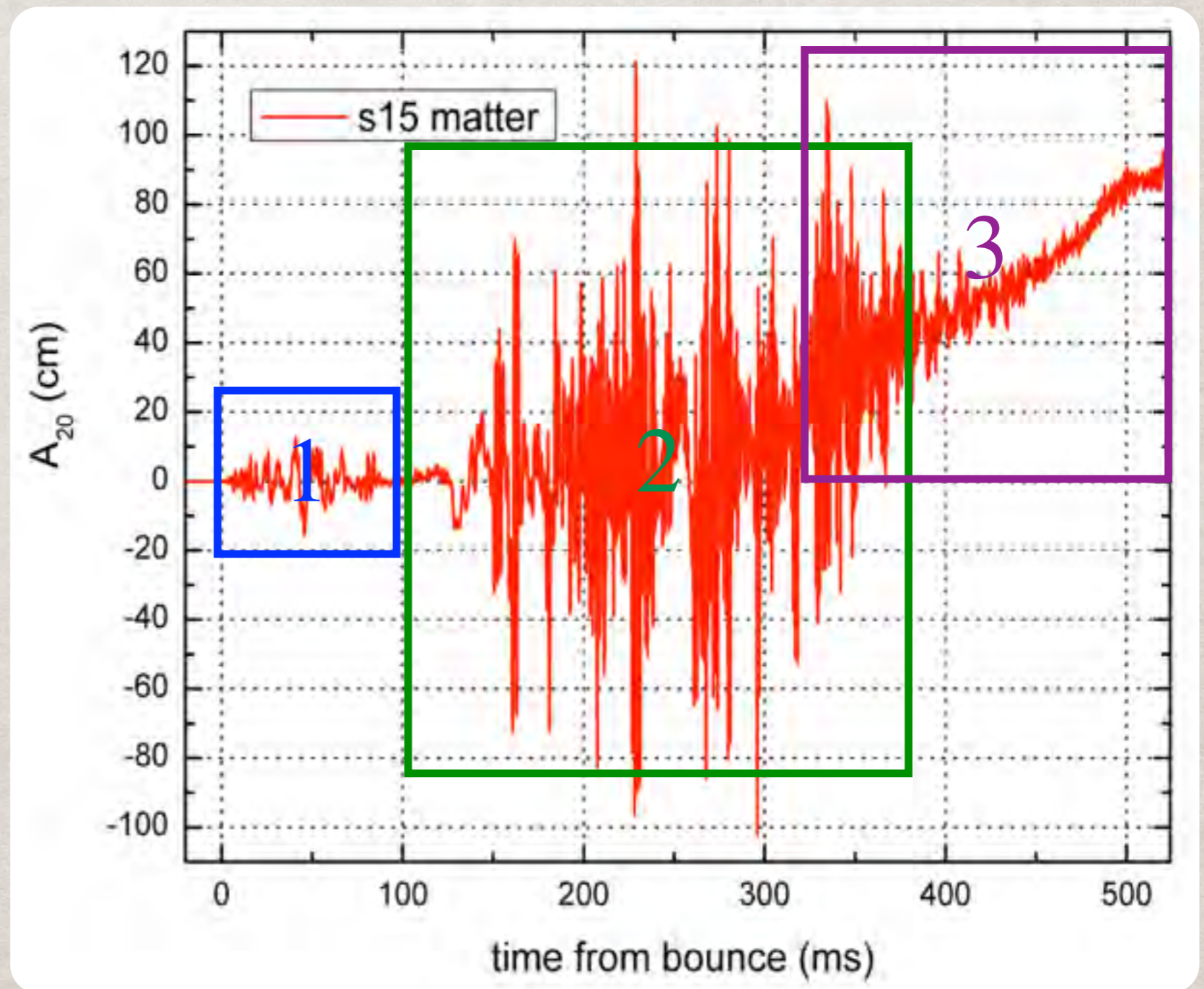
Gravity Wave signal shows 3 separate phases

1) Prompt  
Convection & Early  
Shock Deceleration

2a) Shock Motions  
lead to lower-  
frequency envelope.

2b) Impingement of  
downflows on the  
PNS, leads to  
higher-frequency  
variations.

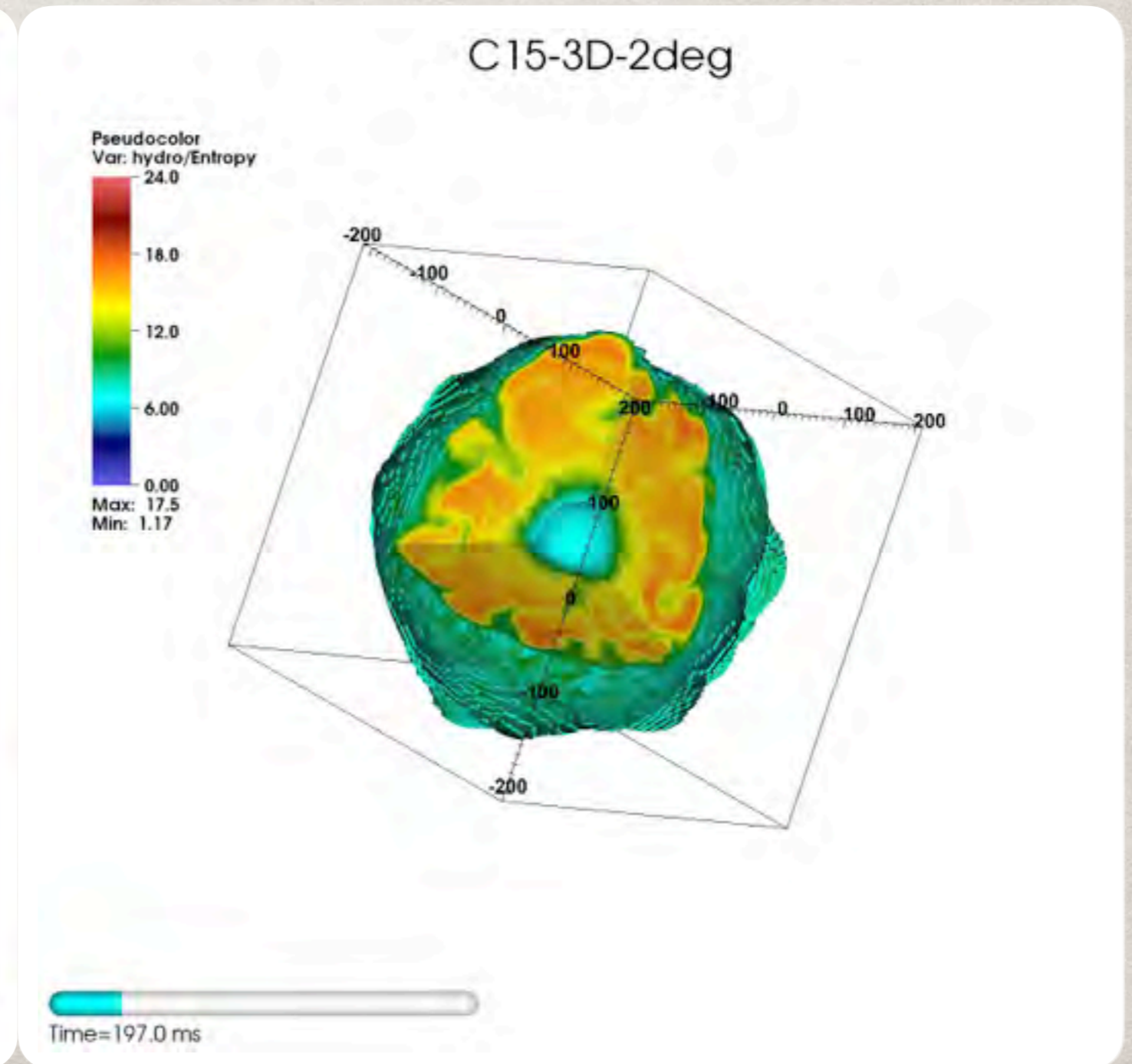
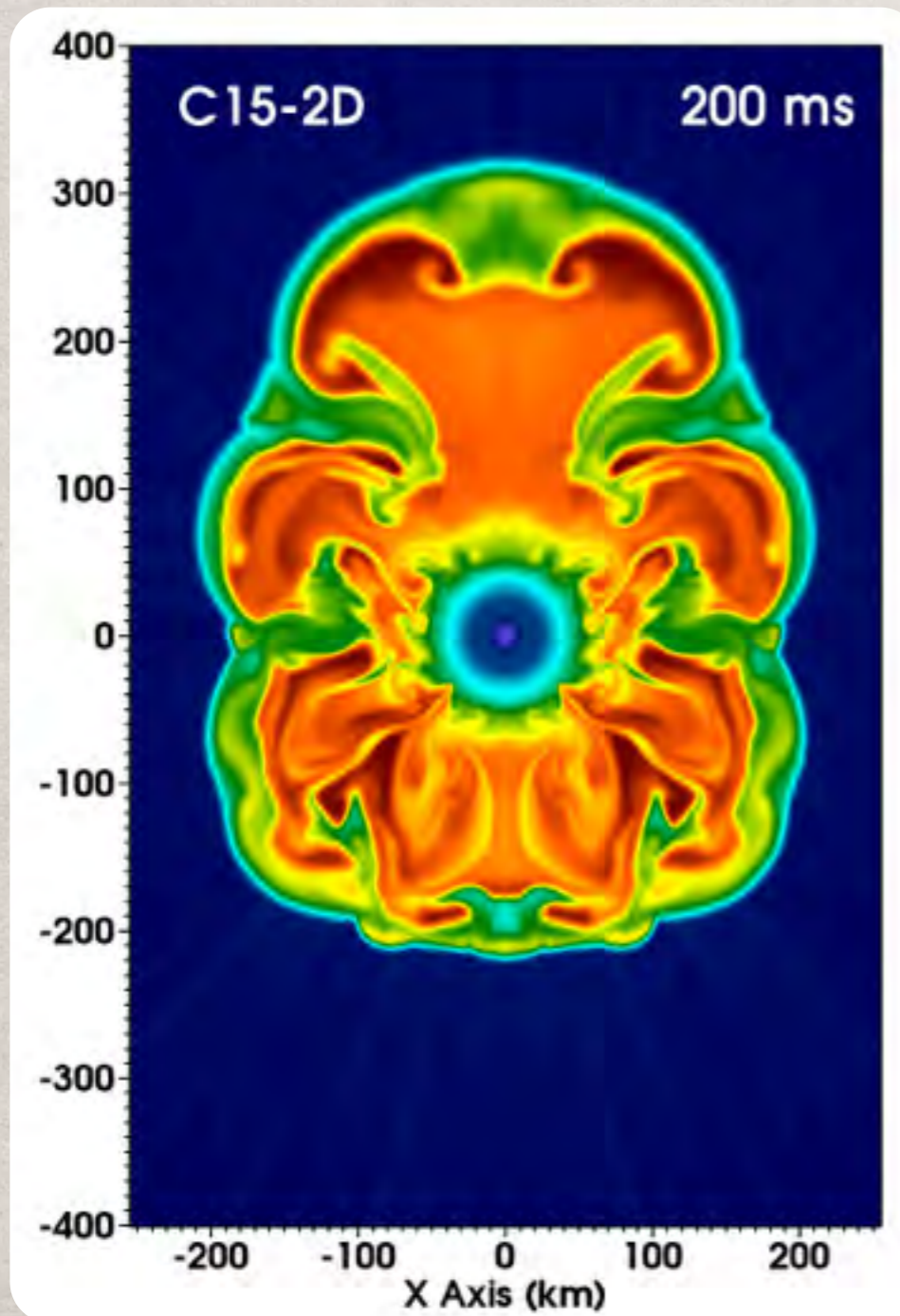
3) Prolate Explosion/Deceleration at Shock



# HOW DOES 3D COMPARE?

2D models tend to explode preferentially along [the symmetry axis](#).

This tendency alone points to the need for 3D models, .

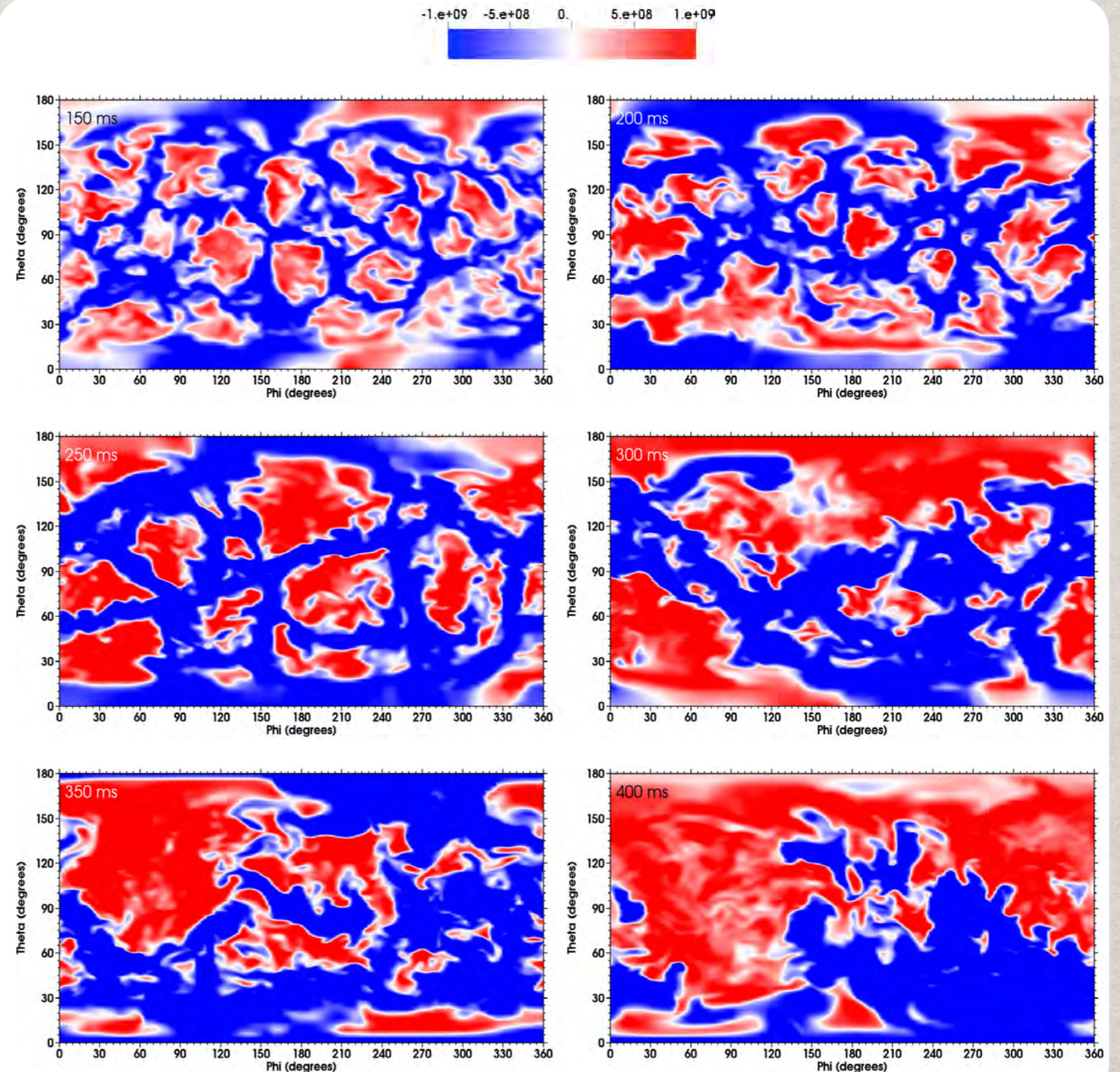


# GROWING PLUMES

The explosion in 3D (as well as 2D) is preceded by the progress to **fewer, larger plumes**, see Fernandez (2015).

However, in 2D this progress is **very rapid**.

These larger plumes allow **neutrino heating** to do work on the shock.



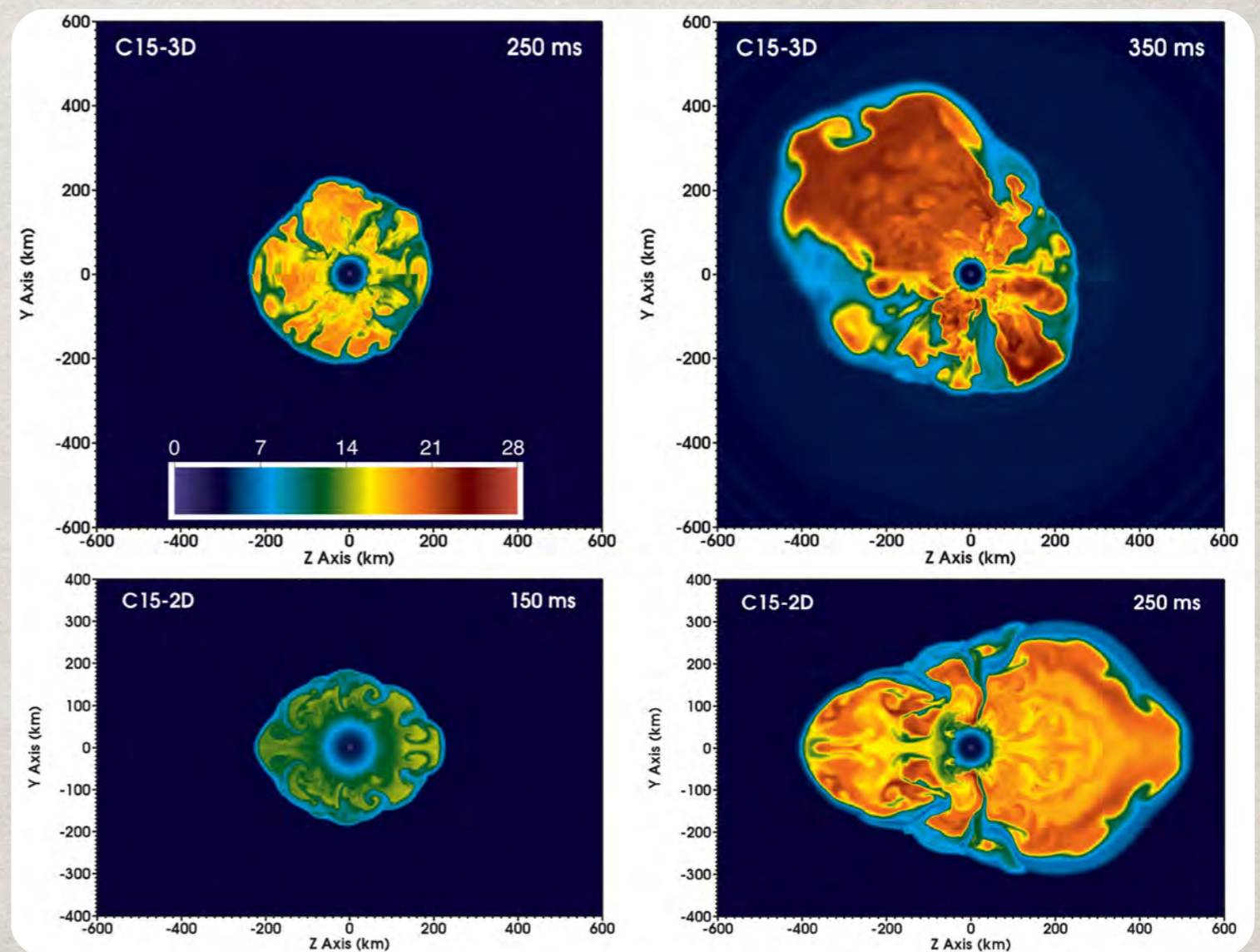
# RAYLEIGH-TAYLOR VS TURBULENCE

The [Rayleigh-Taylor Instability](#), driven in CCSN by neutrino heating, favors large scale plumes, regardless of dimensionality.

In 2D, the [turbulent cascade](#) also favors organizing small scale motion into larger scale flows.

However, in 3D, the cascade favors [tearing apart large scale flows](#).

Thus in 3D, without the assistance of the cascade, R-T requires [more heating](#), and hence [more time](#), to develop.

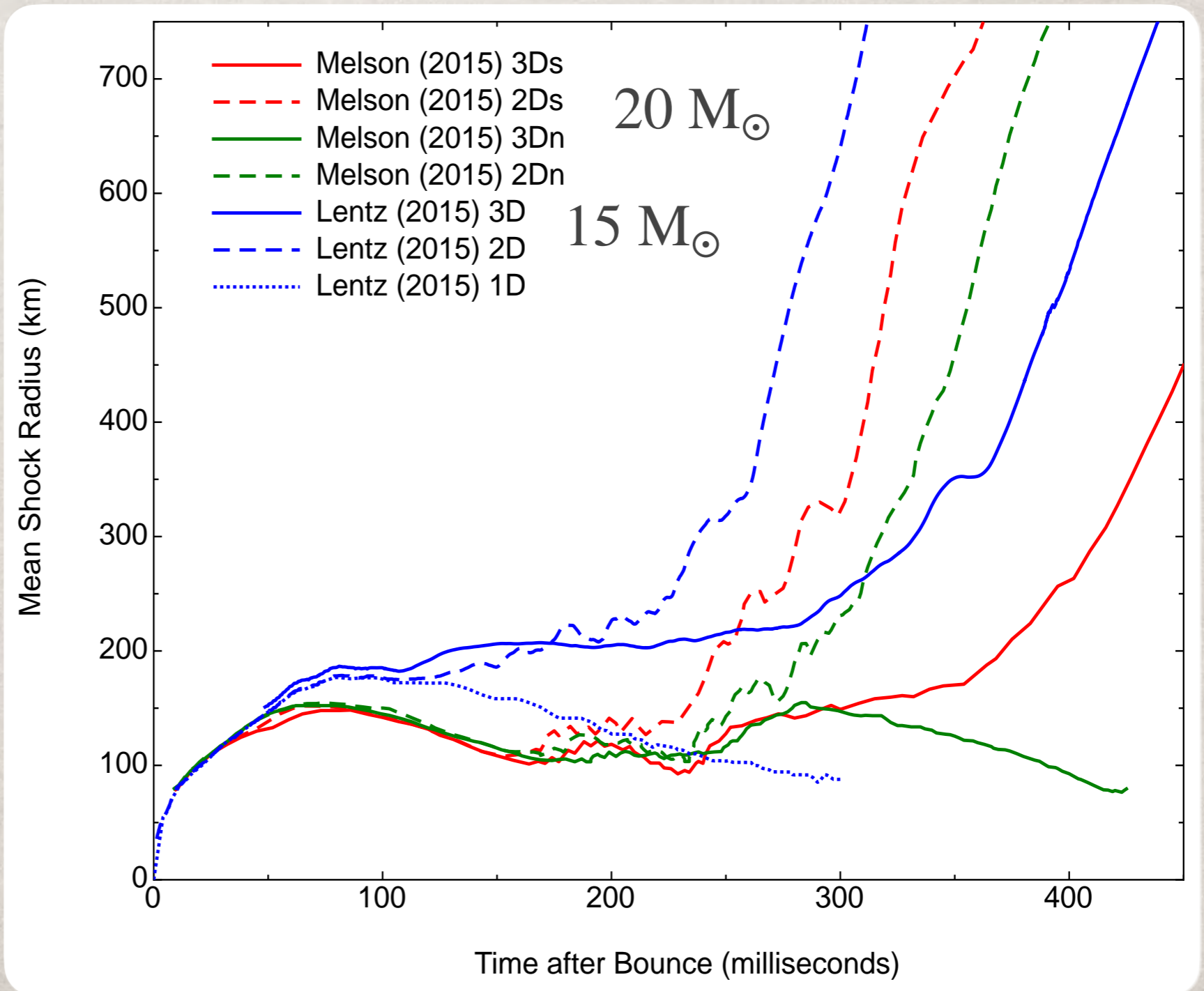


# 3D DELAYS

In both 2D and 3D, explosions are preceded by the development of **large scale convective flows** that span the heating region.

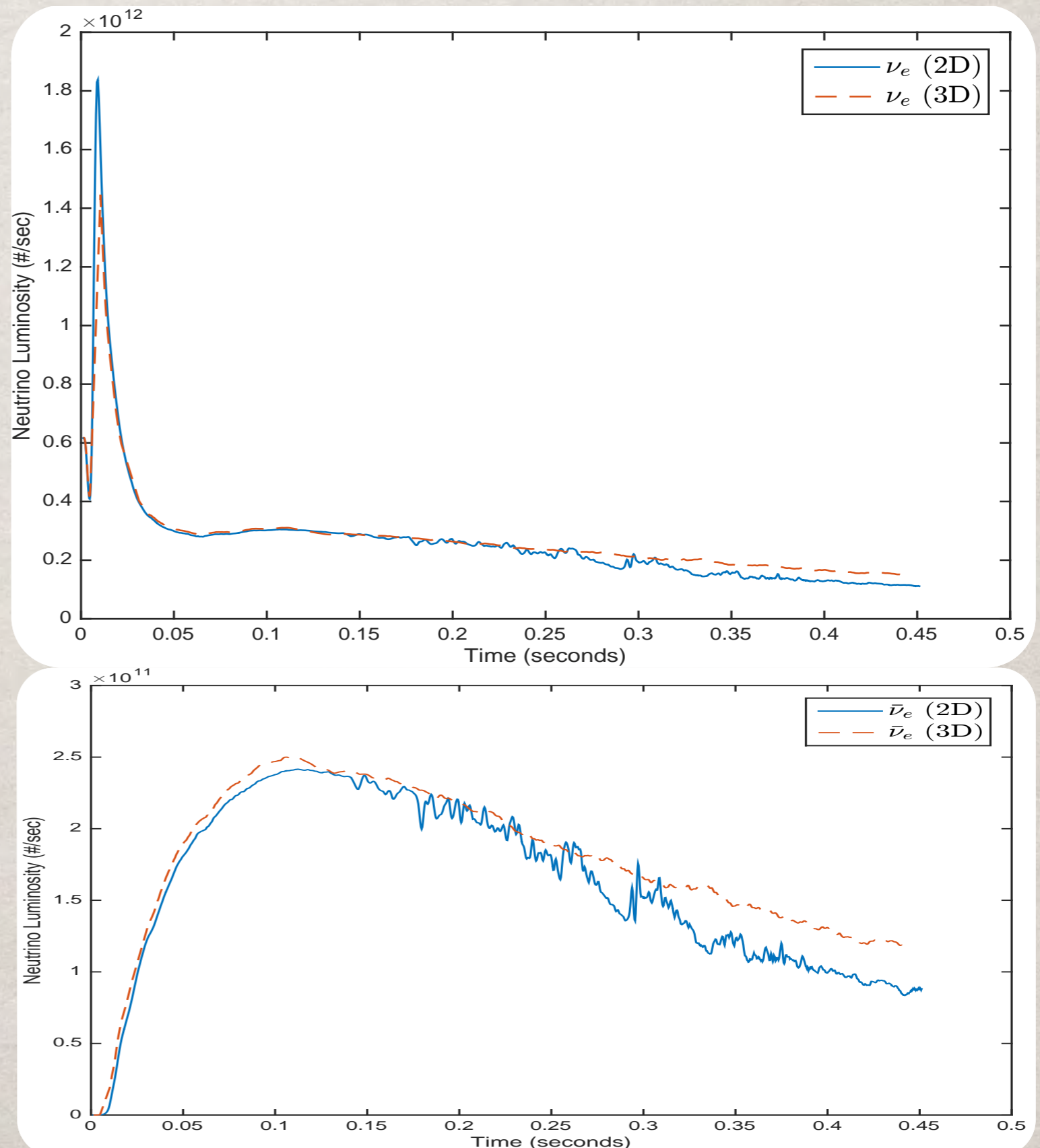
Consensus is that in 2D models the convective plumes develop too rapidly, leading to an **earlier onset of explosion**.

Understanding the complete effects of 3D will require models that **exceed a second** in supernova time.



# 3D (IN) VARIABILITY

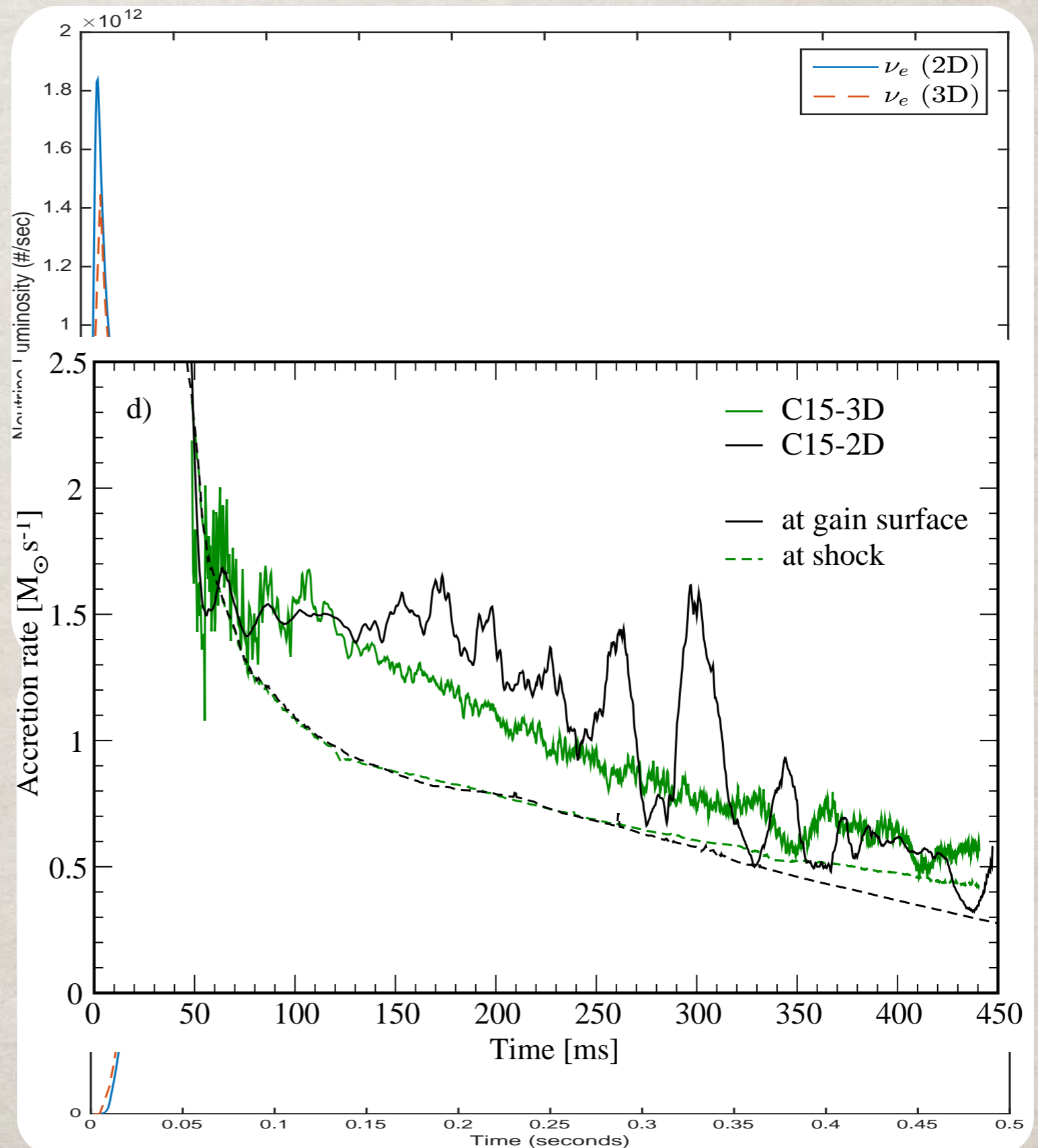
One fascinating difference between 2D and 3D is the strong **reduction in variability** in the 3D models.



# 3D (IN) VARIABILITY

One fascinating difference between 2D and 3D is the strong **reduction in variability** in the 3D models.

In place of the **single downflow** often seen in 2D, accretion in 3D flows more paths and is therefore steadier.

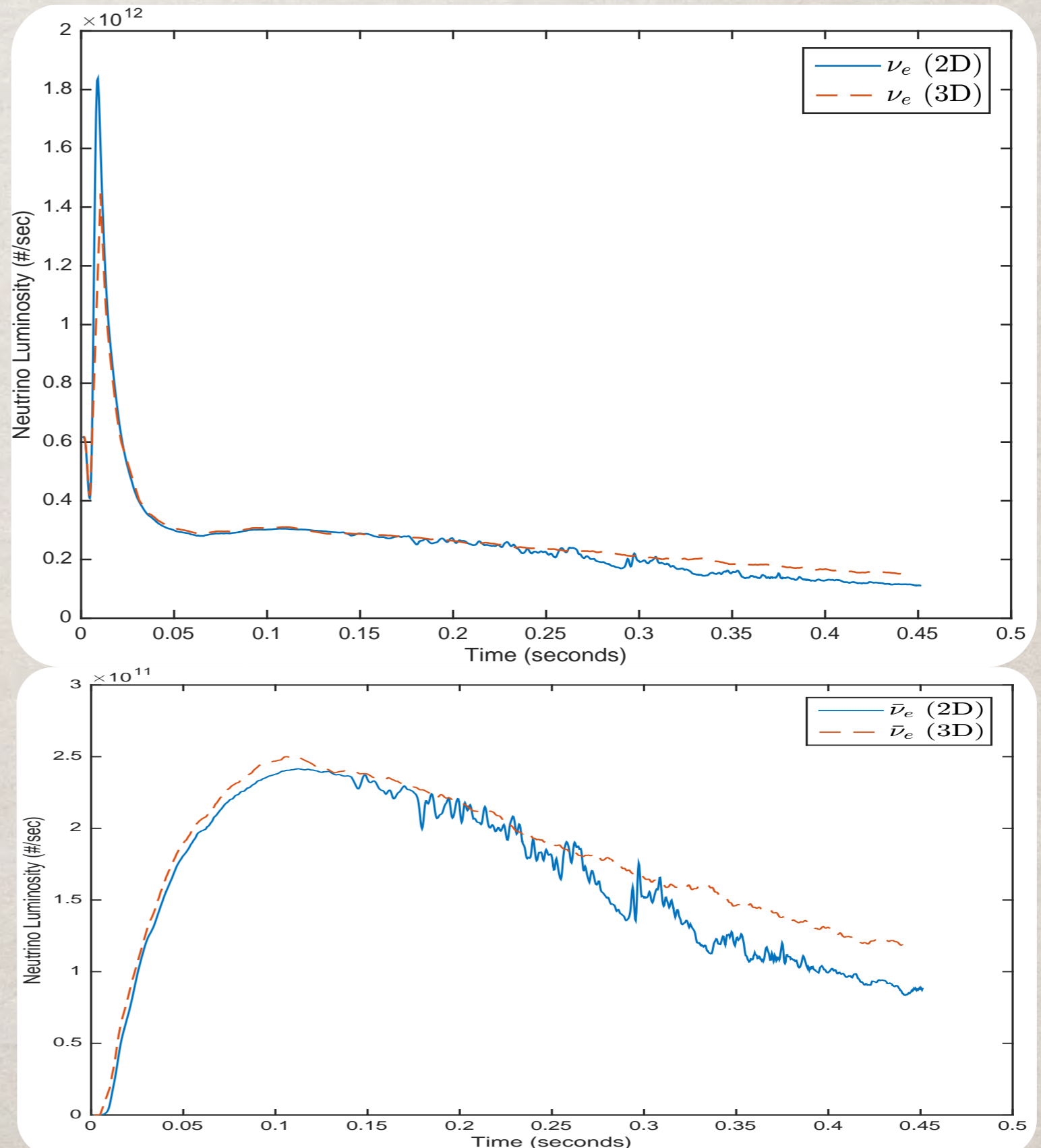


# 3D (IN) VARIABILITY

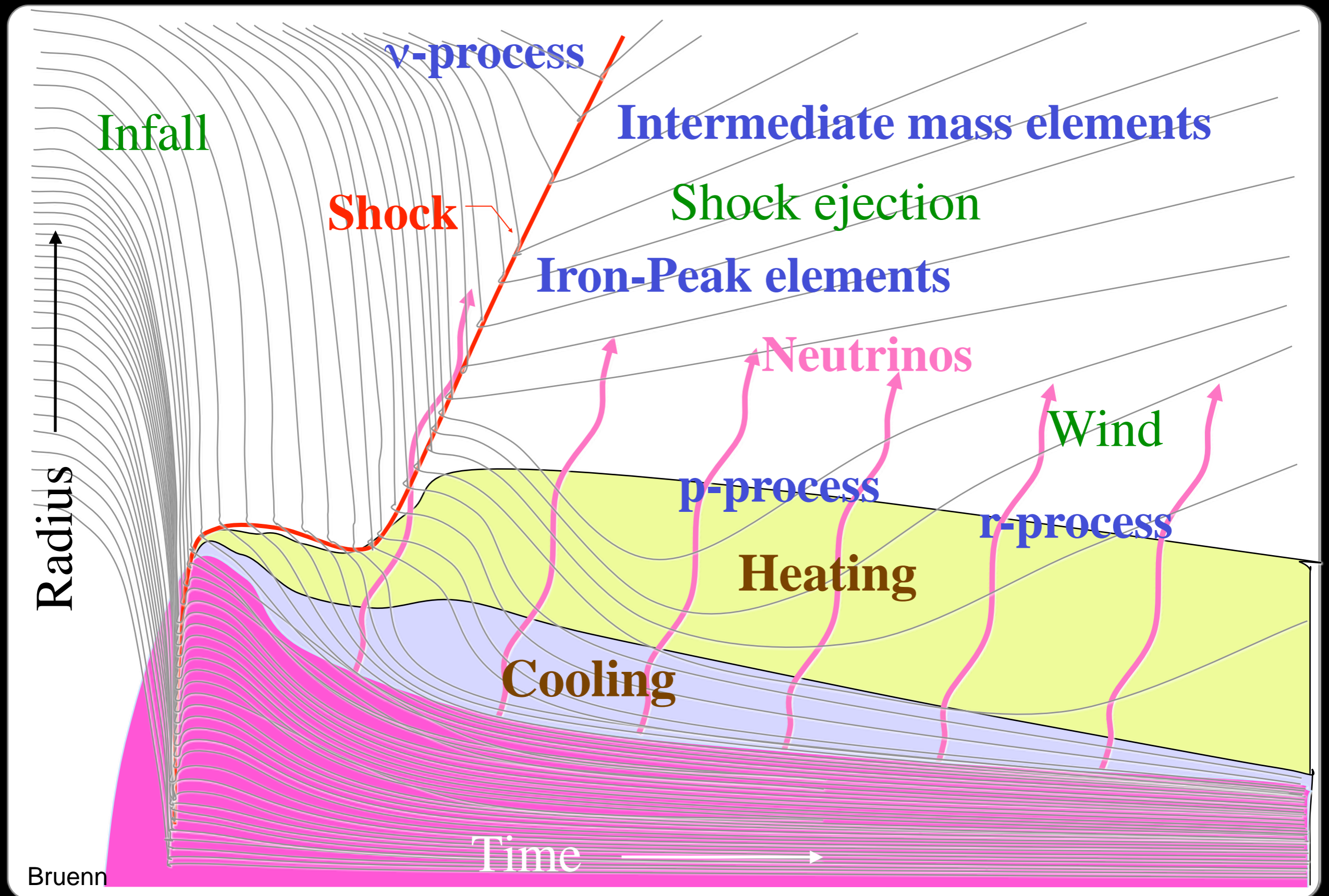
One fascinating difference between 2D and 3D is the strong **reduction in variability** in the 3D models.

In place of the **single downflow** often seen in 2D, accretion in 3D flows more paths and is therefore steadier.

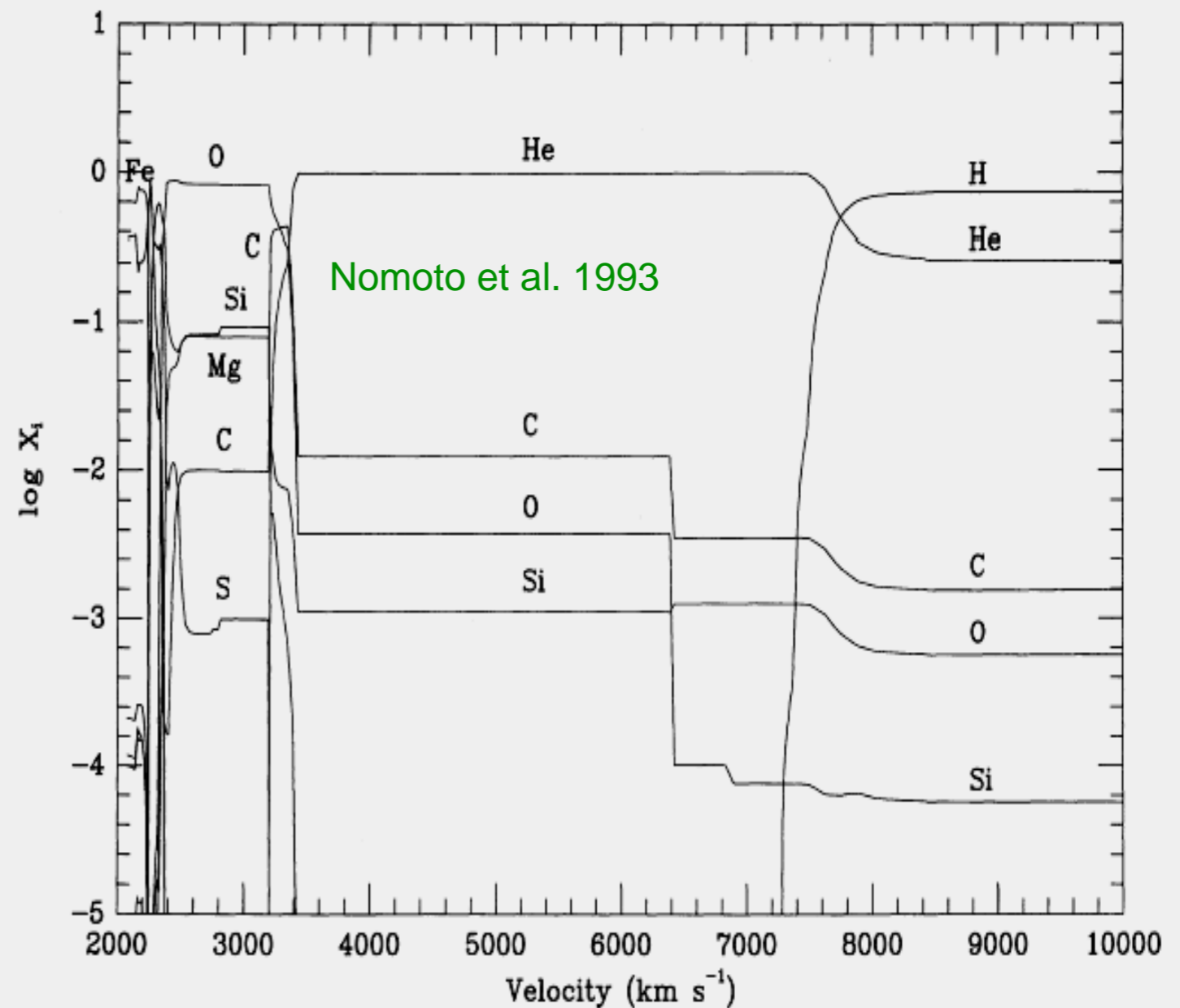
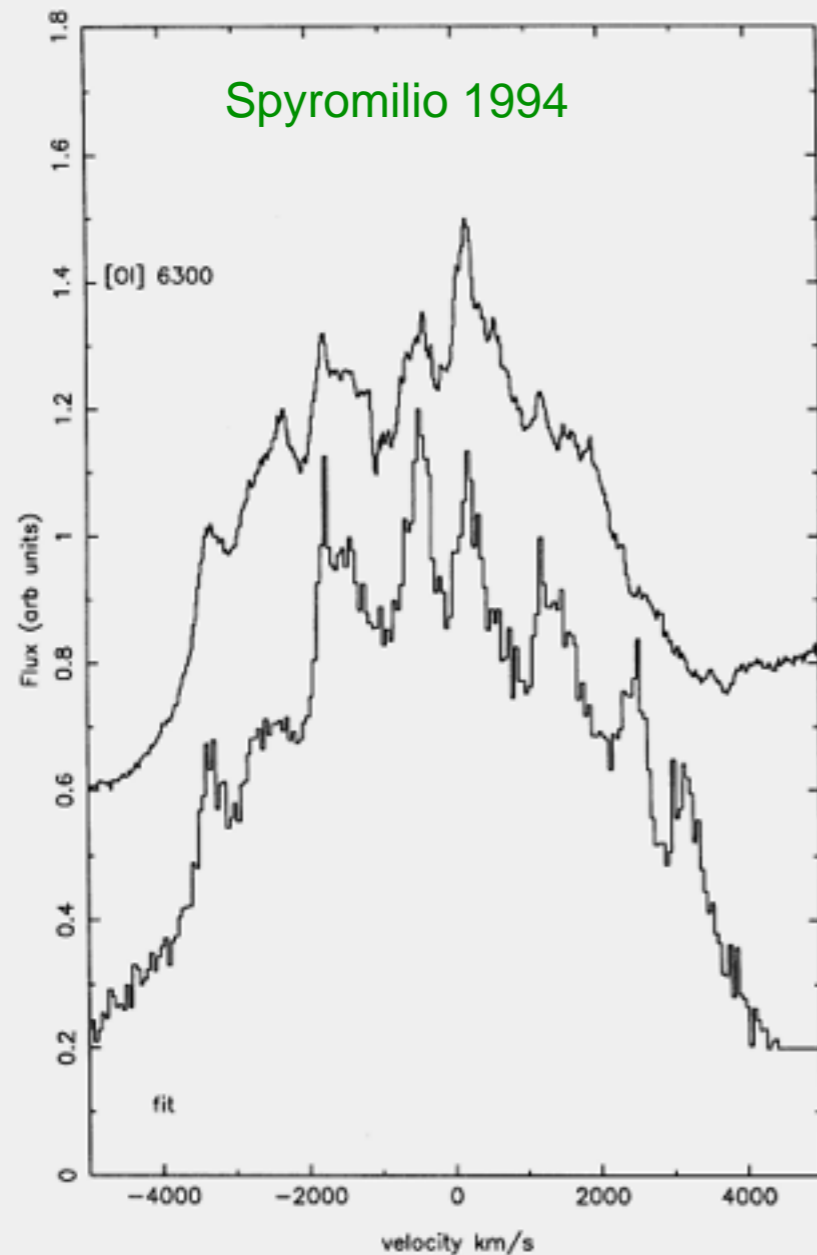
**Timing of explosion** is also evident in the 2D model, but less so (at least thus far) in the 3D model.



# SUPERNOVA NUCLEOSYNTHESIS



# TUNING THE EXPLOSION



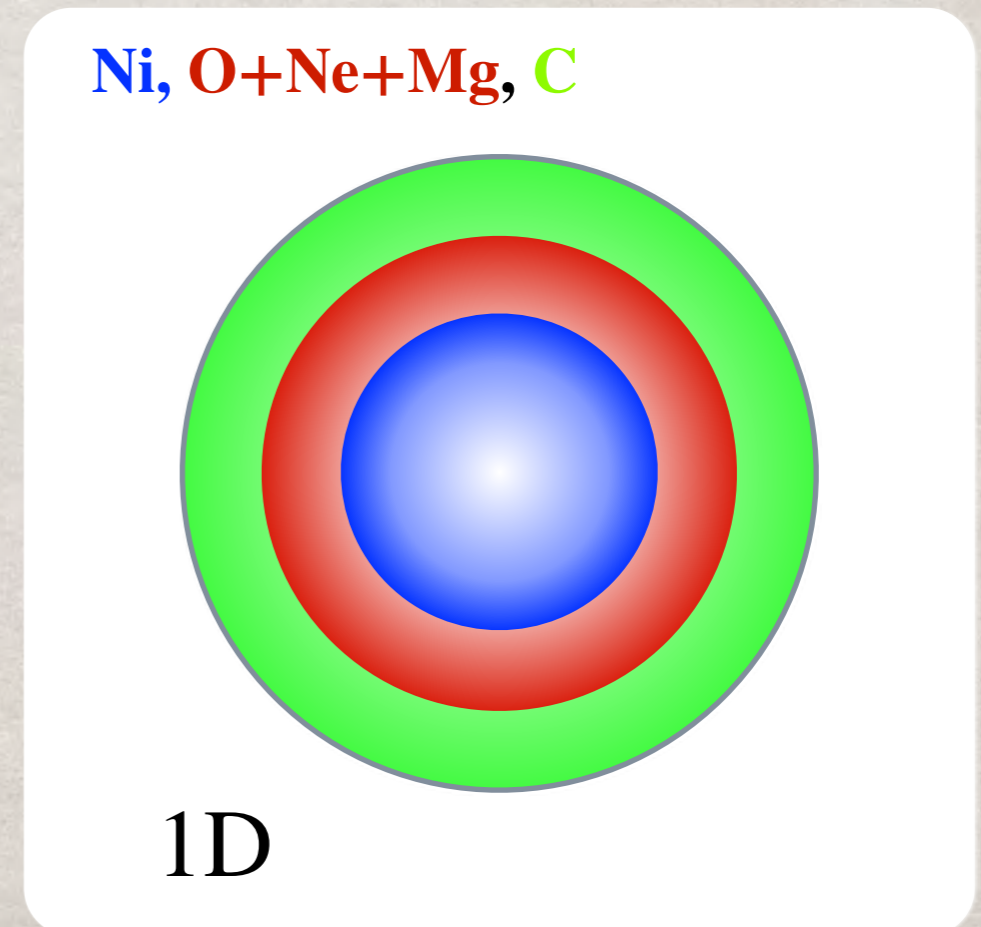
In parameterized nucleosynthesis models, 2 parameters, the **Bomb/Piston energy** and the **mass cut**, are constrained by observations of **explosion energy** and mass of  $^{56}\text{Ni}$  ejected.

# UNLEARN THE ONION

Observations tell us that the explosion, and the ejected elements, are **asymmetric**. Yet we rely on spherically symmetric models to understand supernova nucleosynthesis.



≠



# UNLEARN THE ONION

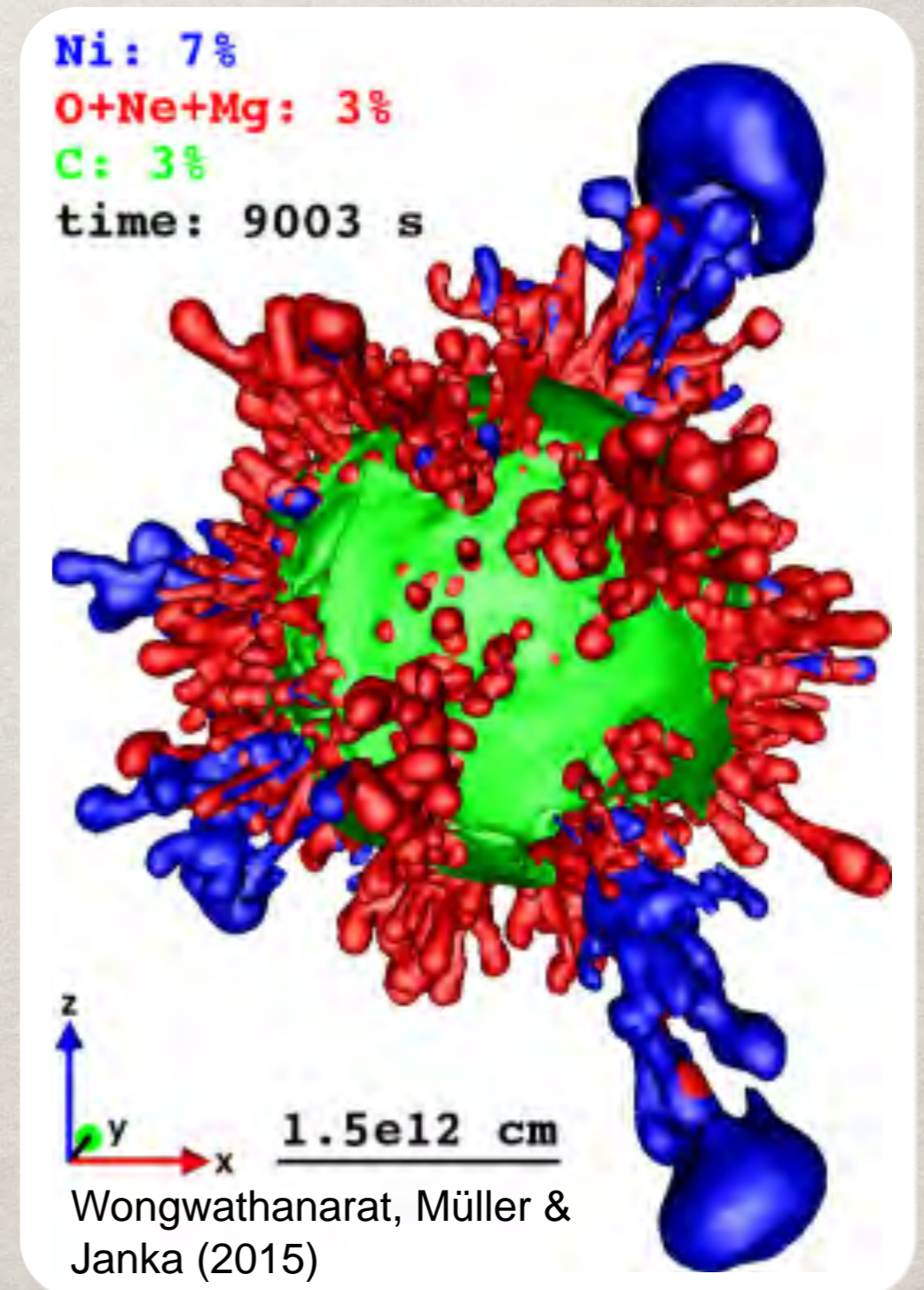
Observations tell us that the explosion, and the ejected elements, are **asymmetric**. Yet we rely on spherically symmetric models to understand supernova nucleosynthesis.

This colors our discussion, for example the notion that the **matter created closest to the neutron star** is most sensitive to the “**mass cut**”.



?

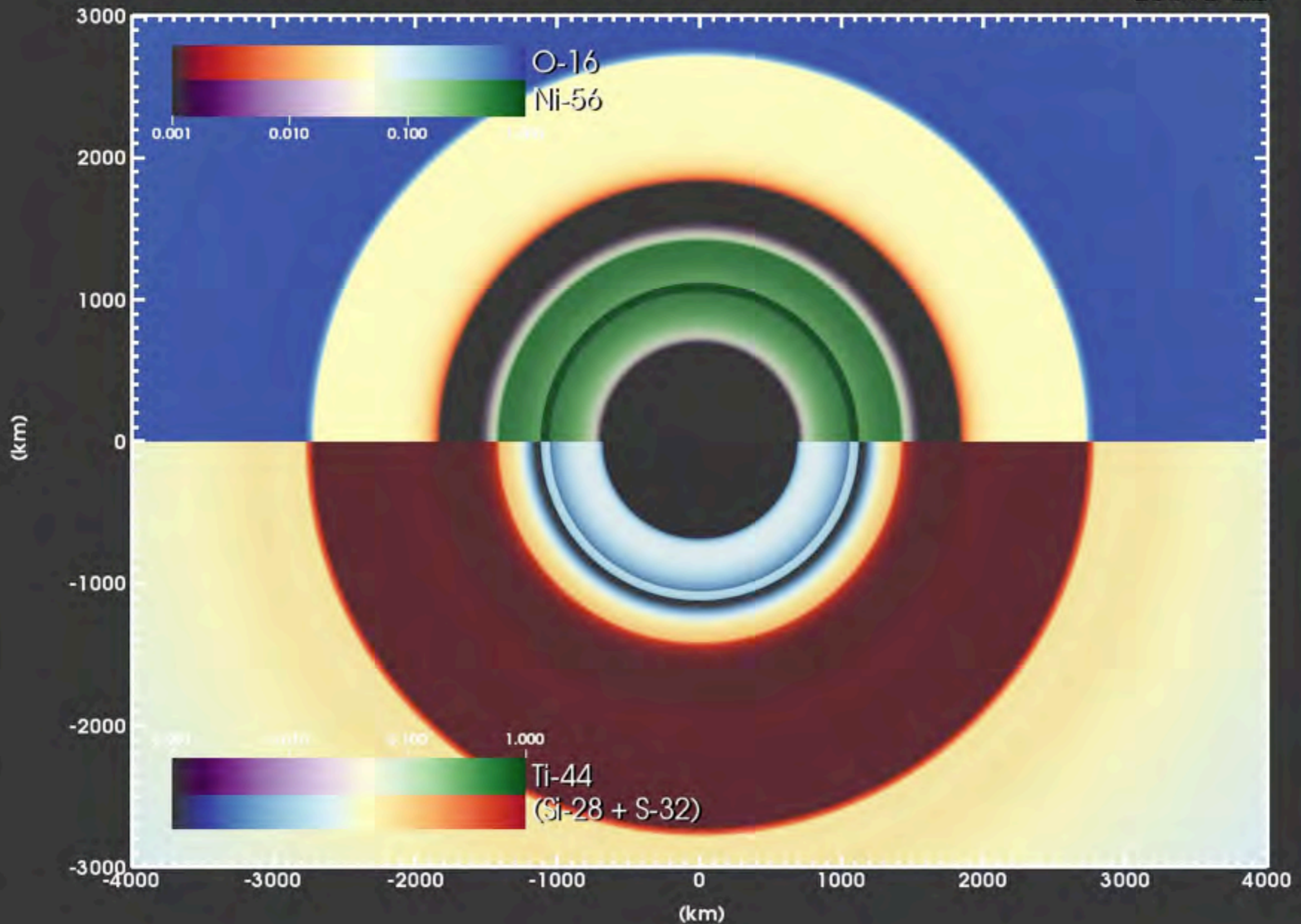
=



# NUCLEOSYNTHESIS: THE MOVIE

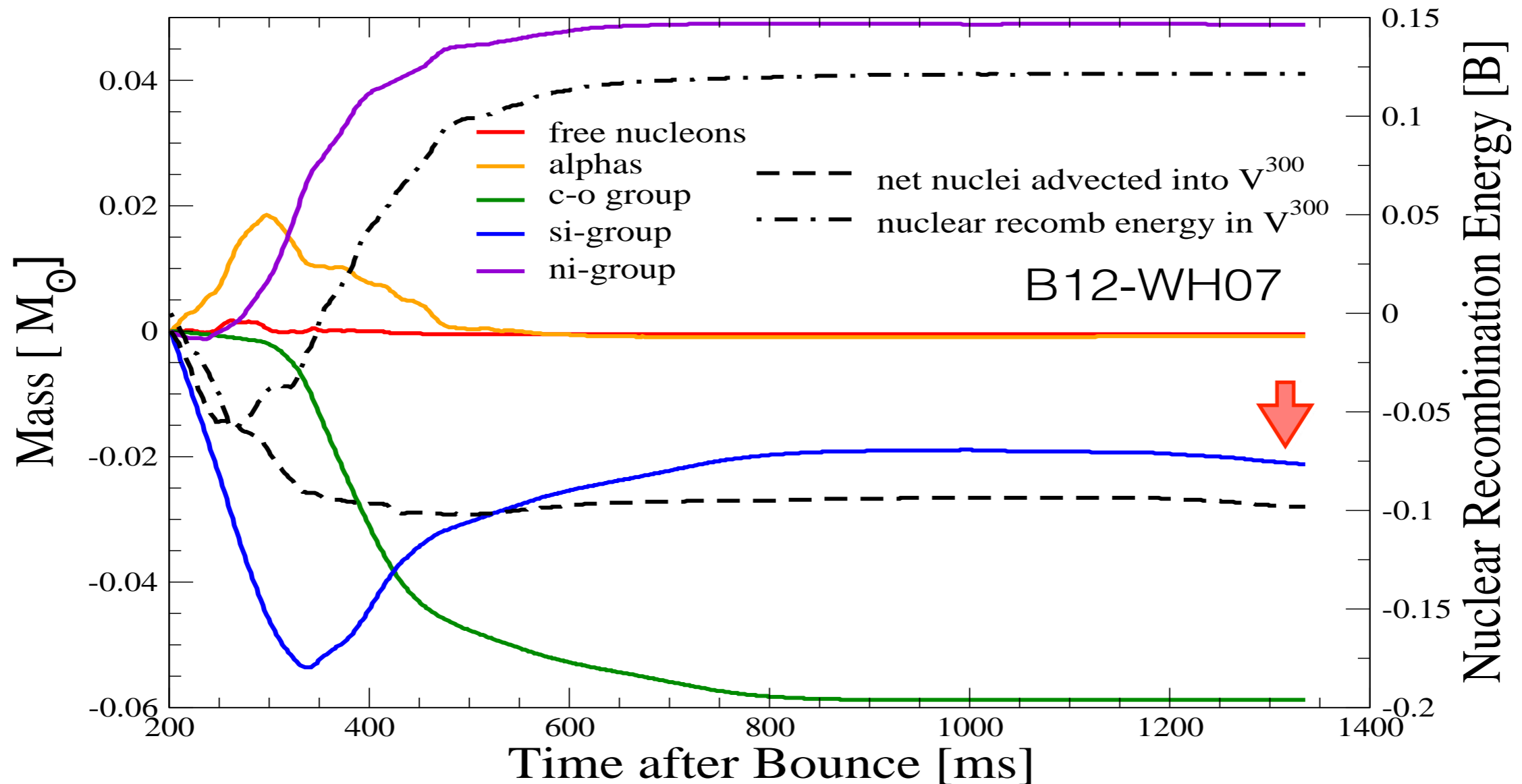
Chimera model: B12-WH07

-258.2 ms



# FINISHED COOKING?

By 800–900 ms after bounce, **shock burning** in the  $12 M_{\odot}$  model is **nearly complete** with shock temperature  $\sim 2$  GK.



Matter continues to **fall inward** of 300 km beyond one second, predominantly from cut-off down flows.

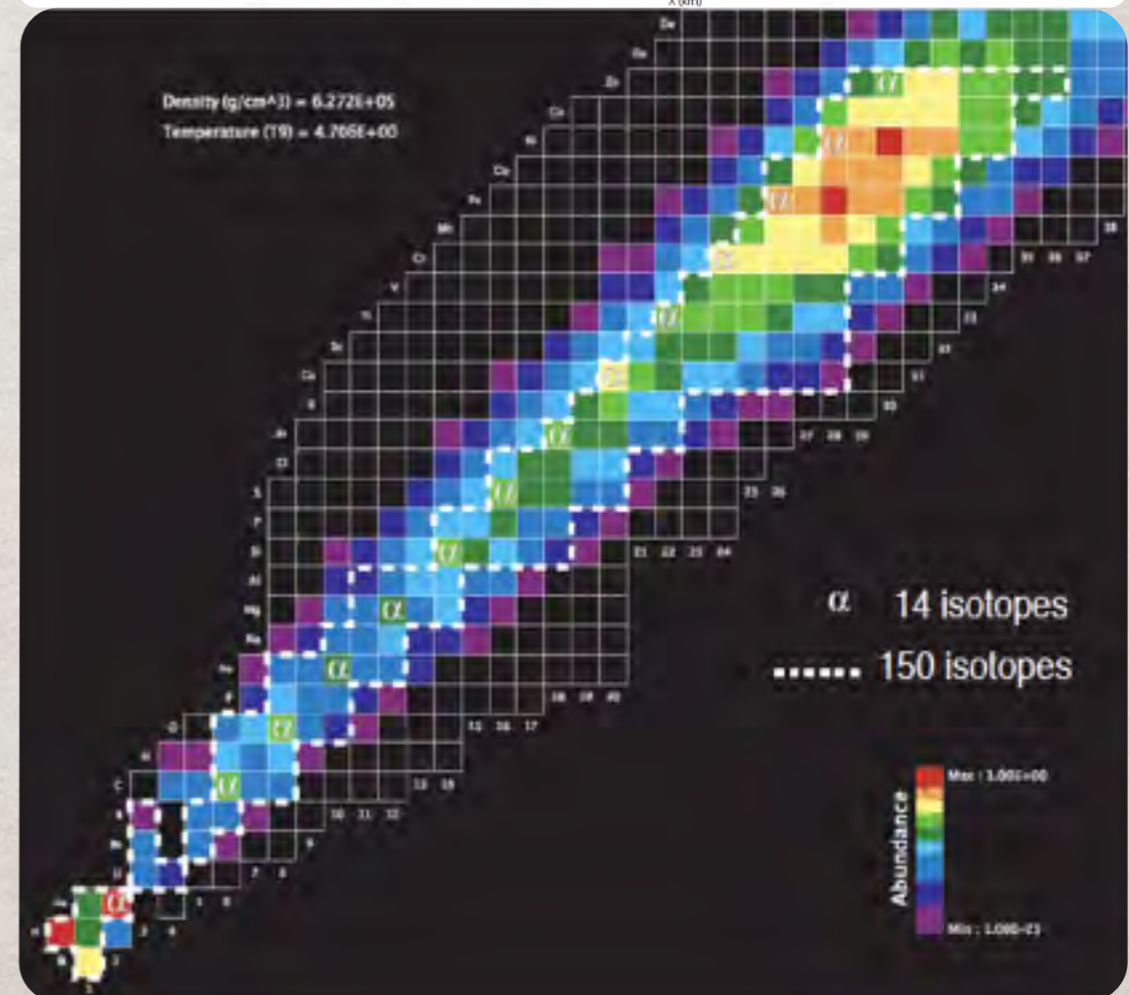
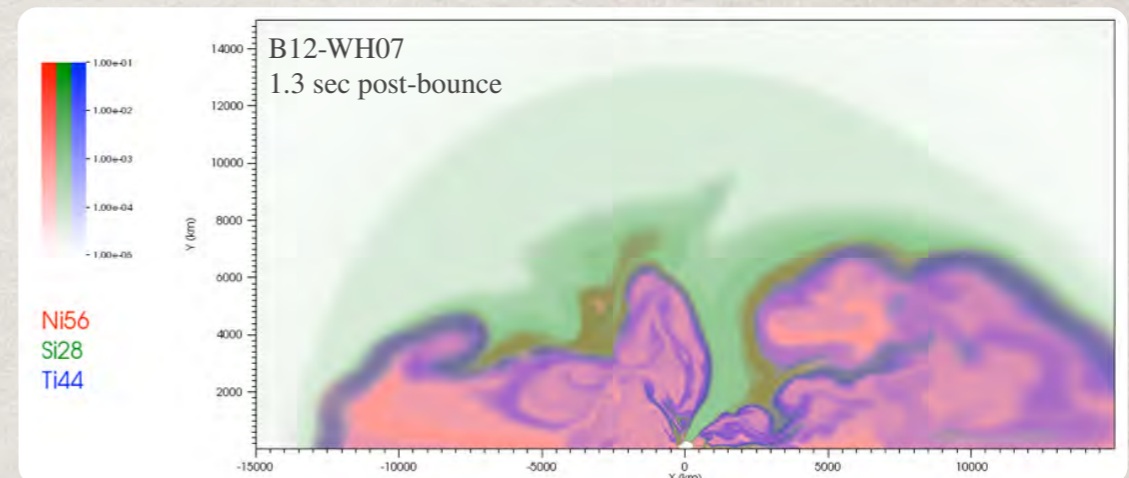
# NUCLEOSYNTHESIS LIMITS

We can calculate nucleosynthesis directly with the  $\alpha$ -network (plus neutrons, protons and auxiliary heavy) in CHIMERA.

As the mass cut resolves, we can examine the nucleosynthesis with **increasing accuracy**.

But parameterized models consider **hundreds** (or even thousands) of **species** within the supernova simulation.

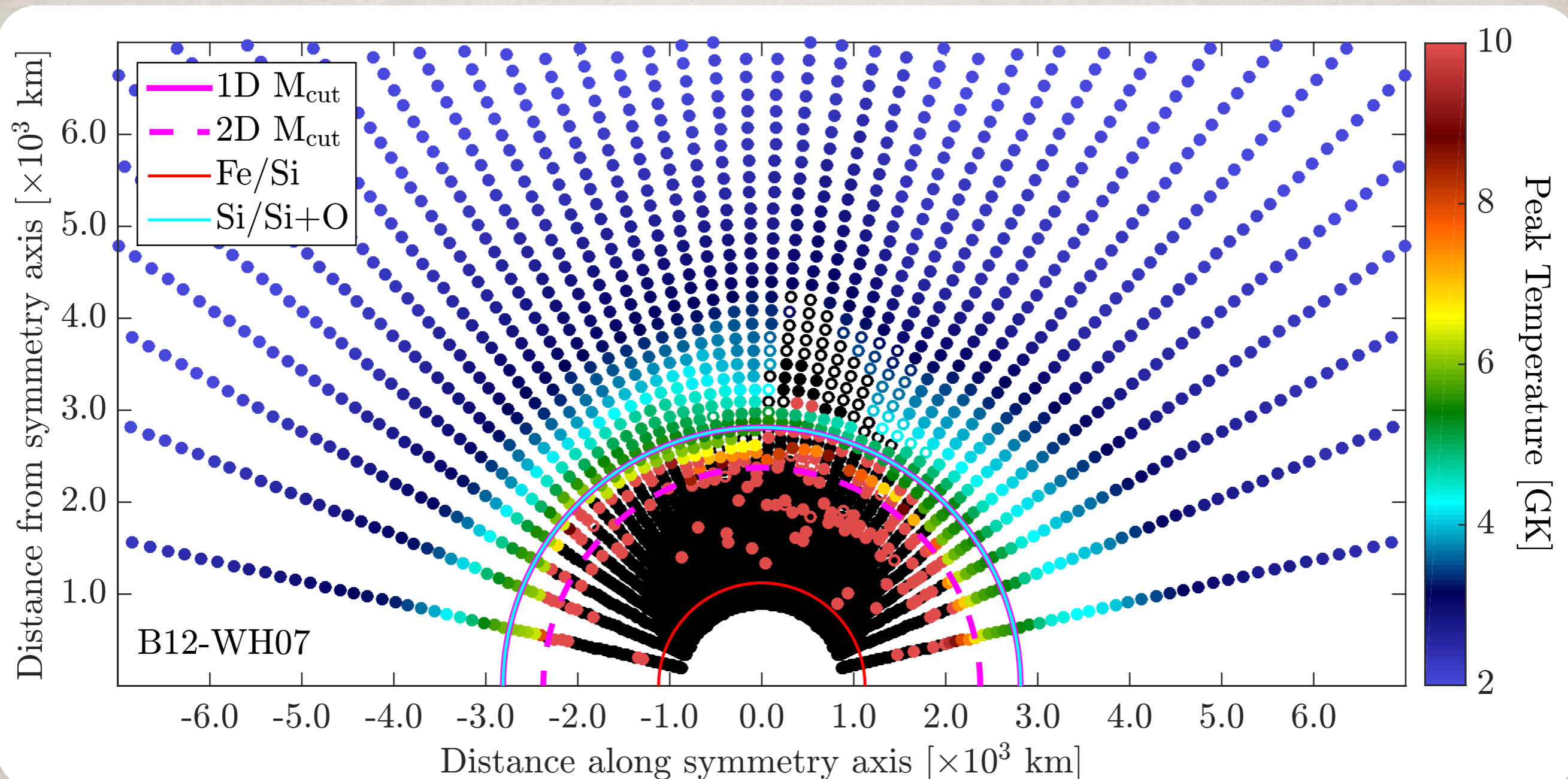
Doing the same in CHIMERA requires post-processing of Lagrangian tracer particles, or using a **larger network** within the supernova models.



# TRACING THE MASS CUT

Post-processing of **tracer particles** is required for nucleosynthesis predictions beyond the built-in network,  $\alpha$ -network or otherwise.

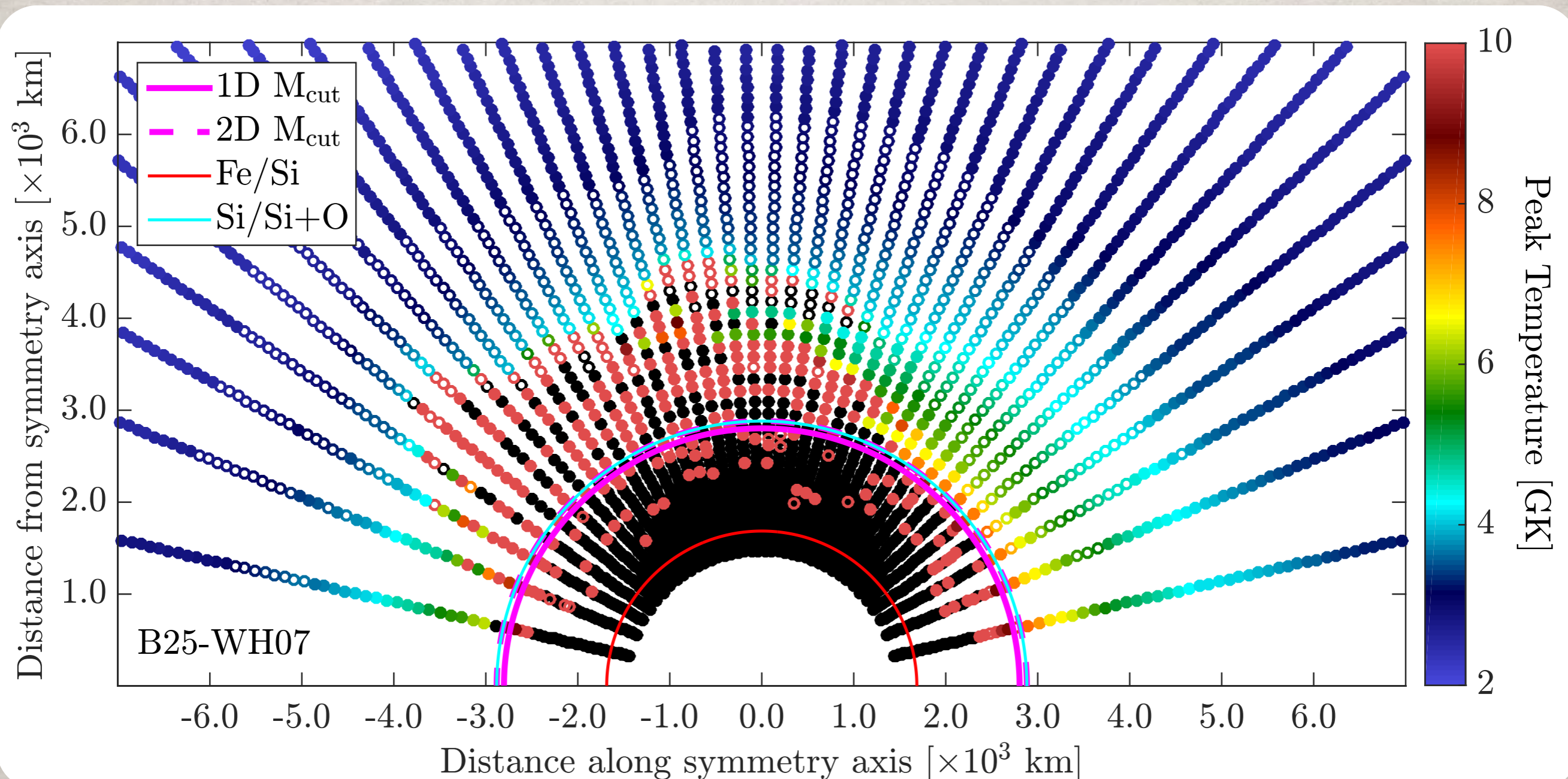
Their Lagrangian view also reveals the complexity of the **mass cut**.



# TRACING THE MASS CUT

Post-processing of **tracer particles** is required for nucleosynthesis predictions beyond the built-in network,  $\alpha$ -network or otherwise.

Their Lagrangian view also reveals the complexity of the **mass cut**.

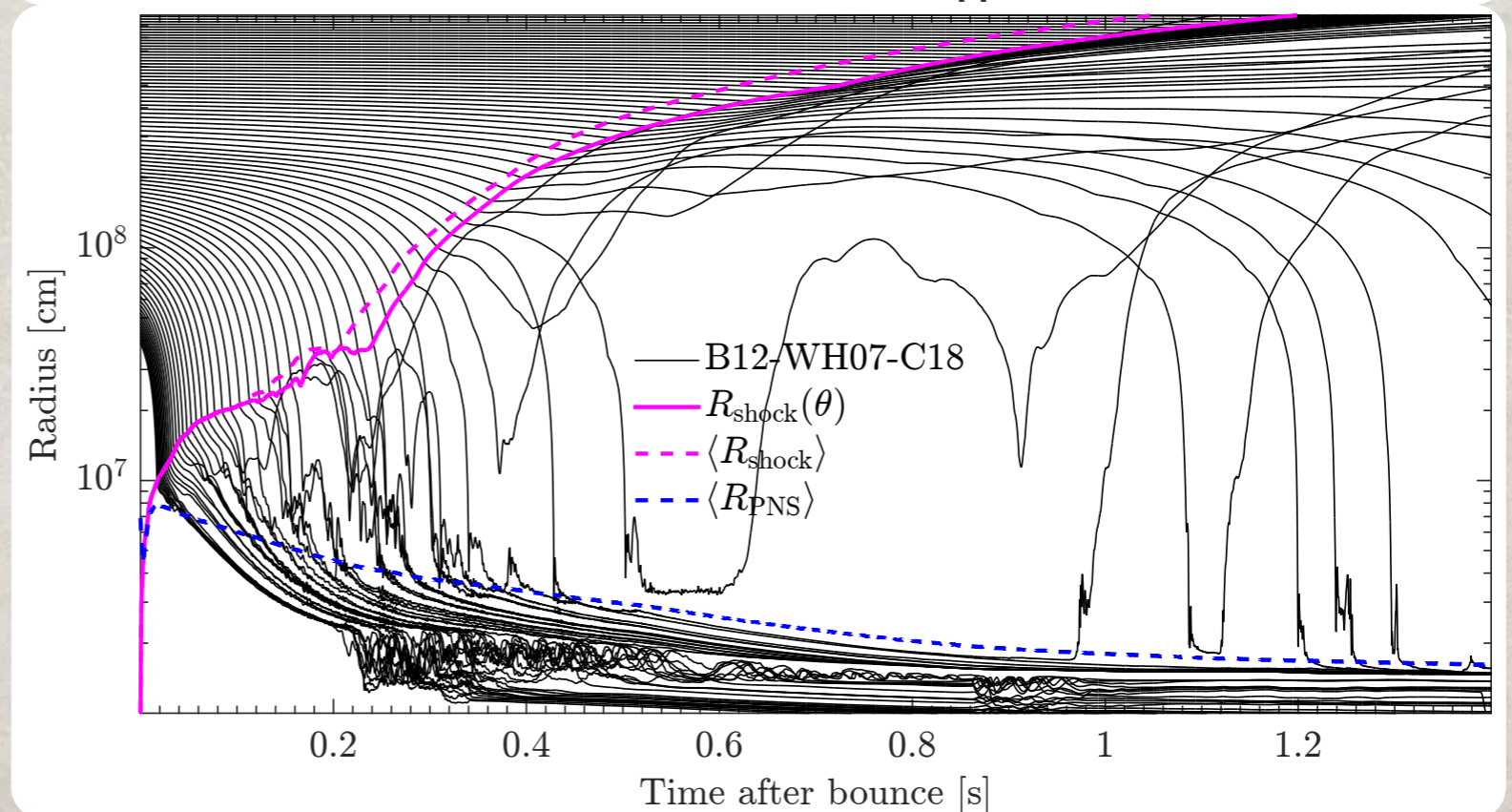
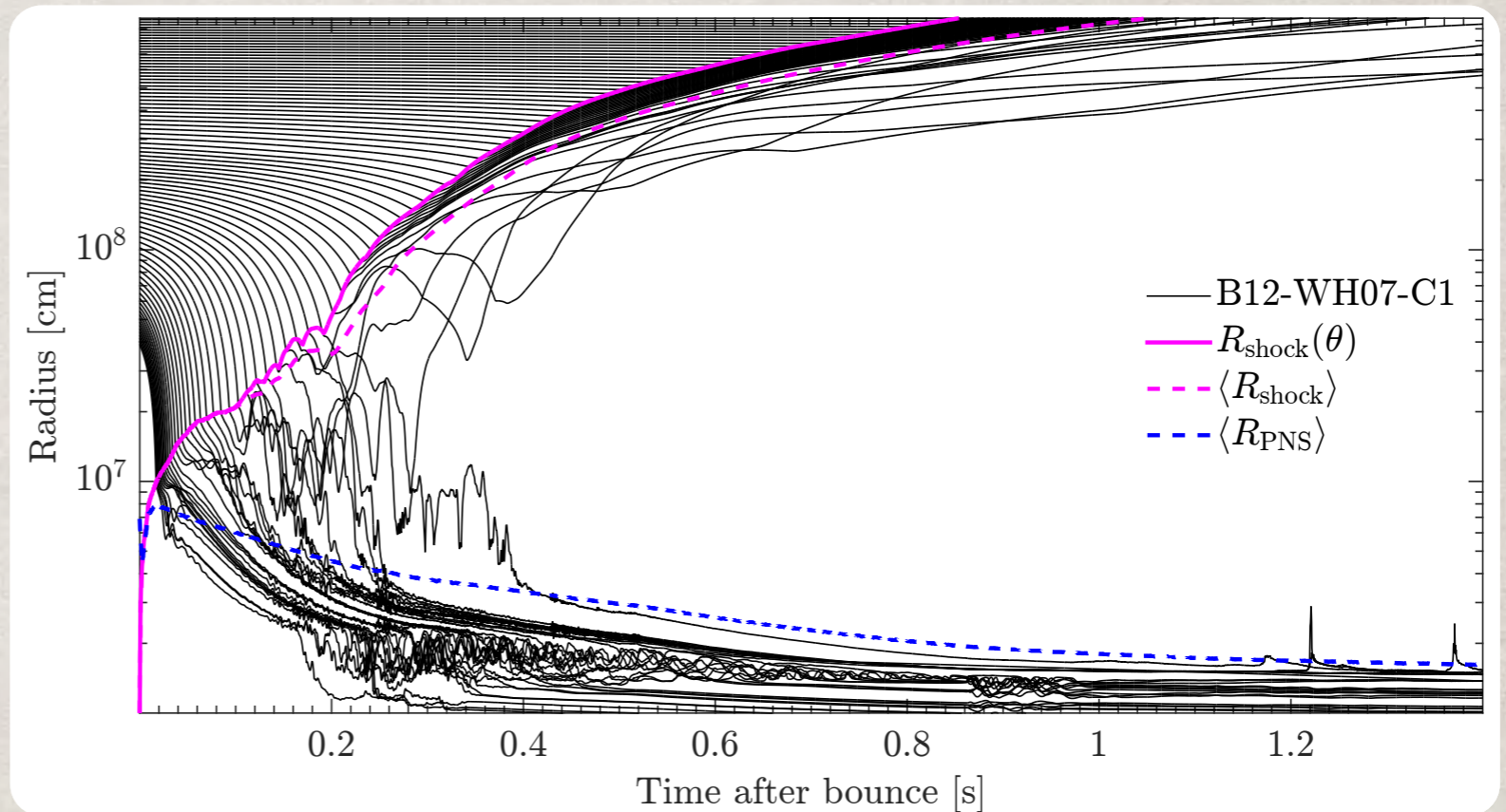


# LATITUDE DEPENDENCE

With 40 columns of tracers in each model, we can examine the fate of the star as a function of latitude.

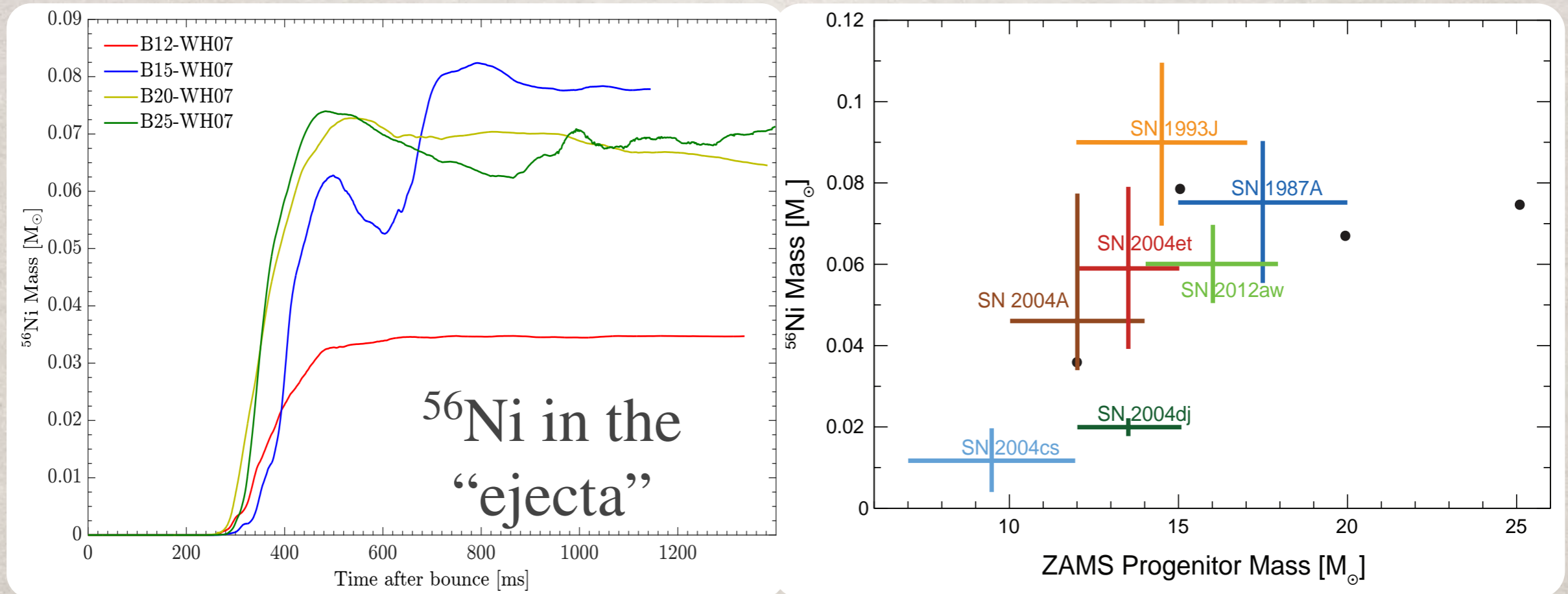
Near the pole, separation between ejecta and PNS develops rapidly and robustly.

Matter from near the equator continues to accrete and be ejected through the end of the simulations.



# NICKEL MASS

Beyond the explosion energy, perhaps the most important observable is the **mass of  $^{56}\text{Ni}$** , because of its relation to the light curve.



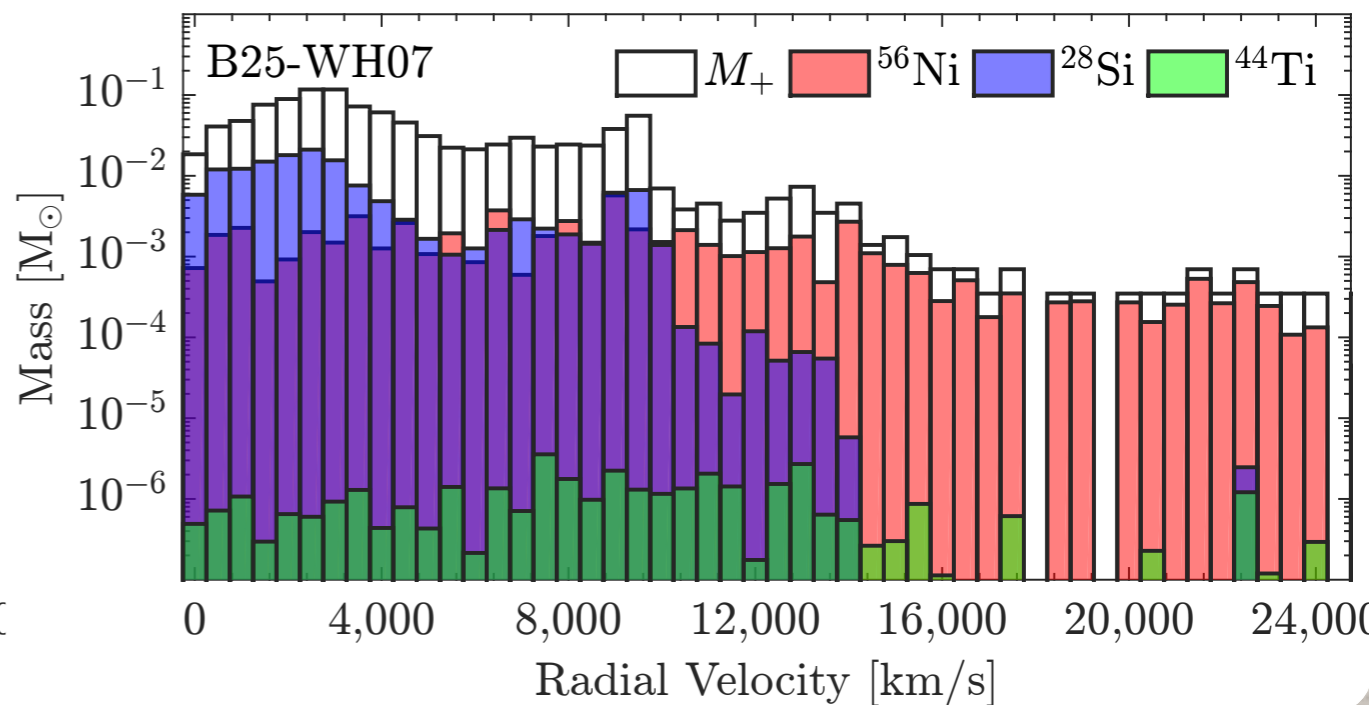
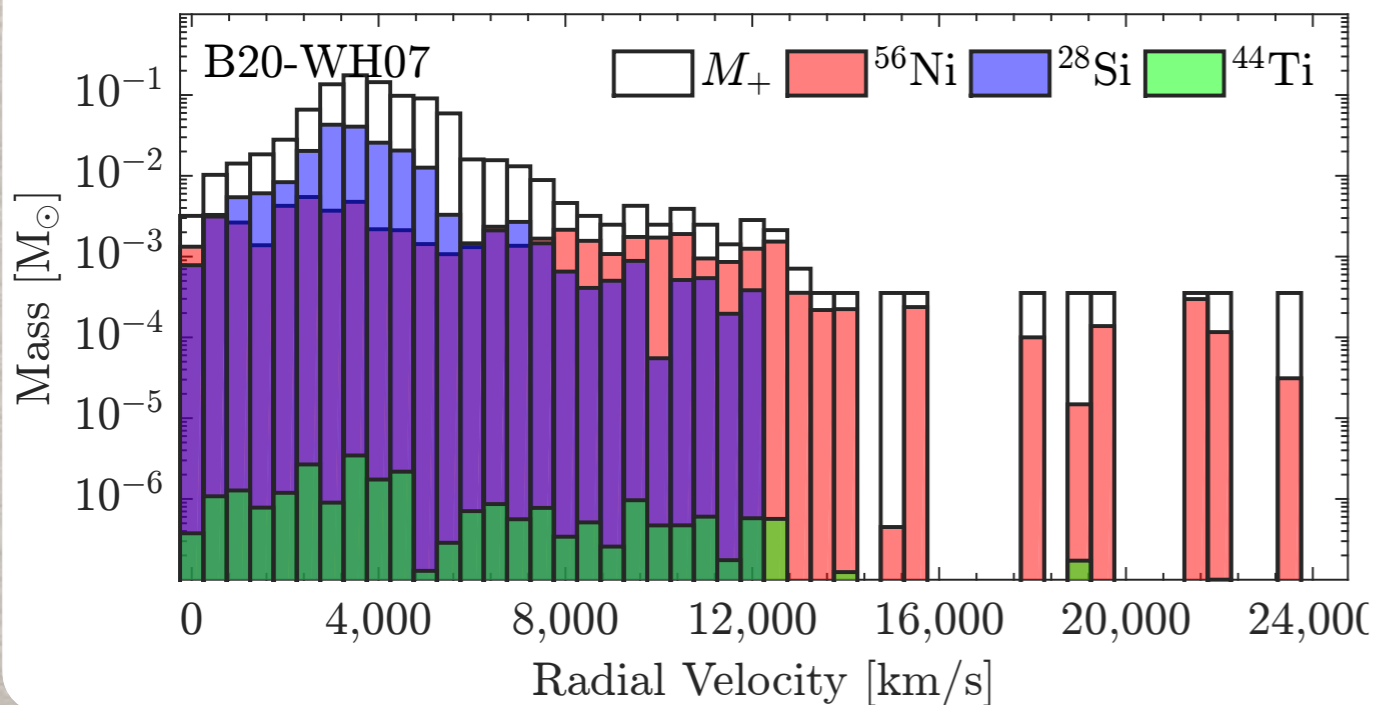
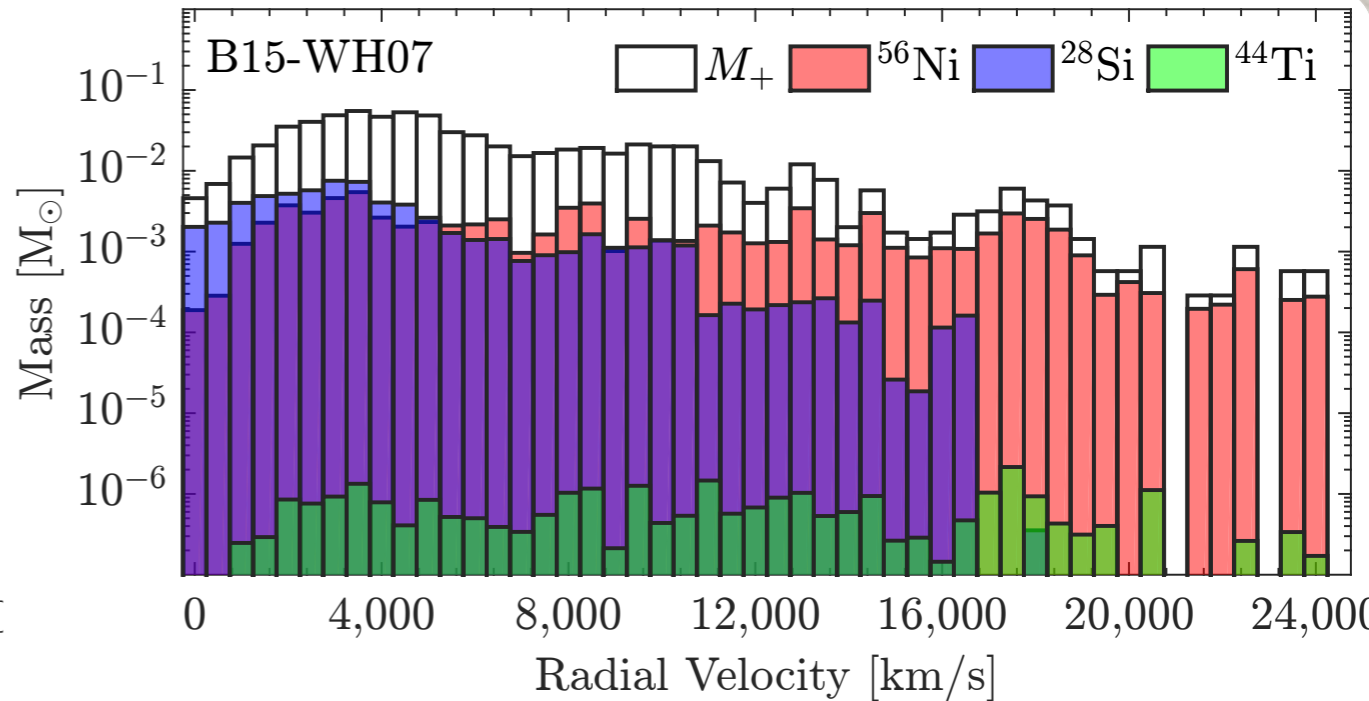
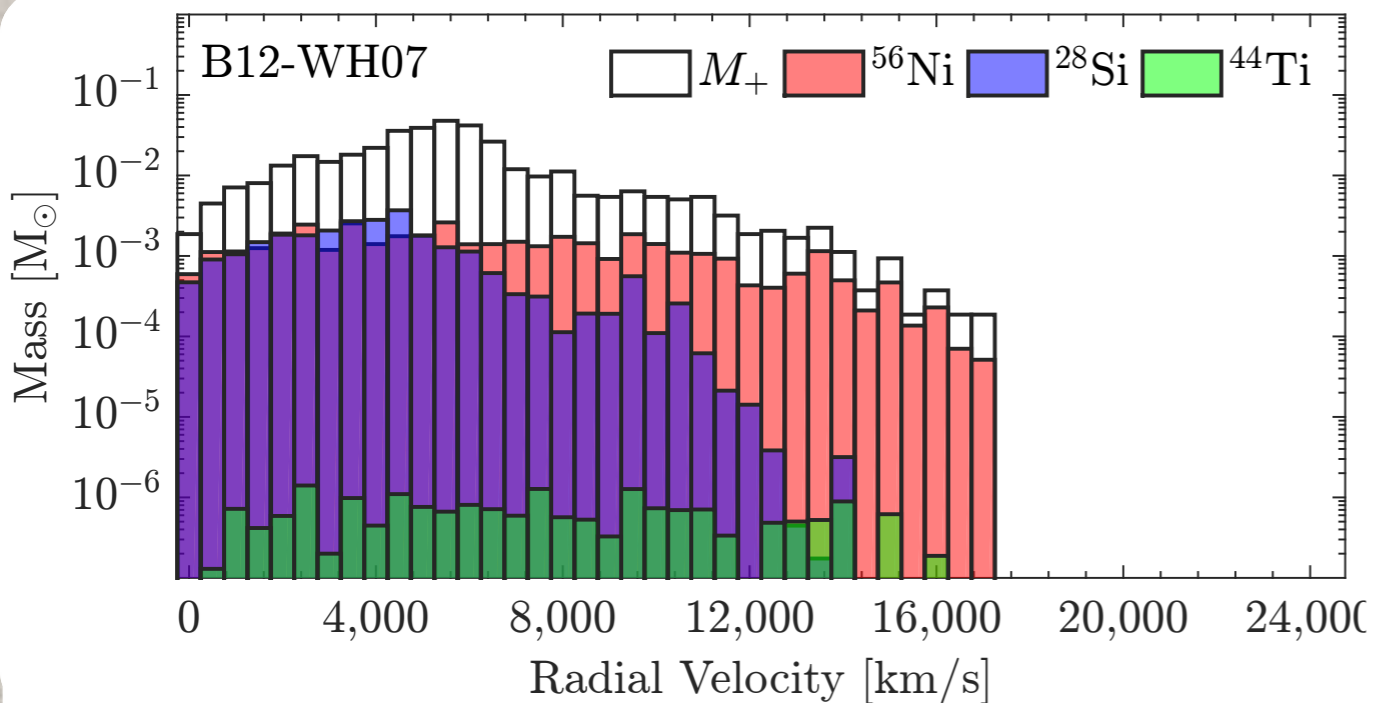
The ejected  $^{56}\text{Ni}$  mass **saturates in time** with the explosion energy.

Results are reasonable, when compared to **observations**.

**Fallback over longer timescales is uncertain.** Recent studies are finding differing results on fallback and  $^{56}\text{Ni}$  has higher velocity.

# VELOCITY DISTRIBUTION

Unlike 1D, **Nickel** and **Titanium** have higher velocities than **Silicon** and Oxygen, thus they are not preferentially sensitive to fallback.

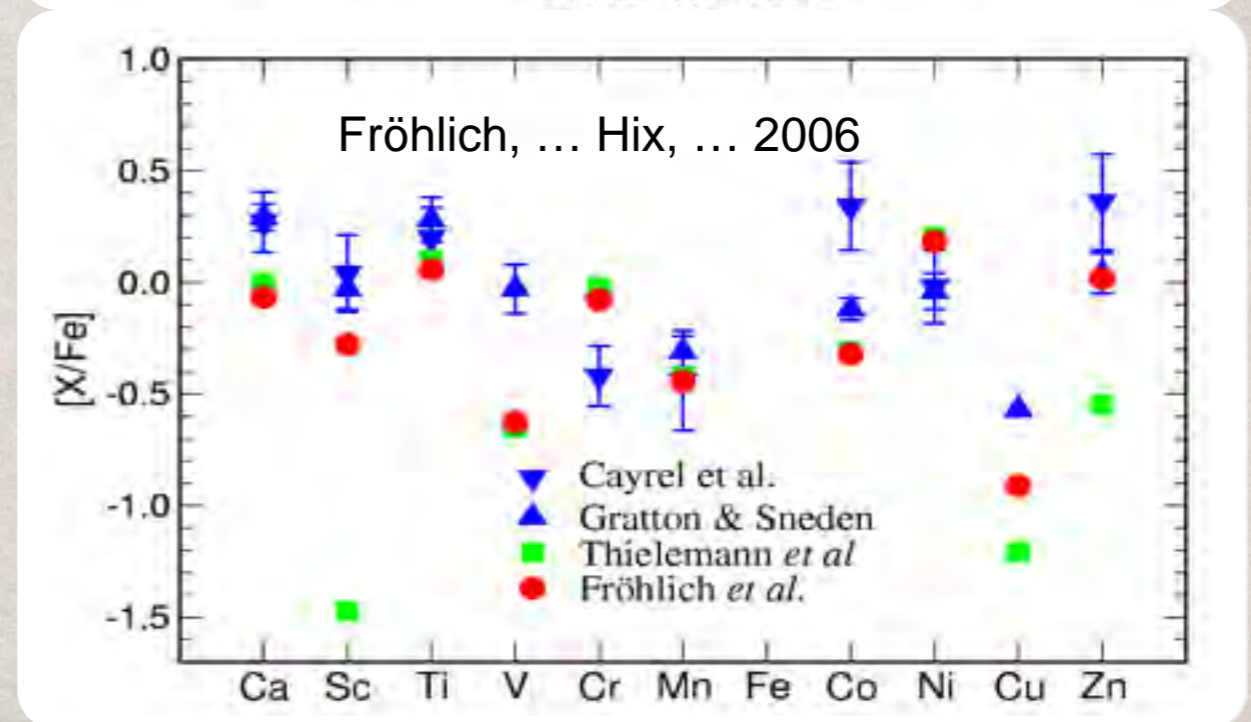
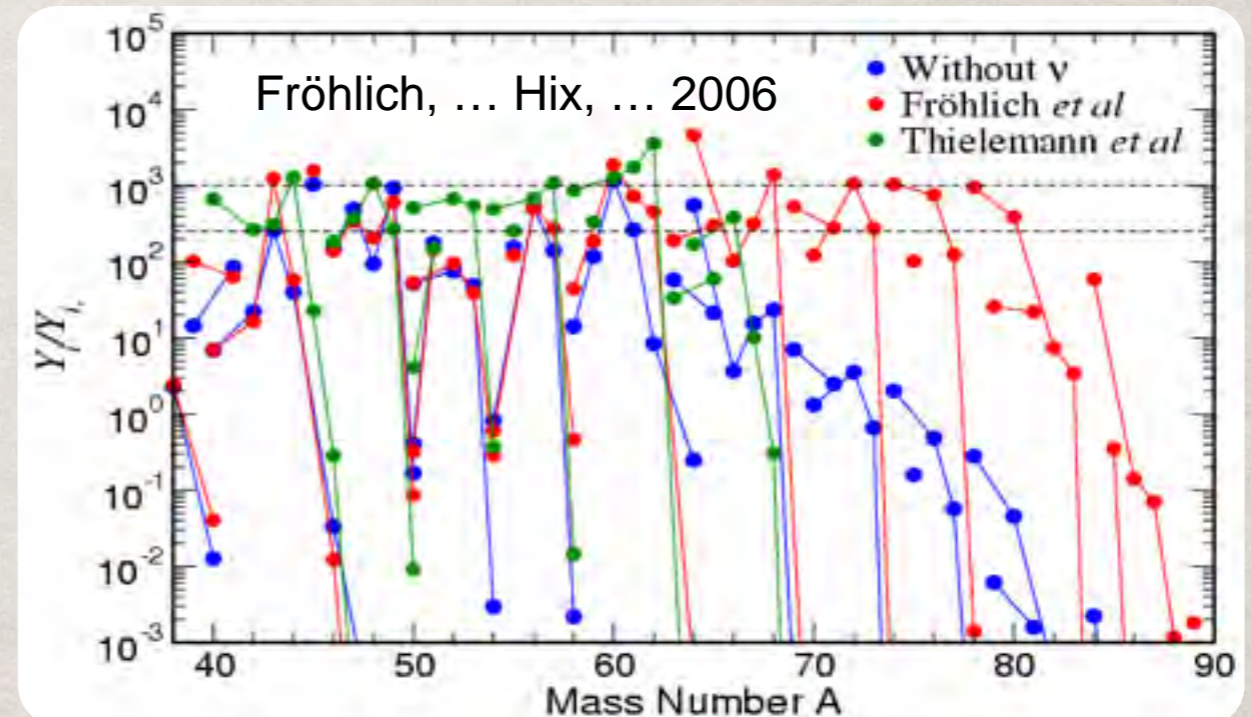


# NEUTRINOS & NUCLEOSYNTHESIS

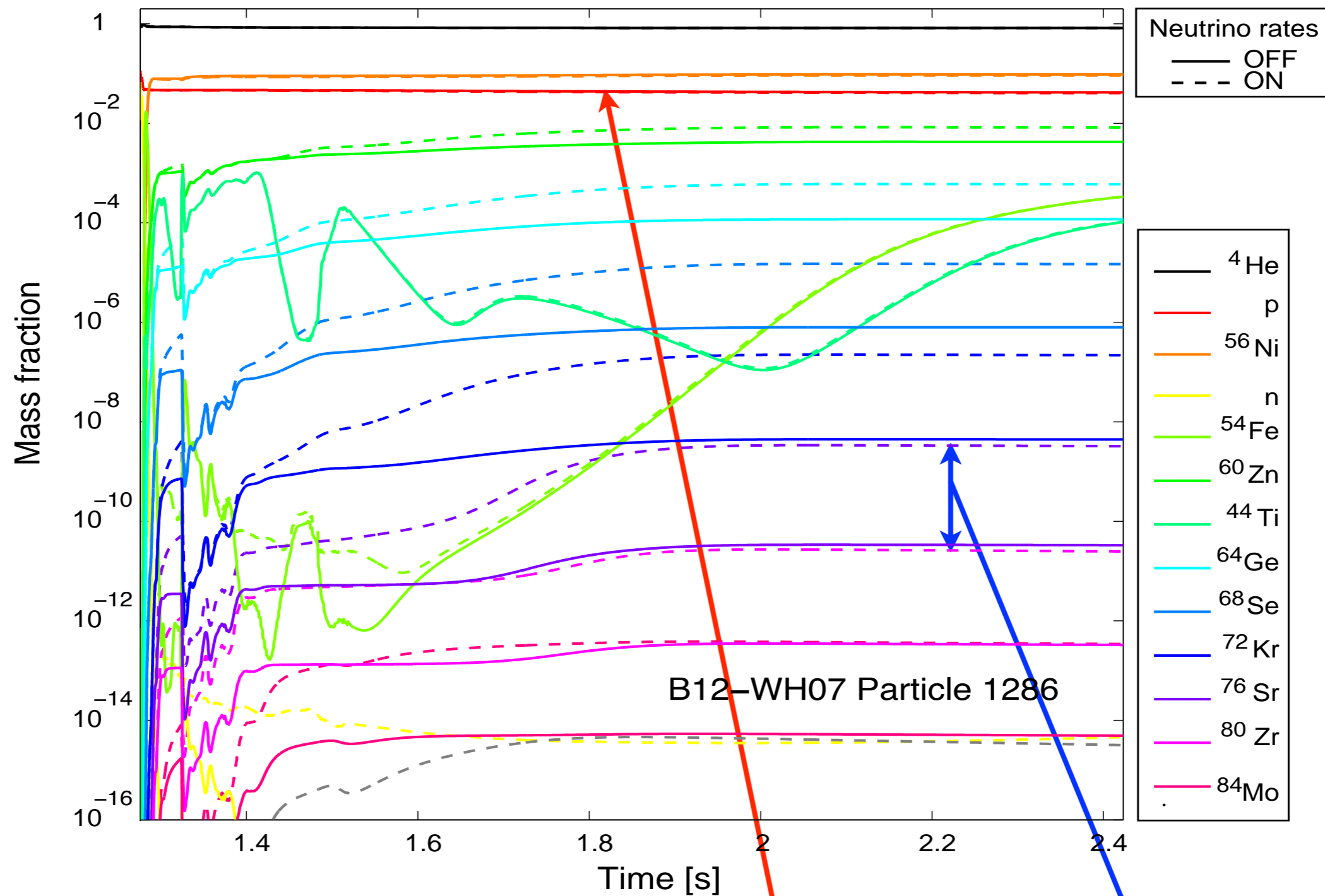
Despite the perceived importance of neutrinos to the core collapse mechanism, models of the nucleosynthesis have largely ignored this important effect.

Nucleosynthesis from  $\nu$ -powered supernova models shows several notable improvements.

1. Over production of neutron-rich iron and nickel reduced.
2. Elemental abundances of Sc, Cu & Zn closer to those observed in metal-poor stars.
3. Potential source of light p-process nuclei ( $^{76}\text{Se}$ ,  $^{80}\text{Kr}$ ,  $^{84}\text{Sr}$ ,  $^{92,94}\text{Mo}$ ,  $^{96,98}\text{Ru}$ ).



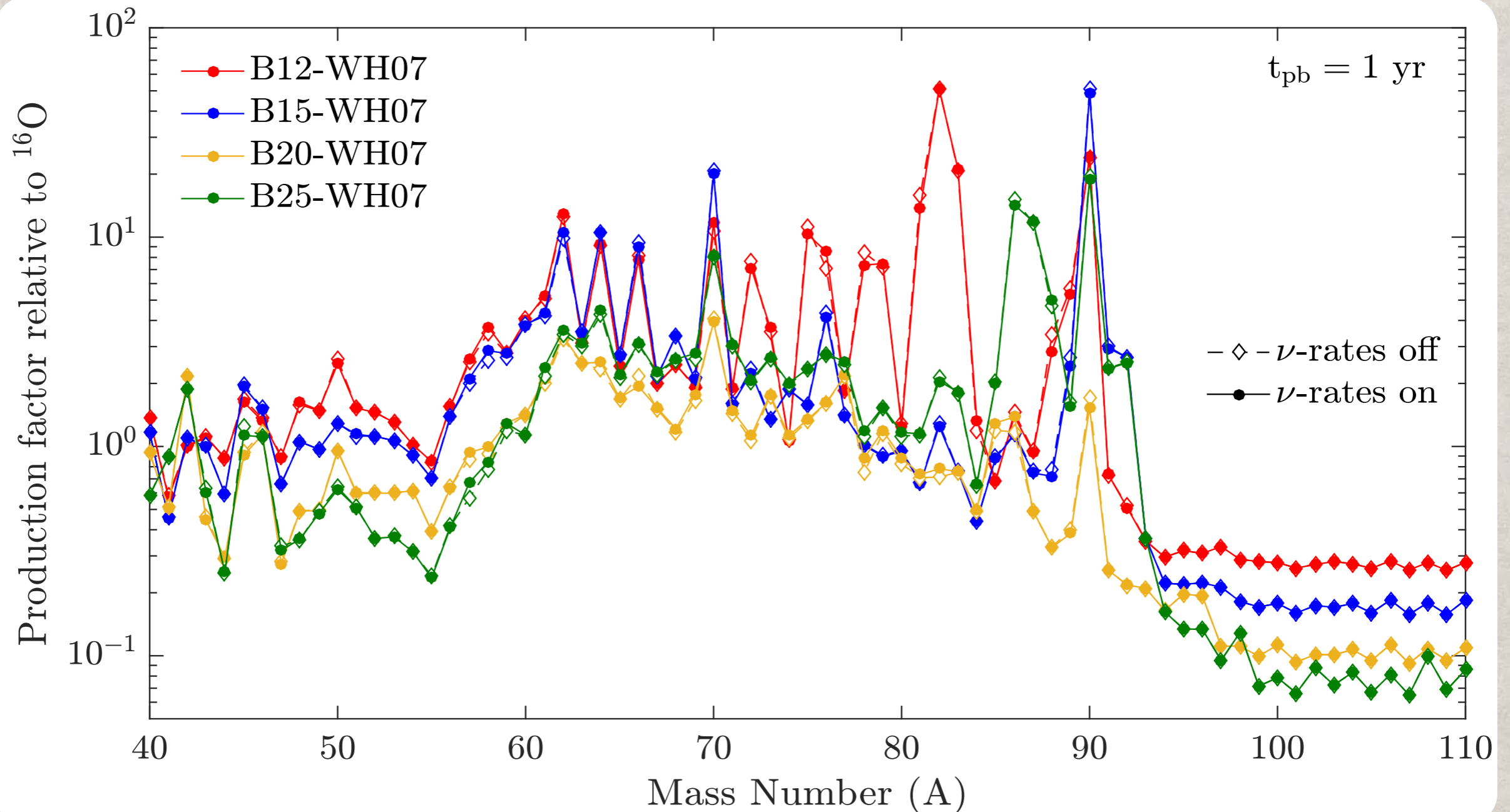
# VP-PROCESS ...



Our preliminary results show **proton-rich ejecta**, but the  **$\nu p$ -process** (dotted lines) occurs for only a handful of particles.

# ... IS MISSING

The  $\nu p$ -process is very weak in these models.

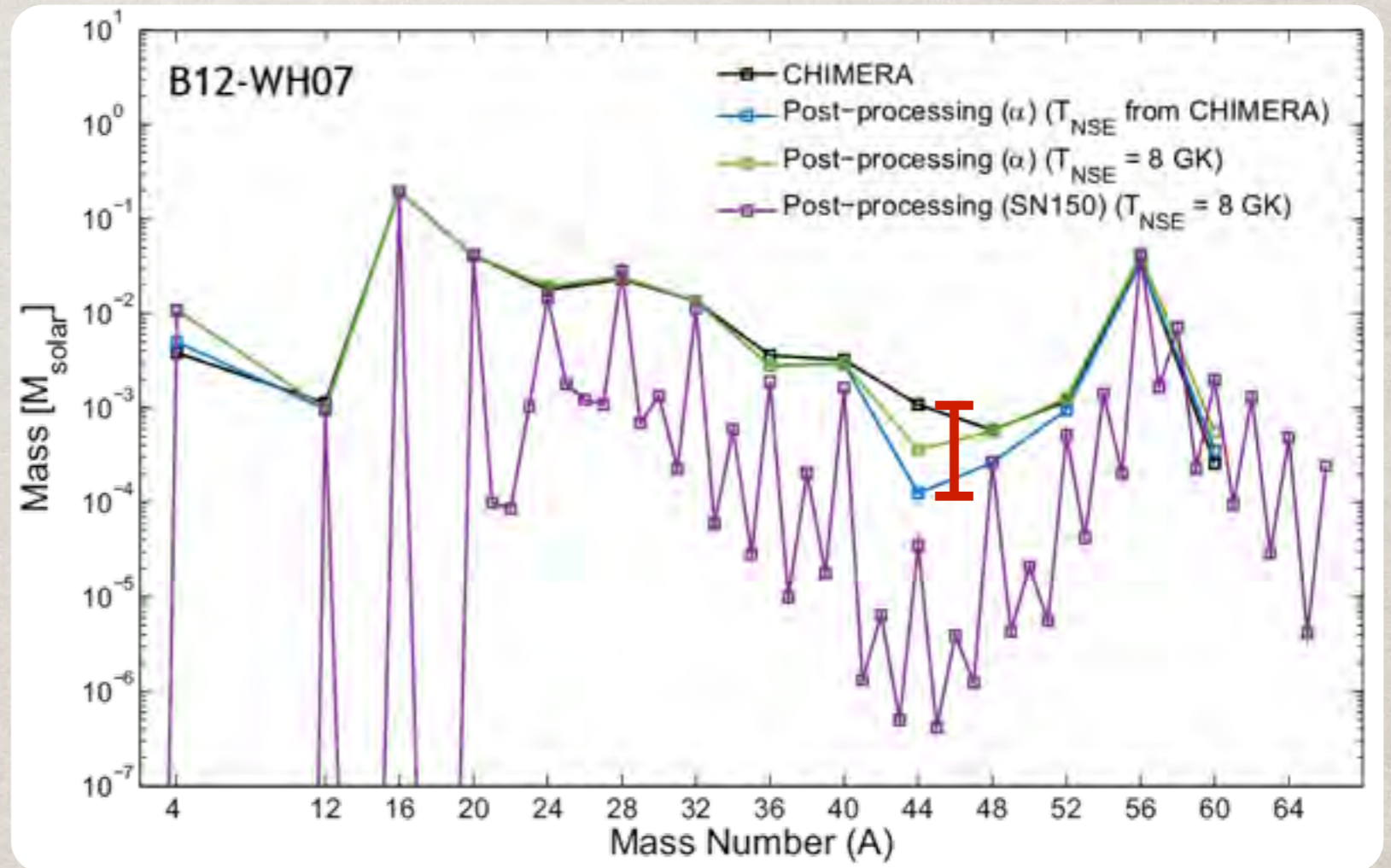


The suppression of the PNS wind is delaying or preventing a strong  $\nu p$ -process from occurring.

# NUCLEOSYNTHESIS TESTING

By computing the post-process nucleosynthesis in the **same fashion** as that built into CHIMERA, we learn about the limits of the tracers.

Products of  $\alpha$ -rich freezeout are **poorly captured** by the post-processing.

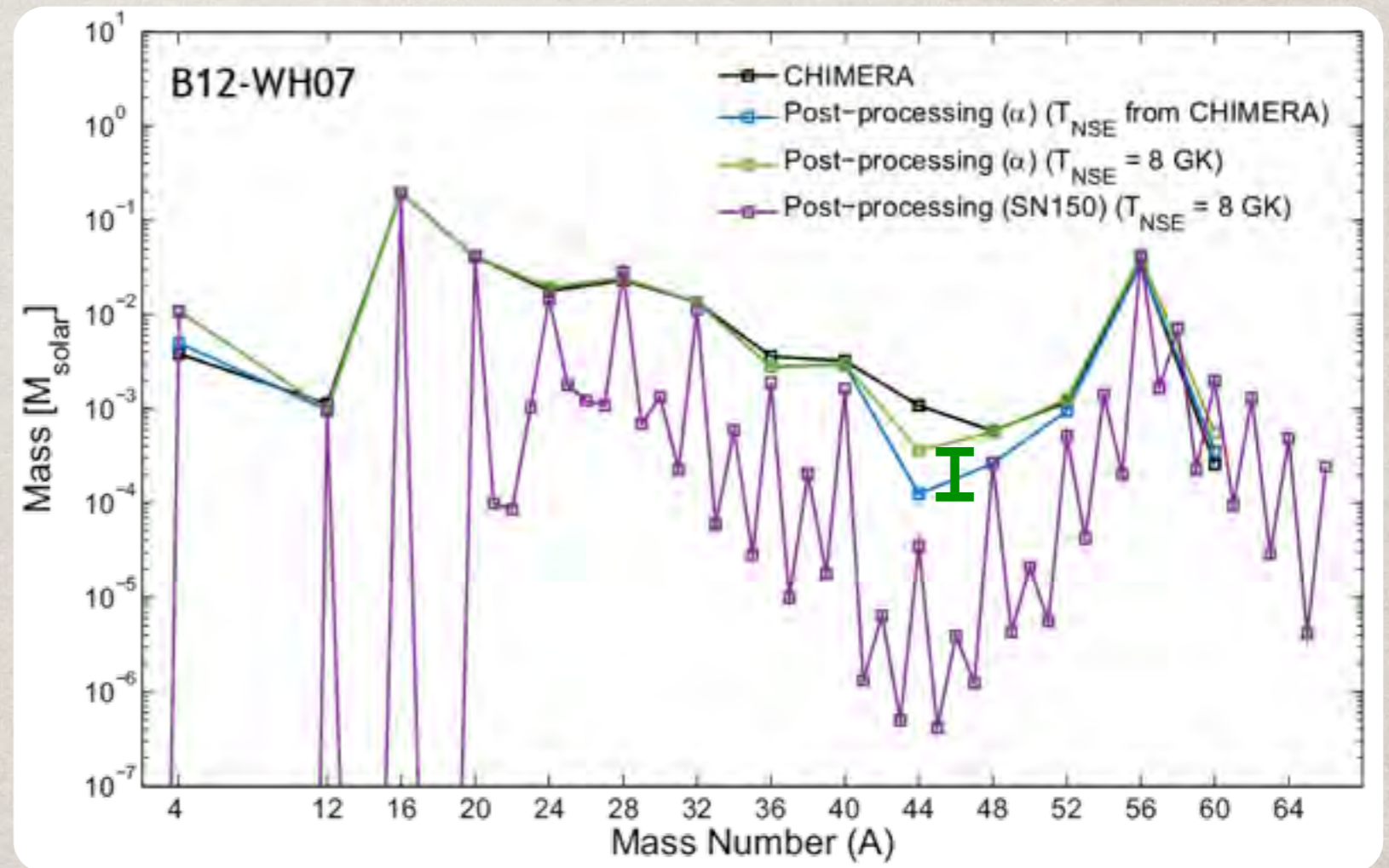


# NUCLEOSYNTHESIS TESTING

By computing the post-process nucleosynthesis in the **same fashion** as that built into CHIMERA, we learn about the limits of the tracers.

Products of  $\alpha$ -rich freezeout are **poorly captured** by the post-processing.

Accurately capturing the  $\alpha$ -rich freezeout also requires **transitioning out of NSE** at temperatures  $> 6$  GK.



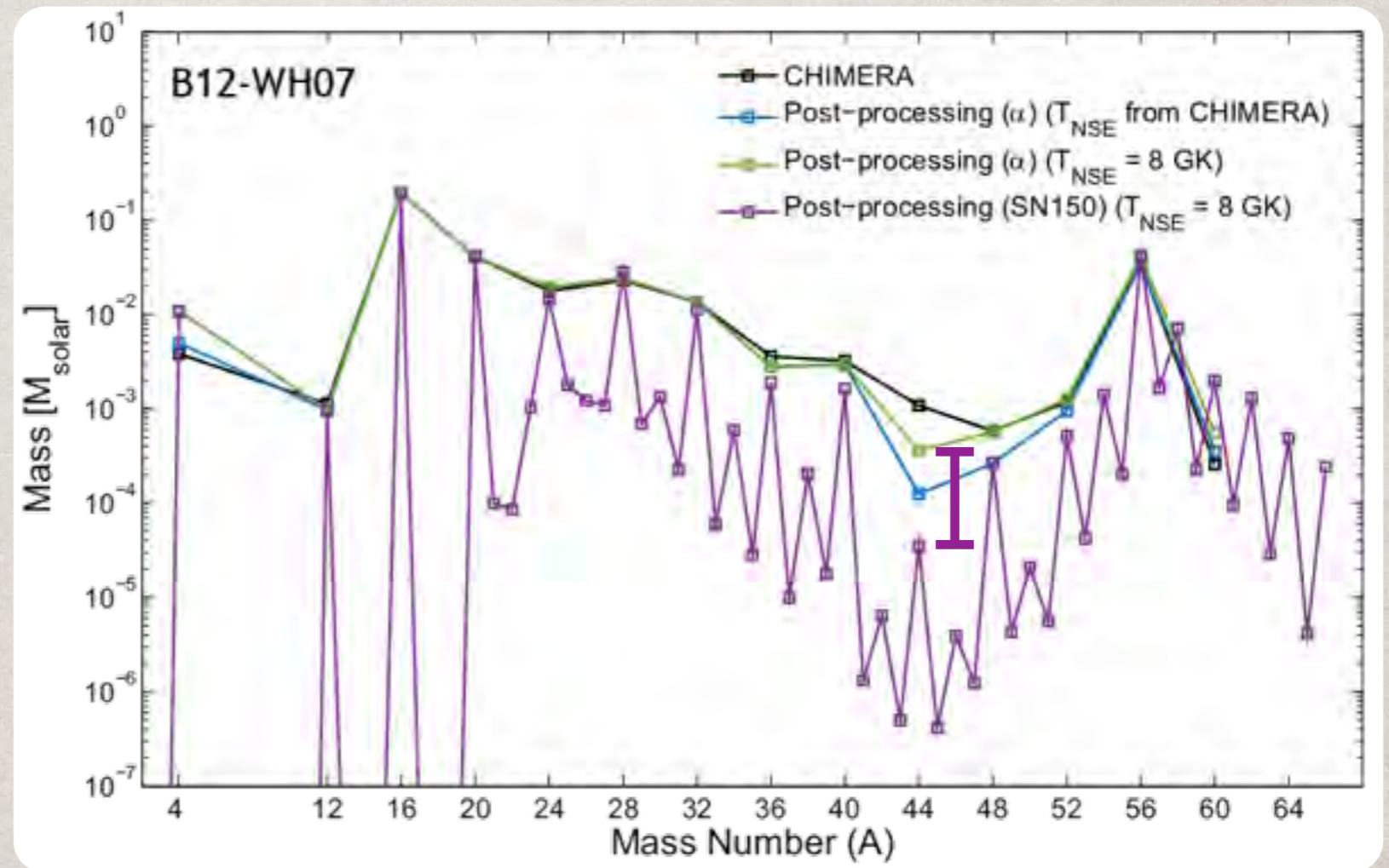
# NUCLEOSYNTHESIS TESTING

By computing the post-process nucleosynthesis in the **same fashion** as that built into CHIMERA, we learn about the limits of the tracers.

Products of  $\alpha$ -rich freezeout are **poorly captured** by the post-processing.

Accurately capturing the  $\alpha$ -rich freezeout also requires **transitioning out of NSE** at temperatures  $> 6$  GK.

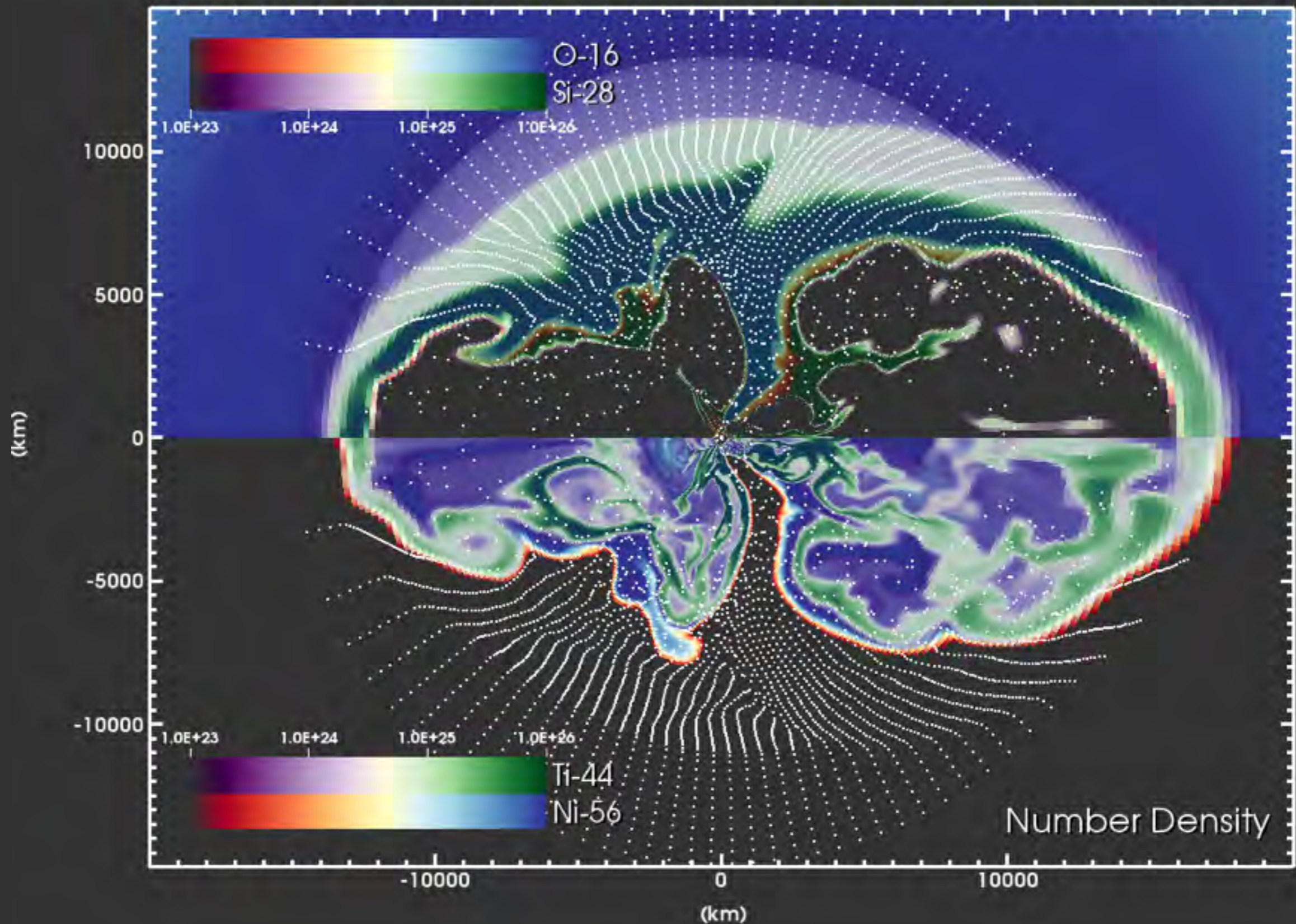
The limitations of the  $\alpha$ -network, when compared to a **more realistic network**, are most evident in the  $\alpha$ -rich freezeout and for  $A > 56$ .



# TRACKING LOW DENSITY

Chimera model: B12-WH07

1336.0 ms



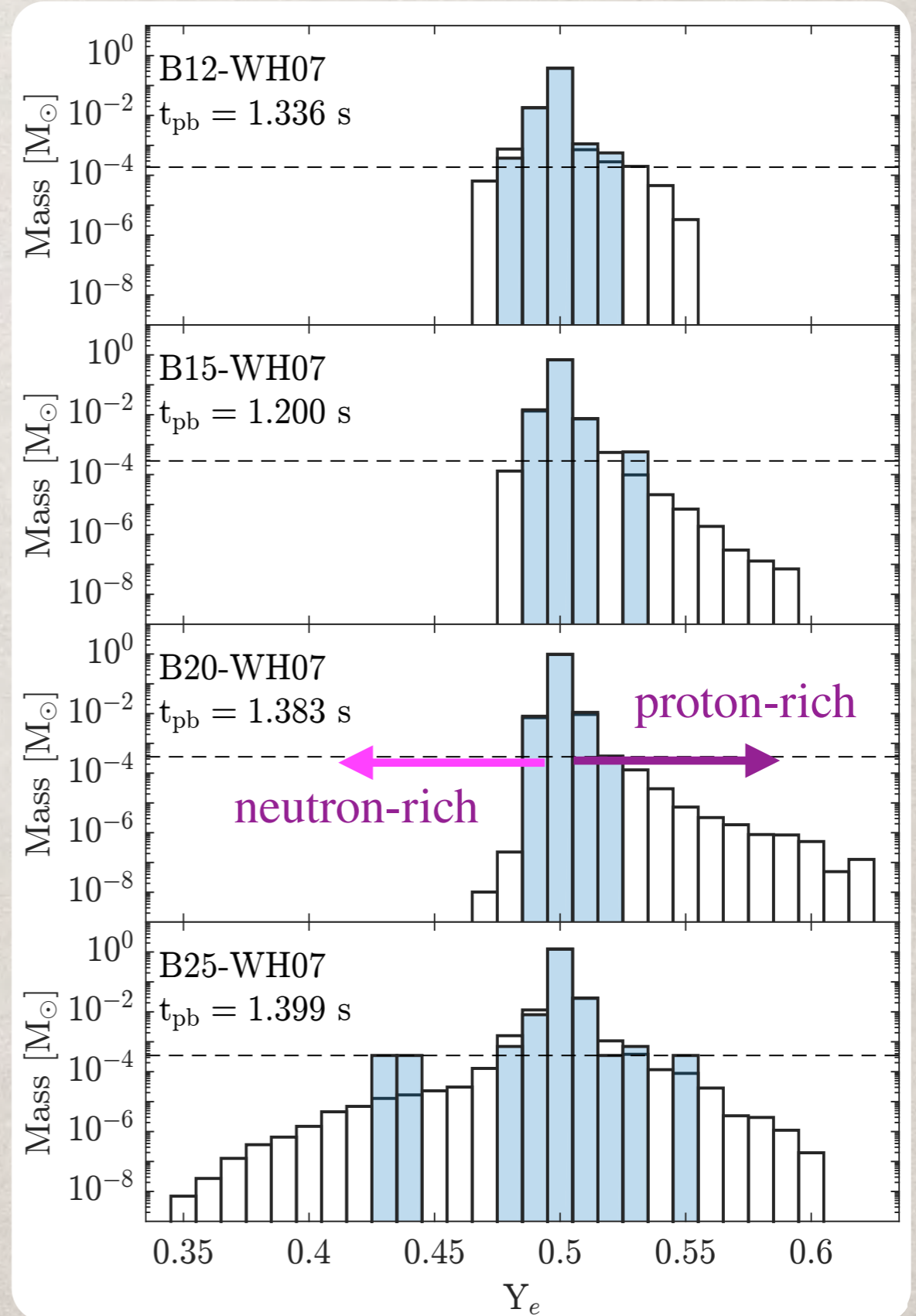
# TRACER RESOLUTION

Another view of the limitations of the tracer resolution is the **distribution in the electron fraction** of the ejecta.

Tracer resolution clearly **limits the production of more exotic species.**

For the B-series, run to 1.2-1.4 s after bounce, **this is the largest uncertainty**, though it only affects  $\alpha$ -rich freezeout.

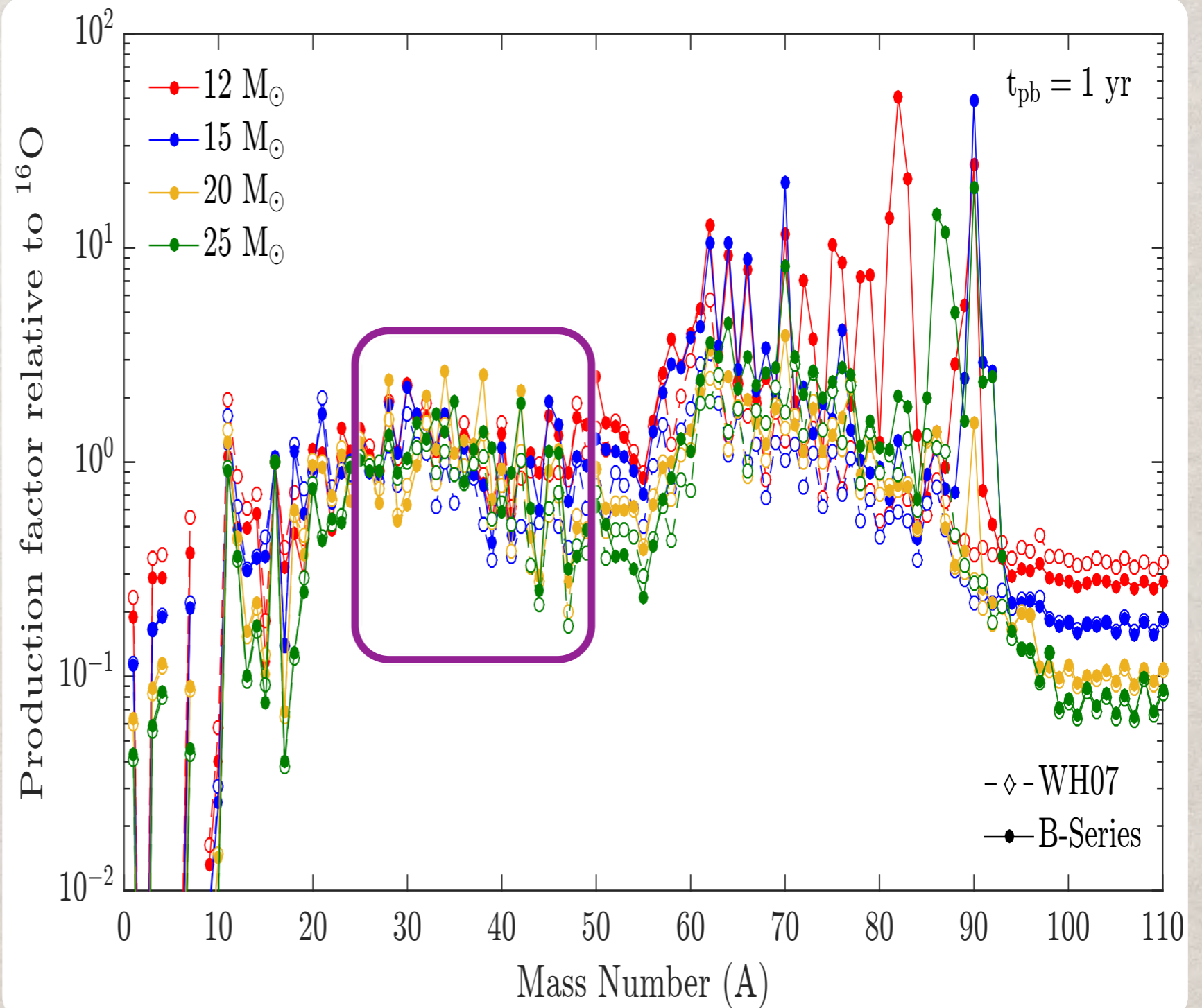
Model	Particles	$M_{\text{tracer}} [M_{\odot}]$
B12-WH07	4000	$1.87 \times 10^{-4}$
B15-WH07	5000	$2.86 \times 10^{-4}$
B20-WH07	6000	$3.55 \times 10^{-4}$
B25-WH07	8000	$3.49 \times 10^{-4}$



# COMPARING TO 1D

Until we can replace 1D CCSN models in all of their applications, we can use the 2D models to identify **areas of concern**.

Intermediate mass elements, up to  $A=50$ , are **similar**, though significant isotopic differences exist.

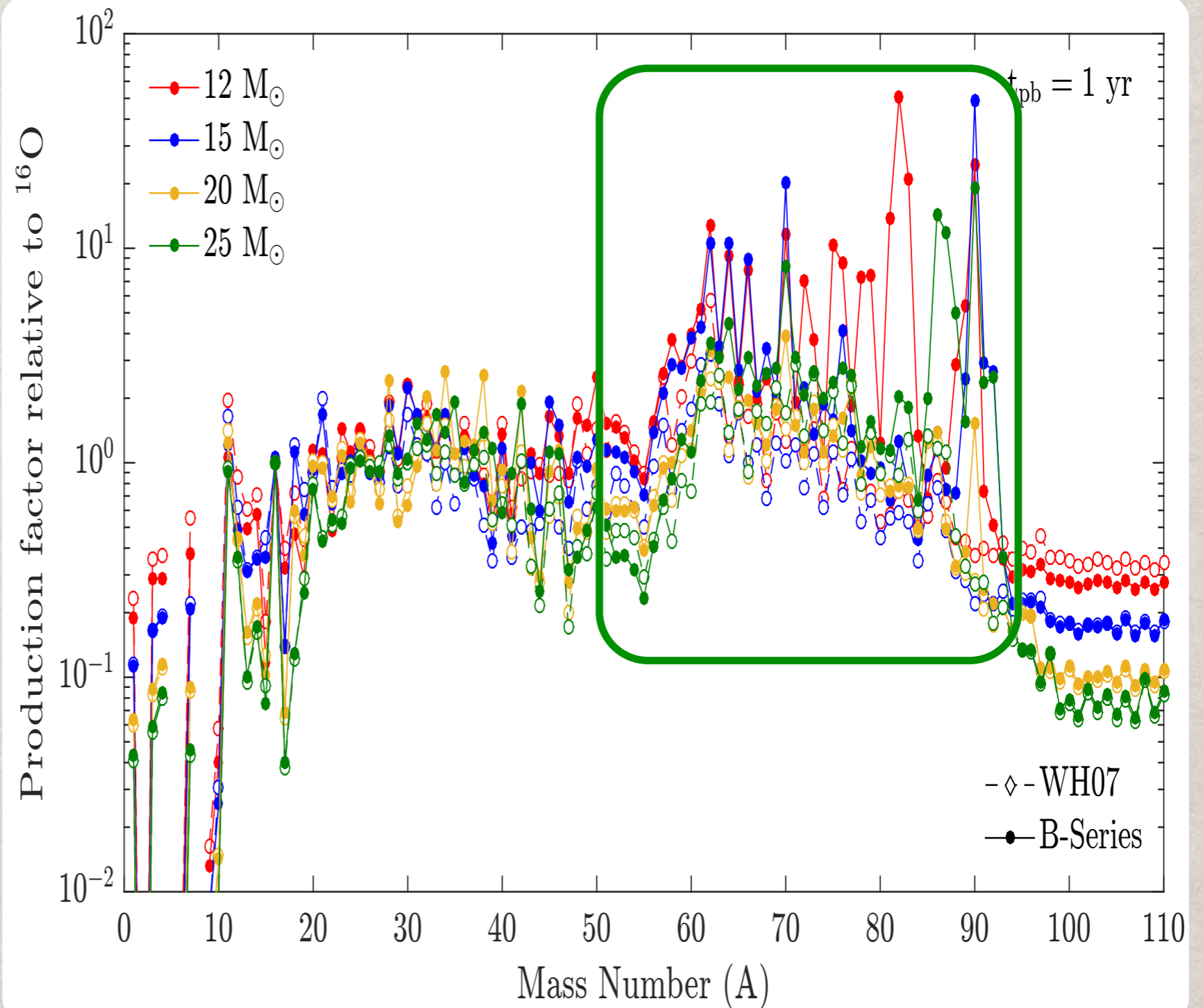


# COMPARING TO 1D

Until we can replace 1D CCSN models in all of their applications, we can use the 2D models to identify **areas of concern**.

Intermediate mass elements, up to  $A=50$ , are **similar**, though significant isotopic differences exist.

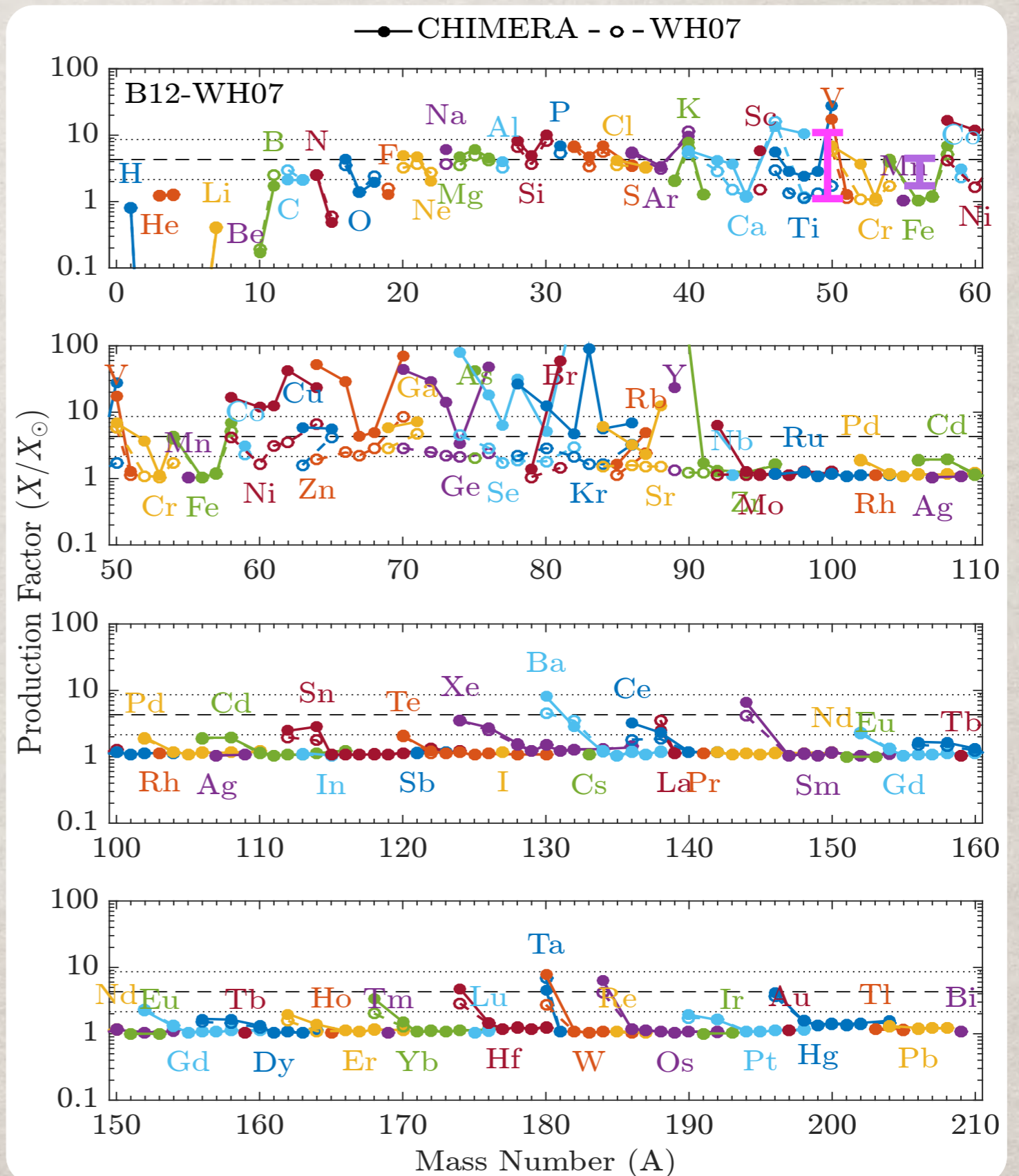
**Iron peak and heavier**, up to  $A=90$ , the **differences get larger**.



# ISOTOPIIC COMPARISON

Isotopic comparisons reveal significant differences from 1D on both the proton-rich and neutron-rich sides.

Ejection of small quantities of neutron-rich, ( $Y_e < 0.45$ ), low entropy matter produces significant amounts of neutron-rich intermediate mass isotopes like  $^{48}\text{Ca}$  and  $^{54}\text{Cr}$ .

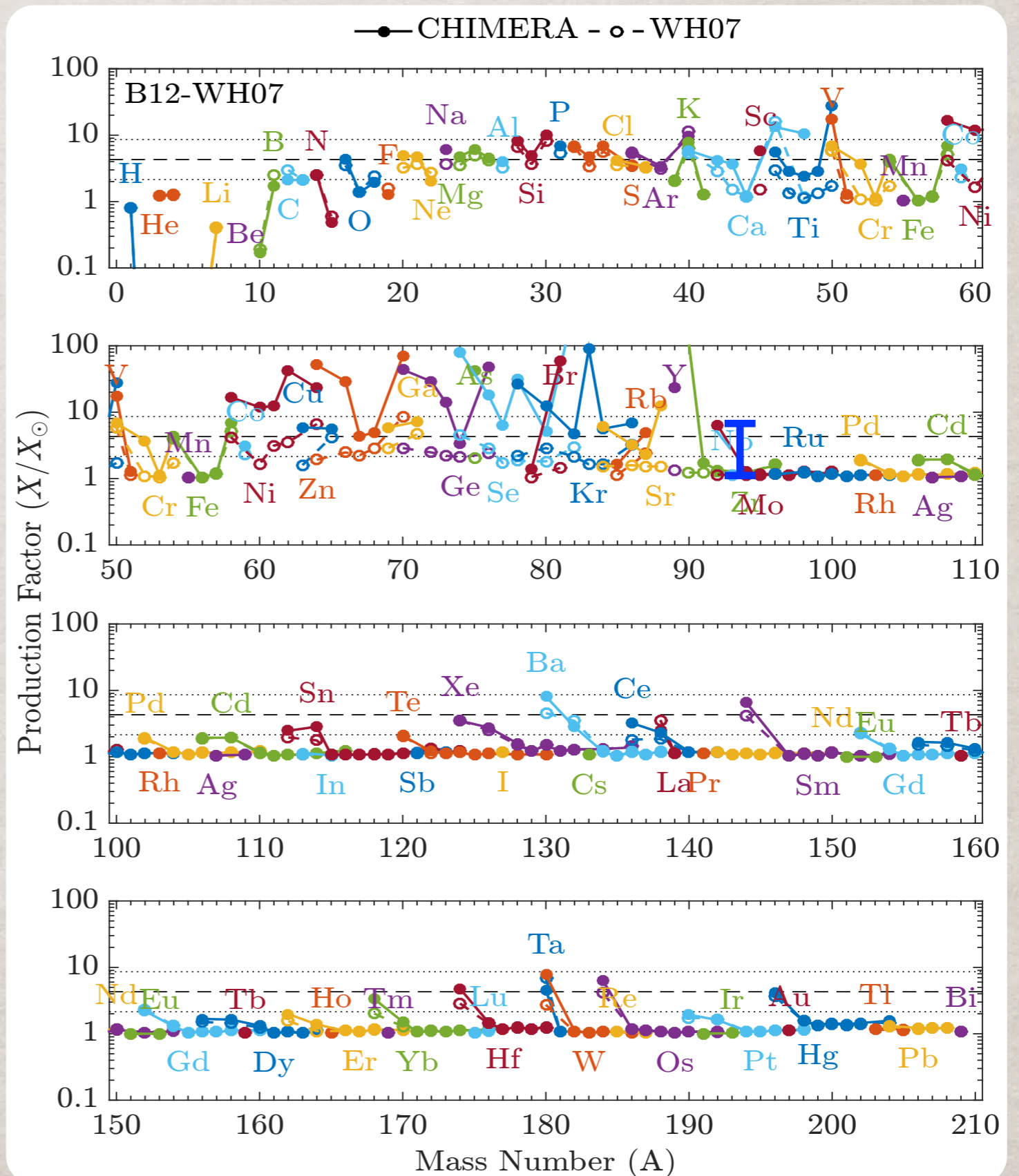


# ISOTOPIIC COMPARISON

Isotopic comparisons reveal significant differences from 1D on both the proton-rich and neutron-rich sides.

Ejection of small quantities of neutron-rich, ( $Y_e < 0.45$ ), low entropy matter produces significant amounts of neutron-rich intermediate mass isotopes like  $^{48}\text{Ca}$  and  $^{54}\text{Cr}$ .

Ejecta with somewhat higher  $Y_e$  ( $< 0.48$ ) and entropy produces  $^{92}\text{Mo}$ .



# MAGIC OF $^{48}\text{Ca}$

$^{48}\text{Ca}$ , with 20 protons and 28 neutrons, is a doubly-magic nucleus.

Fe45	Fe46 20 ms 0+	Fe47 27 ms	Fe48 44 ms 0+	Fe49 70 ms (7/2-)	Fe50 150 ms 0+	Fe51 305 ms 5/2-	Fe52 8.275 s 0+	Fe53 8.51 m 7/2-	Fe54 0+	Fe55 2.73 y 3/2-	Fe56 0+	Fe57 1/2-	Fe58 0+
	ECp	ECp	ECp	ECp	ECp	EC	EC	EC	5.8	EC	91.72	2.2	0.28
Mn44	Mn45	Mn46 41 ms	Mn47 100 ms	Mn48 158.1 ms 4+	Mn49 382 ms 5/2-	Mn50 283.88 ms 0+	Mn51 46.2 m 5/2-	Mn52 5.591 d 6+	Mn53 3.74E+6 y 7/2-	Mn54 312.3 d 3+	Mn55 5/2-	Mn56 2.5785 h 3+	Mn57 85.4 s 5/2-
		ECp	ECp	ECp	ECp	EC	EC	EC	EC	EC,β <sup>-</sup>	100	β <sup>-</sup>	β <sup>-</sup>
Cr43 21 ms (3/2+)	Cr44 53 ms 0+	Cr45 50 ms	Cr46 0.26 s 0+	Cr47 500 ms 3/2-	Cr48 21.56 s 0+	Cr49 42.3 m 5/2-	Cr50 1.8E+17 y 0+	Cr51 27.7025 d 7/2-	Cr52 0+	Cr53 3/2-	Cr54 0+	Cr55 3.497 m 3/2-	Cr56 5.94 m 0+
ECp,ECα,...	ECp	ECp	EC	EC	EC	EC	ECEC 4.345	EC	83.789	9.501	2.365	β <sup>-</sup>	β <sup>-</sup>
V42	V43 800 ms (7/2-)	V44 90 ms (2+)	V45 547 ms 7/2-	V46 422.37 ms 0+	V47 32.6 m 3/2-	V48 15.9735 d 4+	V49 330 d 7/2-	V50 1.4E+17 y 6+	V51 7/2-	V52 3.743 m 3+	V53 1.61 m 7/2-	V54 49.8 s 3+	V55 2.54 s (7/2-)
	EC	ECα	EC	EC	EC	EC	EC	EC,β <sup>-</sup> 0.250	99.750	β <sup>-</sup>	β <sup>-</sup>	β <sup>-</sup>	β <sup>-</sup>
Ti41 80 ms 3/2+	Ti42 199 ms 0+	Ti43 59 ms 7/2-	Ti44 63 y 0+	Ti45 184.8 m 7/2-	Ti46 0+	Ti47 5/2-	Ti48 0+	Ti49 7/2-	Ti50 0+	Ti51 5.76 m 3/2-	Ti52 1.7 m 0+	Ti53 32.7 s (3/2-)	Ti54 0+
ECp	EC	EC	EC	EC	8.0	7.3	73.8	5.5	5.4	β <sup>-</sup>	β <sup>-</sup>	β <sup>-</sup>	
Sc40 182.3 ms 4-	Sc41 596.3 ms 7/2-	Sc42 681.3 ms 0+	Sc43 3.891 h 7/2-	Sc44 3.927 h 2+	Sc45 7/2-	Sc46 83.79 d 4+	Sc47 3.3492 d 7/2-	Sc48 43.67 h 6+	Sc49 57.2 m 7/2-	Sc50 102.5 s 5+	Sc51 12.4 s (7/2-)	Sc52 8.2 s 2+	Sc53
ECp,ECα,...	EC	EC	EC	EC	100	β <sup>-</sup>	β <sup>-</sup>	β <sup>-</sup>	β <sup>-</sup>	β <sup>-</sup>	β <sup>-</sup>		
Ca39 859.6 ms 3/2+	Ca40 0+	Ca41 1.03E+5 y 7/2-	Ca42 0+	Ca43 7/2-	Ca44 0+	Ca45 162.61 d 7/2-	Ca46 0+	Ca47 4.536 d 7/2-	Ca48 6E+15 y 0+	Ca49 8.718 m 3/2-	Ca50 1.9 s 0+	Ca51 10.0 s (3/2-)	Ca52 4.6 s 0+
EC	96.941	EC	0.647	0.135	2.086	β <sup>-</sup>	0.004	β <sup>-</sup>	β <sup>-</sup> ,β <sup>-</sup> 0.187	β <sup>-</sup>	β <sup>-</sup>	β <sup>-</sup>	β <sup>-</sup>
K38 7.636 s 3+	K39 3/2+	K40 1.277E+9 y 4-	K41 3/2+	K42 12.360 h 2-	K43 22.3 h 3/2+	K44 22.13 m 2-	K45 17.3 m 3/2+	K46 10 s (2-)	K47 17.50 s 1/2+	K48 6 s (2-)	K49 1.26 s (3/2+)	K50 472 ms (0-,1,2-)	K51 365 ms (1/2+,3/2+)
EC	93.2581	EC,β <sup>-</sup> 0.0117	6.7302	β <sup>-</sup>	β <sup>-</sup>	β <sup>-</sup>	β <sup>-</sup>	β <sup>-</sup>	β <sup>-</sup>	β <sup>-</sup>	β <sup>-</sup>	β <sup>-</sup>	β <sup>-</sup>

Making  $^{48}\text{Ca}$  requires **neutron-rich** conditions, but if **temperature gets too high**, it will burn to form neutron-rich iron or nickel.

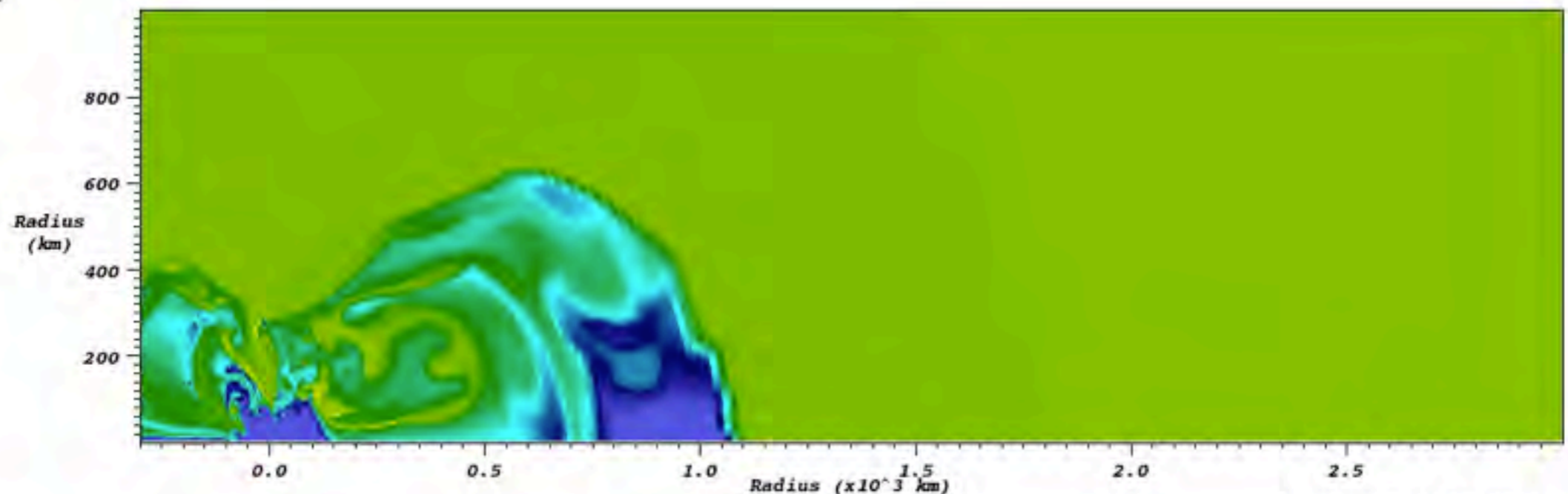
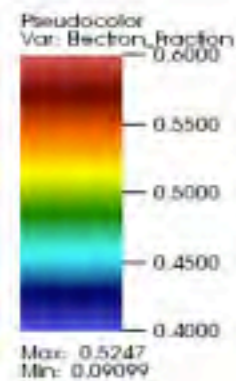
# STRIPPING A NEUTRON STAR

Relatively cold, but neutron-rich, matter is **trapped in the neutron star** and not ejected in the parameterized spherically symmetric models.

In the self-consistent, multi-dimensional models, accretion streams occasionally **dredge neutron-rich matter off the neutron-star**.

If this matter is **not heated** too much by subsequent interactions, such matter can be the source of  $^{48}\text{Ca}$ .

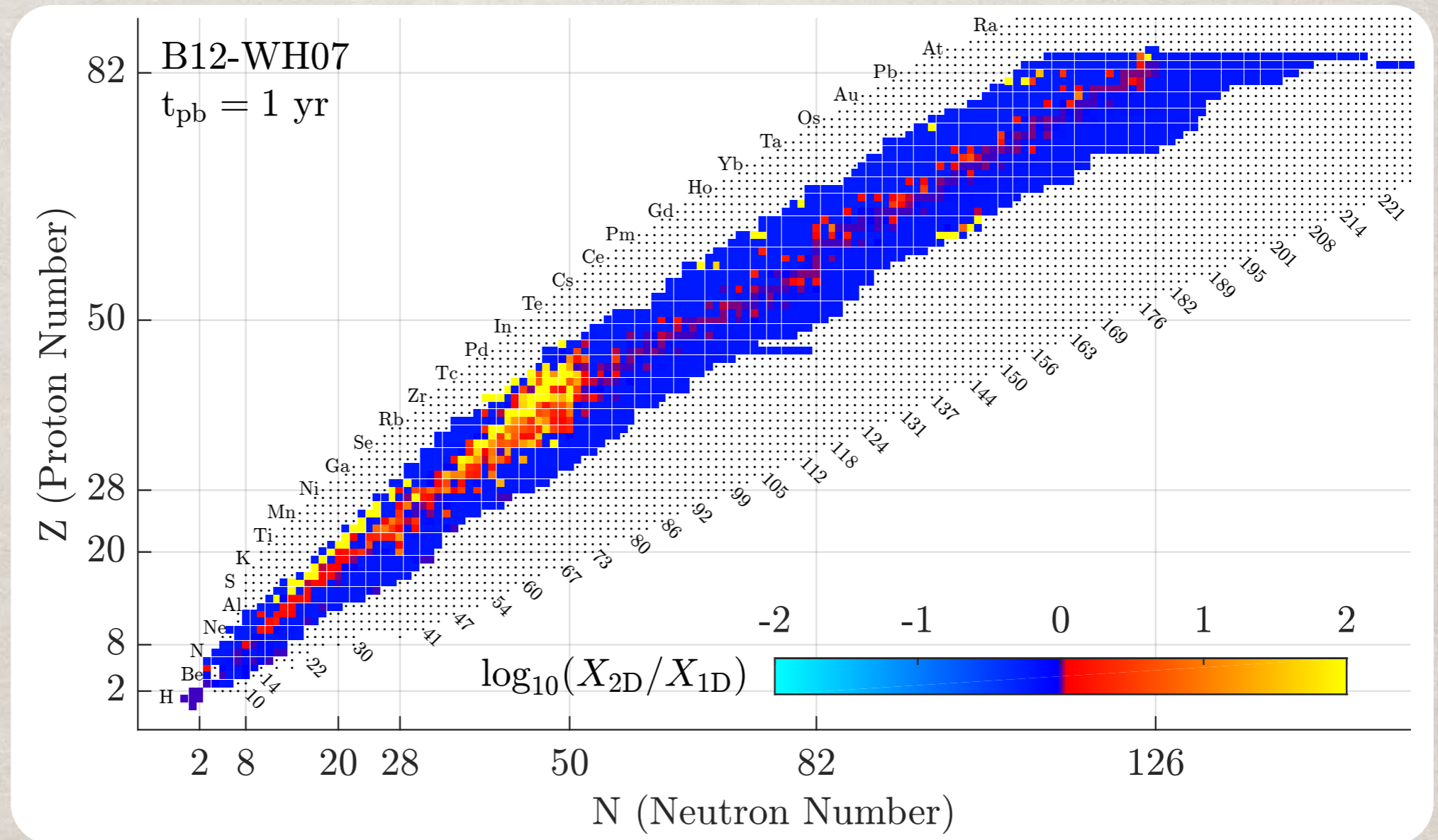
Frame 01329  
Time (elapsed) +0518.4  
Time (bounce) +0255.2



Tue May 22 04:04:02 2012

# THERMODYNAMIC VARIETY

Multi-dimensional dynamics allows the ejecta to experience a **wider variety** of temperature, density, electron fraction and neutrino exposure.



Deeper Mass Cut results in modest increase in intermediate mass and iron-group elements.

# CONCLUSIONS

Examining the nucleosynthesis of CCSN with models that self-consistently treat the explosion mechanism requires running the models to **times > 1 second** after bounce for uncertainties like the mass cut, thermodynamic extrapolation, etc. to become tractable.

Even then, **low post-processing resolution** is a significant uncertainty.

Differences from 1D models are seen in differing amounts of iron peak and intermediate mass elements as a result of changes in the **explosion timing** and **mass cut**.

The ejection of significantly more **proton-rich matter** as well as small quantities of **neutron-rich matter** can change the production of individual isotopes by orders of magnitude.

**Neutrino-Driven wind** is strongly **suppressed** by accretion.

There is **considerable commonality** in the production of species from NSE freezeout between lower mass CCSN and ECSN.

# PEEK AT THE FUTURE

DB: d9.6-2d-00329.silo

Cycle: 0

Time: 0.363247

Z9.6 2D sn160

